DILLA UNIVERSITY

SCHOOL OF GRADUATE STUDIES

THE COMPETITION BETWEEN SUPERCONDUCTIVITY AND SPIN DENSITY WAVE SODIUM DOPED BARIUM IRON ARSENAIDE ($Ba_{1-x}Na_xFe_2As_2$) SUPERCONDUCTORS

A THESIS SUBMITED TO THE DEPAERTMENT OF PHYSICS IN PARTIAL FULFILMENT OF THE REQUIREMENT FOR THE DEGREE OF MASTER OF SCIENCES IN PHYSICS

BY

GETACHEW YALEW

JUNE, 2021

DILLA ETHIOPIA

APROVAL SHEET OF THESIS

The undersigned hereby certify that they have read and recommended to the school of graduate studies for acceptance a thesis entitled **"the competition between superconductivity and spin density wave in sodium doped barium iron arsenide ($Ba_{1-x}Na_xFe_2As_2$) superconductor "** by Getachew Yalew in partial fulfillment of the requirements for the degree of Master of Science in physics.

Approved by:

Advisor's Name: ---------- signature: ----------date----------

Chairman's Name: ----------signature: ----------date----------

Internal Examiner's Name: ---------- signature: ----------date----------

External Examiner's Name: ----------signature: ----------date----------

DILLA UNIVERSITY

Date----------

Author : Getachew Yalew Emirie

Title: The Competition between Superconductivity and Spin Density Wave in Sodium Doped Barium Iron Arsenide ($Ba_{1-x}Na_xFe_2As_2$) Superconductor

College: Natural and computational science

Department: physics

Degree: M.Sc. **Convection**: June Year: 2021G.C

Permission is here with granted to Dilla University to circulate and have copied for non-commercial purposes, at its discretion, the above title upon the request of individuals or institutions.

Signature of Author

TABLE OF CONTENTS

List of figures vi
Abstract vii
Acknowledgement viii
CHAPTER ONE 1
General introduction 1
1 Back ground of the study 1
1.1 Zero electrical resistance and Meissner's effect 3
1.2 The BCS theory 3
1.3 Types of superconductivity 5
1.5 Statement of the problem 7
1.6 Significance of the study 7
1.7 Scope of the study 7
1.8 Objectives of the study 8
1.8.1 General objectives 8
1.8.2 Specific objectives 8
CHAPTER TWO 9
2. Review of related literature 9
2.1 High temperature superconductors 9
2.2 Cuprate superconductors 9
2.3 Iron-Based Superconductors 10
2.4 The main family of iron based superconductors 13
2.5 Barium iron arsenide ($BaFe2As2$) 16
2.6 Sodium doped $BaFe2As2$ ($Ba1-xNaxFe2As2$) 18
2.5 Spin Density Wave (SDW) 24
CHAPTER THREE 25
3. Methodology 25
3.1 The green function formalism 25
3.2 Equation of motion 26
CHAPTER FOUR 28
4. Formulation of the problem 28
4.1 The model Hamiltonian 28
4.2 Pure superconducting state for hole doping barium iron arsenide superconductors 29
4.3 Calculating Superconducting transition temperature with magnetic order parameter 39
4.4 Magnetic transition temperature and magnetic order parameter 57

4.5 Energy gap for pure superconducting order parameter state 64
CHAPTER FIVE 66
5. Results and discussion 66
CHAPTER SIX 69
6. Conclusions 69
Outline of the thesis 70
References 71
Declaration 79

List of figures

Figure 1.1: Experimental data by H.K. Onnes [1]----------**2**

Figure 1.2 : History of the increase of superconducting transition temperature----------2

Figure 1.3: Meissner effect (a) magnetic field penetrating a superconductor above critical temperature ($T > T_c$) (b) magnetic field expelled from a superconductor below critical temperature ($T < T_c$) ---------- 3

Figure 1.4 : A diagram showing the formation of Cooper pairs [2]----------4

Figure 1.5: Types of superconductors. (a) type I superconductors and (b) type II superconductors [8]----------6

Figure 2.1: Several representative classes of the iron-based materials [34]----------16

Figure 2.2: Crystal structure of $BaFe_2As_2$----------17

Figure 2.3: Phase diagram of $Ba_{1-x}Na_xFe_2As_2$----------23

Figure 2.4: Spin Density Wave (SDW) ----------24

Figure 5.1:Temperature vs Superconducting order parameter the graph which is drawon by using Equation (4.3.84)----------67

Figure 5.2: Magnetic transition temperature vs magnetic order parameter the graph which is drawon by using Equation (4.3.81)----------67

Figure 5.3: Superconducting transition temperature vs Magnetic ordering parameter for $Ba_{1-x}Na_xFe_2As_2$ Equation (4.3.56) is used to draw the graph---------- 68

Figure 5.4 : Superconducting and magnetic transition temperature as a function of magnetic order parameter of $Ba_{1-x}Na_xFe_2As_2$----------68

Abstract

The interplay between magnetism and superconductivity has awoken profound interest in the field of condensed matter physics. In this thesis the competition between superconductivity and spin density wave in hole doped barium iron arsenic ($Ba_{1-x}Na_xFe_2As_2$) superconductor has been investigated based on two band model of Hamiltonian. Employing retarded double time temperature dependent green's function with the two model Hamiltonian, the expression for superconducting transition temperature (T_c) and spin density wave transition temperature (T_m) as a function of magnetic order parameter (M) have been found. The mathematic expression and the graph T_C as function magnetic order parameter shows that the superconducting transition temperature does not increase rather it decreases as the magnetic order parameter increase, but the graph of magnetic transition temperature as a function of magnetic order parameter show that SDW transition temperature increases with the increase of magnetic order parameter. The intersection region in merged graphs of Tc as a function of magnetic order parameter and Tm as a function of magnetic order parameter show that the possible coexistence of superconductivity and spin density wave in $Ba_{1-x}Na_xFe_2As_2$ superconductors exist in some range of order parameter The result that in the merged graph has revealed in abroad agreement with experimental observation.

.

Acknowledgement

First of all, I would like to thank almighty God about help me until this time. Then I would like to thank my advisor Dr Dagne Atnafu for his continuous support, assistance and follow up, during the Course work and the thesis work. I truly admire him for his friendly approach with immeasurable and valuable contribution throughout the whole period of the research work. I am grateful to all members of my family for their various supports; especially thanks to my brother Yeshambel Yalew and my friend Teshome Ayele who support me on materials and continuous idea sharing during graduate's time. Lastly I would like to thanks to Dilla University in addition to physics department for giving knowledge by preparing MSc program.

CHAPTER ONE

General introduction

1 Back ground of the study

Superconductivity (SC) is a phenomenon of zero electrical resistance. It was first discovered by the Dutch physicist Heike Kimberling Onnes in Holland in 1911[1].The phenomenon of superconductivity, in which the electrical resistance of certain materials completely vanishes at low temperatures. Onnes, was the first to liquefy helium (which boils at 4.2 Kelvin at standard pressure). In 1911 Onnes and one of his assistants discovered the Phenomenon while studying the resistance of metals at low temperatures .They studied mercury because very pure samples could easily be prepared by distillation. Most of the physical properties of superconductors, such as the heat capacity, the critical temperature, critical current density, and critical field vary from material to material at which superconductivity is destroyed.

The coexistence of superconductivity and magnetism has been an interesting topic in condensed matter physics and it has been studied experimentally and theoretically for many years. These two cooperative phenomena were thought to be antagonistic [1]. According to BCS (Bardeen, Cooper, and Schrieffer) theory, a superconductor expels a magnetic field, which in turn destroys superconductivity. However, both superconductivity ordering and magnetic ordering have been seen in harmony (coexisting) in some of alkali earth compounds. The coexistence of superconductivity and antiferromagnetic is quite peaceful and very weakly influences each other [2]. The historic measurement of superconductivity in mercury is shown in Figure 1.1.

As in many other metals, the electrical resistance of mercury decreased steadily upon cooling, but dropped suddenly at 4.2K, and became undetectably small. Soon after this discovery, many other elemental metals were found to exhibit zero resistance when their temperatures were lowered below a certain characteristic temperature of the material, called the critical temperature, T_c [1].

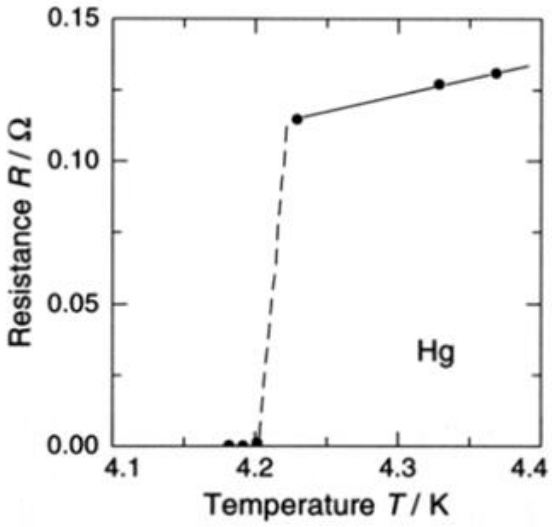

Figure1.1: Experimental data by H.K. Onnes [1]

In 1934 Goter and Casimir [3] introduced a phenomenological theory of superconductivity based on the assumption that in the superconducting state, there are two components of the conducting electron fluid normal and superconducting. The properties of the normal electrons are identical to those of the electron system in a normal metal, whereas, the superconducting paired electrons are responsible for the anomalous properties. During the 75 years that followed, many studies were made to understand how superconductors work. Over that time, various alloys were found that showed superconductivity at higher temperatures as indicated in figure (1.2).

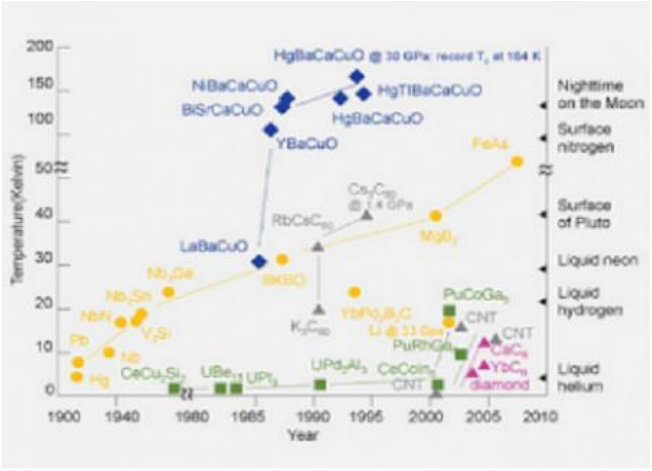

Figure1.2: History of the increase of superconducting transition temperature

1.1 Zero electrical resistance and Meissner's effect

It was assumed that, superconductivity was a manifestation of perfect conductors. If a perfect conductor is cooled below a critical temperature in the presence of an applied magnetic field, the field will be trapped in the interior of the conductor, but it will be expelled if the field is applied after it is cooled below the critical temperature. In 1933 Meissner and Ochsenfeld [4], discovered that superconductors are materials that expel magnetic fields (become perfect diamagnetic) from their interior when cooled below their critical temperature (t_c) .This property not only implies that magnetic fields are excluded from superconductors.

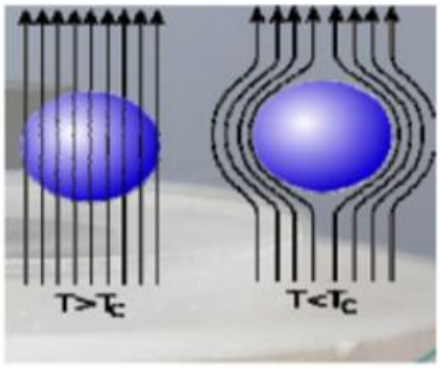

Figure1.3: Meissner effect (a) magnetic field penetrating a superconductor above critical temperature ($T > T_c$) (b) magnetic field expelled from a superconductor below critical temperature ($T < T_c$) [4].

1.2 The BCS theory

According to classical physics, part of the resistivity of a metal is due to collisions between free electrons and thermally displaced ions of the metal lattice and part is due to scattering of electrons from impurities or defects in the metal. This classical model could never explain the superconducting state since the electrons in a material always suffer from some collisions and therefore resistivity can never be zero. Until the discovery of the BCS theory, no one could explain why electrons enter the superconducting state and why electrons in this state are not scattered by impurities and lattice vibrations.

The microscopic theory of superconductivity (BCS) [2] discovered in 1957 has had good success in explaining the features of superconductors according to which two electrons in the superconductor are able to form a bound pair called a Cooper pair which experiences an attractive interaction. This notion at first seems counter intuitive since electrons normally repel one another because of their like charges. However, a net attraction is achieved when the electrons interact with each other via

the motion of the crystal lattice as the lattice structure is momentarily deformed by a passing electron as shown in the Figure (1.4). The passage of electron 1 causes nearby ions to move inward towards the electron resulting in a slight increase in the concentration of positive charge in this region. Electron 2 approaches before the ions return to their equilibrium positions and being attracted to the distorted (positively charged) region. The net effect is a weak attractive force between the two electrons (Cooper pairs). It can be said that, the attractive force between two electrons is an electron lattice-electron interaction (phonon mediated), where the crystal lattice serves as the mediator of the attractive force.

Cooper pair in a superconductor consists of two electrons having opposite momenta and spin [5]. Cooper pairs are formed in a shell of width of order (K_BT_c) around the Fermi surface. Their radius is small as compared to the average distance between electrons. Hence, between electrons forming Cooper pairs there are so many Cooper pairs [6].The very essential feature of the BCS theory is that once the Cooper pairs are formed, they will have the same wave function, as regards to both the center of mass and the relative coordinate. BCS theory also showed that, the energy difference between the free state of the electron (i.e., energy of individual electron- a case of normal state) and the paired state (the energy of paired electron- a case of superconducting state) appears as the energy gap at the Fermi surface. The normal electron states are above the energy gap in the semiconductors and insulators. Since pairing is completed at 0 k, the difference in energy of free and paired electron states (i.e., normal and superconducting electron states) is maximum, that means energy gap is maximum at absolute zero. At ($T = T_c$), pairing is dissolved and energy gap reduces to zero.

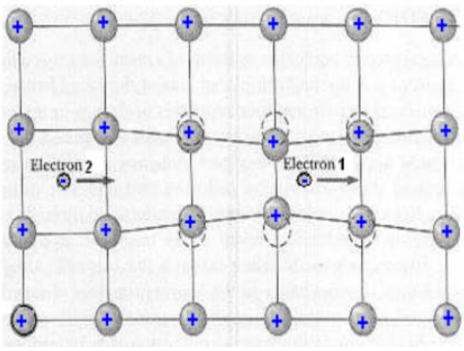

Figure1.4 : A diagram showing the formation of cooper pairs [2].

1.3 Types of superconductivity

Superconducting materials can be divided into two types based on their response to magnetic field. They are type I and type II superconductors. There is no difference in the mechanism of superconductivity in the two types of superconductors. They have similar thermal properties at the superconductor-normal transition in zero magnetic fields. But the Meissner effect is entirely different. A good type I superconductor excludes a magnetic field until superconductivity is destroyed suddenly and then the fields penetrates completely. A good type II superconductor excludes the field completely, up to field (Hc1). Above (Hc1) the field is partially excluded, but the specimen remains electrically superconducting. At a much higher field, the flux penetrates completely and superconductivity vanishes. High magnetic fields destroy superconductivity and restore the normal conducting state. Depending on the character of this transition, we may distinguish between type I and II superconductors. It is found that the internal field is zero (as expected from the Meissner effect) until a critical magnetic field, (Hc), is reached where a sudden transition to the normal state occurs [7]. This results in the penetration of the applied field into the interior.

Most of the pure elements type I superconductors [8]. Type II superconductors; on the other hand, respond differently to an applied magnetic field. An increasing field from zero results in two critical fields, (Hc1) and (Hc2). At (Hc1) the applied field begins to partially penetrate the interior of the superconductor. However, the superconductivity is maintained at this point. The superconductivity vanishes above the second, much higher, critical field, (Hc2). For applied fields between (Hc1) and (Hc2), the applied field is able to partially penetrate the superconductor, so the Meissonier effect is in complete, allowing the superconductor to tolerate very high magnetic fields.

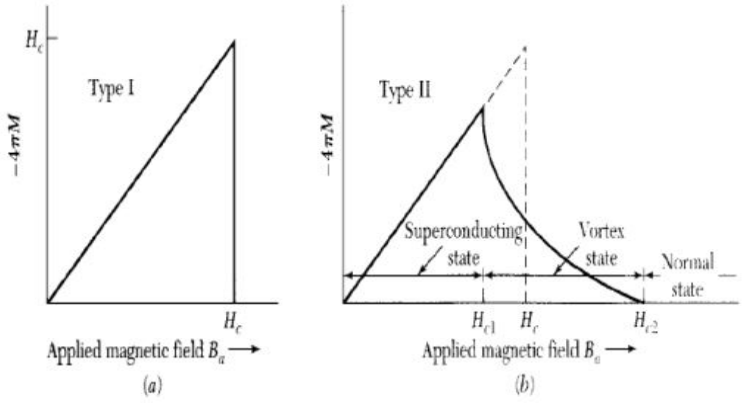

Figure 1.5: Types of superconductors (a) type -I and (b) type- II superconductors (8)

1.4 Superconductivity and Magnetism in Iron Based Superconductor

A type I superconductor in a magnetic field will completely repel all field lines. This is called the Meissner effect, and it is an example of perfect diamagnetism. The perfect exclusion of a magnetic field can be explained by using Faraday's law. Recall that the integral over a closed loop of E dotted with ds is equal to the rate of change of the magnetic flux. Since no potential difference can exist in a superconductor (there is no resistance to make ones possible), then the magnetic field inside a superconductor cannot change.

Physicists predicted that the magnetic field would remain in the superconductor, even once the external field was turned on. However, when the experiment was carried out, the magnetic field was expelled from the conductor as soon as Tc was reached. This proved that not only can the magnetic field not change, but it must be zero inside a superconductor. Surface currents in a superconductor act to exactly counter any applied magnetic field, and this is how one can levitate a magnet above a superconductor. Since the first discovery of superconductivity (SC) a century ago, the effects of magnetic impurities and the possibility of magnetic ordering in superconductors has been a central topic of condensed matter physics. Due to strong spin scattering, it has generally been believed that the conduction electrons cannot be both magnetically ordered and superconducting [9]. Even though it is thought that Cooper pairs in cuprates, heavy fermions, and Fe based compounds are mediated by spin actuations [10].

Superconductors generally occur after suppressing the magnetic ordering either through chemical doping or the application of hydrostatic pressure [11]. However, there is growing evidence for the coexistence of superconductivity with either ferromagnetic (FM) or antiferromagnetic (AFM) ordering. With the decrease of temperature (T), some of these systems show magnetic ordering before the superconducting transition (T_c) [12], some are ordered in a reversed sequence, some have the two orderings occur concomitantly [13], and some show reentrant superconductivity (partially) overlapping with a magnetically ordered phase [14]. Despite extensive investigations of interaction between SC and magnetic moments, there is so far no unified theory for the coexistence of SC and magnetism. With the lack of theoretic guidance, the existing experimental findings lead to two schools of thought: one is that both orders result from the same conduction electrons as evidenced by their synchronized magnetic and superconducting orders [15], and the other is that there are two separate sets of electrons responsible for magnetic ordering and superconductivity, respectively [13]. The discovery of superconductivity in Fe-based compounds has sparked enormous interest in

the scientific community. Though superconductivity is induced after suppressing the AFM ordering, it can coexist with either remaining AFM ordering or new FM ordering [1]

1.5 Statement of the problem

Superconductivity is a phenomenon of zero electrical resistance that current flows in a conductor without stropping for long period of times, this current affects the conductor warm up and broken. One problem that existed in the study of high-temperature superconductors was too high a resistivity in the electrical contacts .At different doping level concentration their superconducting property changes. Superconductivity is usually lost when magnetism is turn on. Magnetism and superconductivity are usually contradictory at low temperature at a much higher field, the flux penetrates completely and superconductivity vanishes. Superconductivity in the oxide materials was limited to very low temperatures. Electron doping with Cu or hole doping with Cr does not yield superconductivity. When a material is changed to superconductor its structure changes.

1.6 Significance of the study

The result of this research work will have a great importance in filling the scientific gap, providing information about superconducting properties of elements, alloys and compounds. Superconducting wire can carry immense electrical currents with no heating, which allows it to generate large magnetic fields. We have obtained the self-consistent gap equations, and the expressions for the transition temperatures and order parameters. By calculating the temperatures as a function of order parameters, we have presented possible cases of phase coexistence /separation among the SDW and superconducting phases. The study will also use to know about suppression of magnetic order parameter for the emergence of superconductivity. All compounds exhibit a magnetically ordered state, which suppresses the superconducting states. Superconductors are used in world life.

1.7 Scope of the study

This study has been specifically focused on analyzing or investigating factors affecting superconductivity among this are either hole doping or electron doping of at different concentrations. The study is concerned on iron based superconductors such as sodium doped barium iron arsenide.

1.8 Objectives of the study

1.8.1 General objectives

The general objective of this thesis is to study the competition between superconductivity and spin density wave in hole doped barium iron arsenide ($Ba_{1-x}Na_xFe_2As_2$) superconductor theoretically.

1.8.2 Specific objectives

The specific objectives of this study will be:

- To correlate the spin density wave ordered parameter and superconductivity ordered parameter in in hole doped ($Ba_{1-x}Na_xFe_2As_2$) Superconductor.
- To calculate the superconducting critical temperature and spin density wave transition temperature of hole doped barium iron arsenide ($Ba_{1-x}Na_xFe_2As_2$) superconductor mathematically.
- To obtain the competition between spin density wave and superconductivity in hole doped barium iron arsenide ($Ba_{1-x}Na_xFe_2As_2$) superconductor.

CHAPTER TWO

2. Review of related literature

2.1 High temperature superconductors

High-temperature superconductors (Tc or HTSc) are materials that have a superconducting transition temperature (T_c) above 30 K (-243.2℃). From 1960 to 1980, 30K was thought to be the highest theoretically possible T_c. There was a great excitement after the discovery of high T_c SC cuprate by Bednorz and Müller in 1986 , for which they were awarded the Nobel Prize in Physics in 1987 [17]. who reported T_c well above 30K in $La_{2-x}Ca_x Cuo_4$ .Their remarkable discovery of superconductivity phenomena led to the discovery of many cuprate systems with transition temperature T_c achieved up to ~ 135 K (T_c ~ 164 K under high pressure) in Hg based cuprates [18]. The subsequent world-wide efforts in search of high T_c SC cuprate raised the transition temperature beyond the liquid nitrogen temperature of 77K for the first time [19].

2.2 Cuprate superconductors

Since the discovery of the 1st high-temperature (high T_c) cuprate superconductor, a quite large number of structures belonging to the cuprate family have emerged. Cuprate superconductors are generally considered to be quasi-two-dimensional materials with their superconducting properties determined by electrons moving within weakly coupled copper-oxide (CuO_2) layers. Neighboring layers containing ions such as lanthanum, barium, strontium, or other atoms act to stabilize the structure and dope electrons or holes onto the copper-oxide layers. The undoped 'parent' or 'mother' compounds are Mott insulators with long-range antiferromagnetic order at low enough temperature. Single band models are gen/nearly considered being sufficient to describe the electronic properties.

The cuprate superconductors adopt a perovskite structure. The copper-oxide planes are checkerboard lattices with squares of O^{2-} ions with a Cu^{2+} ion at the Centre of each square. Chemical formulae of superconducting materials generally contain fractional numbers to describe the doping required for superconductivity. There are several families of cuprate superconductors and they can be categorized by the elements they contain and the number of adjacent copper-oxide layers in each superconducting block.

For example: Yttrium Barium Copper Oxide (YBCO) ($YBa_2\,Cu_3\,O_7$, T_c~92K) and Bismuth Strontium Calcium Copper Oxide (BSCCO) ($BiSr_2\,Ca_1Cu_2O_8 + x$ $(Bi-2212)$, T_c~85K,) and $BiSr_2\,Ca_2Cu_3\,O_{10} + x$ $(Bi-2223)$, T_c~110K. In spite of all these efforts, the mechanism of this new kind of superconductivity has not been clarified yet; it still remains one of the most enigmatic problems of the solid-state physics. The difficulty of this problem is due to the complicated properties, including complicated crystalline structures of materials displaying high T_c, to the presence of a strong anisotropy, to the existence of non-adiabatic effects, to strong electronic correlations, In these complicated materials, several phase transitions (structural, magnetic, superconductor, etc.) occur, and mixed states are allowed, for instance coexistence of superconductivity and ferromagnetism [20]

2.3 Iron-Based Superconductors

Iron-based superconductors contain layers of iron and a pnictogen such as arsenic or phosphorus or a chalcogen.This is currently the family with the second highest critical temperature, behind the cuprates. Interest in their superconducting properties began in 2006 with the first discovery of iron based superconductivity in $LaFePO$ at 4K and gained much greater attention in 2008 after the analogous material $LaFeAs$ (O, F) with transition temperature T_c, of 26 K found by Hobson's group. Since then, many researches have been done on the materials, with T_c reaching as high as 55K by replacing La with Sm.

The 1st report of superconductivity in an iron pnictides, specifically in F-doped $LaOFeP$ below 5 K in 2006 , was hardly noticed and only two years later, when F-doped $LaOFeAs$ was reported to superconductor below 28 K, the potential of iron pnictides as high-temperature superconducting materials was realized [21]. Following this discovery, more than 50 new iron superconductors with the same basic structure were discovered with Tc reaching up to 56 K .The common motive is a planar FeAs layer in which the Fe atoms form a square lattice, tetrahedral coordinated with As atoms placed alternatingly above and below the hollow centers of the squares. Instead of As, the ligand could be another pnictogen (P) or a chalcogen (x=Se or Te), but for simplicity, in this paper we shall refer to it as As.[22].These superconductors are divided in four main families depending on their 3D crystal structure this structure is shown in Figure (2) [23]: The iron chalcogenides are simple tetragonal with the FeX layers stacked on top of each other (11 family).

The iron pnictides have the $FeAs$ layers separated by alkali metals (111 family), or by rare-earth oxygen/fluoride blocking layers (1111 family), in set stacking, or by alkali- earth metals (122 family) in body-centered conductivity in F doped $LaFeAsO$ with T_C of 26 K [24] create. Denoting the chemical formula of these so-called 1111 materials by $RFeAsO$, F doping resulted in the following optimal transition temperatures: 52 K for R = Nd , 52 K for R = Pr, 55 K for R = Sm , 41 K for R = Ce , 36– 50 K for R = Gd ,46 K for R = Tb , and 45 K for R = Dy . To date, the highest transition temperature for the iron-based superconductors is 56 K observed in a sample of $Gd_{1-x}\ Th_x\ FeAsO$ [25].These superconducting transition temperatures make the Fe-based materials second only to the cuprates and they, therefore, represent the second family of high-T_C super- conductors. It was later shown that F doping was not necessary and similar transition temperatures could be obtained for the case of oxygen deficient $RFeAsO_{1\ \_\ y}$: 28 K for R= La , 42 K for Ce , 53 K for Nd , 48 K for Pr, 55 K for Sm ,53 K for Gd , 52 K for Tb and Dy. Both the F doped and oxygen deficient samples show the same trend for T_C as a function of rare earth ion. Crystal structure of the1111,122, 111, and 11 materials. At room temperature, the $RFeAsO$ materials crystallize in the $P_{4/nmm}$ tetragonal space group resulting in a layered structure with $FeAs$ and RO layers [26] (see Figure 2.1 above. Shortly after the initial activity on the 1111 materials, superconductivity was also discovered in related materials possessing identical $FeAs$ layers with differing spacers.

The discovery of superconductivity with T_C of 38 K in $Ba_{1\ \_\ x}K\ xFe_2\ As_2$ [27] was of particular interest as it was quickly realized that large single crystals of these 122 materials could be grown (unlike the 1111 family).Structurally, at room temperature, the 122 materials exhibit the $ThCr_2Si_2$ crystal structure (space group $I_{4/mmm}$).As is clearly shown in figure 2.1 above, the $FeAs$ layers are very similar to the 1111 materials although neighboring layers along the c-axis have an inverted arsenic coordination. For both the 1111 [28] and 122 [29] materials, it was quickly realized that replacement of Fe with Co would also result in superconductivity, albeit with a reduced T_C when com- pared with doping between $FeAs$ planes. Such behavior is in contrast to that observed in the cuprates where disorder in the copper oxide plane was found to destroy superconductivity.

Superconductivity was also discovered in the 122 materials upon electron doping on the Fe site with Ni], Rh, Ir and Pd or by isoelectronic replacement of Fe with Ru. Interestingly, electron doping with Cu or hole doping with Cr does not yield superconductivity. The large number of potential dopants together with the availability of single crystal samples has made the 122 family of compounds the topic of considerable experimental focus. Superconductivity was also discovered in $LiFeAs$ [30–32] and $Na_{1-x}FeAs$ [33] (111 materials) sharing the same FeAs plane with Li or Na as the spacer as shown in figure 2.1 above. Transition temperatures of 18 K (for $LiFeAs$) and 12–25 K ($Na_{1-x}FeAs$) [33] have been observed dependent on the precise Na concentration. Interestingly, superconductivity seems to appear in the 111 materials in purely stoichiometric material without chemical doping. Finally, the Fe (Se,Te) family of compounds (11 materials) also exhibits superconductivity with a maximum transition temperature (under ambient pressure) of 15k.

Band structure calculations [35] suggested that $FeTe$ may have enhanced superconducting properties.However, pure $FeTe$ is not a superconductor [34] but is complicated by the presence of excess Fe, i.e.The actual chemical formula is $Fe_{1+y}Te$ [36]. It has been suggested that this excess Fe is magnetic and may act as a pair breaking moment destroying superconductivity [37]. Nonetheless, the doped material, $Fe_{1+y}Te_{1-x}Se_x$ does exhibit an enhanced T_C of 15 K with the maximum transition temperature observed for x near 0.5 [34]. The structures of the 1111, 122, 111, and 11 families of materials are shown in figure 2.1 above. The common feature is the presence of an identical $FeAs$ (or FeSe) plane. An interesting trend can be seen in figure 1–the larger the separation between layers, the higher the observed optimal transition temperature.

Two-dimensional (2D) magnetism occurs in the regions of highest T_c and, thus, may be favorable for superconductivity. This trend led to attempts at further separating the $FeAs$ layers and superconductivity with fairly high transition temperatures have been observed in Sr_2VO_3FeAs with a spacer of Sr_2VO_3 and T_C of 37.2 K [38], and doped $Sr_2Sc_{0.4}Ti_{0.6}FeAsO_3$ with a spacer of $Sr_2Sc_{0.4}Ti_{0.6}O_3$ and T_C onset of 45 K (although the resistivity does not reach zero until 7K [39].Although these temperatures still do not exceed the 56 K in the 1111 materials, they are quite high particularly in the case of Sr_2VO_3FeAs as this material is nominally stoichiometric. There is hope that doping of this

and related materials could lead to an increase in transition temperature. Shortly after the discovery of superconductivity in $LaFeAsO_{1-x}F_x$, alculations indicated that conventional electron–phonon coupling was insufficient to explain the high transition temperatures [40], as was later verified experimentally [41].As will be explained below, a ubiquitous magnetically ordered state is present indicating magnetism in close proximity to superconductivity leading one to naturally consider the interplay between magnetism and superconductivity in these materials. In the following section, we will review experimental studies of magnetism in the Fe- based compounds and its influence on superconductivity.

2.4 The main family of iron based superconductors

The family of Fe-based materials comprises over 50 different compounds, identified within just two years after the discovery of $LaFeAsO$ (T_c =26K) in 2008 [42]. Early on, four unique crystallographic structures were shown to support superconductivity. While their composition ranges from the simplest $\alpha - PbO$-type binary element structure to more complicated quaternary structures composed of elements [44].The most known families include; 1111, 122, 111, 11 families and their structure is presented on Figure: 2 [43].

I. 1111-type family

1111 compounds are made up of combination of elements, rare-earth (La, Sm, Gd etc.) transition metal. It comprises compounds with the same structure as $LaFeAsO$, and is the earliest versions of $FeSCs$. Due to their atoms composition ratios of the four elements, they are called the '1111-type'. Show their crystal structure, which is a $ZrCuSiAs$ type structure with a tetragonal $P_{4/nmm}$ space group. [45], this family includes $LaFePO$ and $LaFeAsO_{1-x}F_x$, and $LnFeAsO$ with various lanthanide elements (Ln), Up to now, the highest T_c~56K in1111family of iron-based superconductors has been achieved. The family consists of negatively charged FeP or $FeAs$ layers, where Fe atoms form a planar square lattice, and positively charged LnO layers. With or without doping, electrons are conducting in FeP or $FeAs$ layers [46].The first evidence for the importance of magnetism in the Fe-based superconductors was the concentration dependent phase diagram presented with the initial discovery of superconductivity in F doped $LaFeAsO$ [47]. It was soon shown that the undead $LaFeAsO$ parent compound exhibited spin-density wave (SDW) order below about 150 K [48, 49] .Unexpectedly, $LaFeAsO$ also exhibited a structural phase transition [48] at a temperature slightly above the magnetic

ordering temperature. There is clear competition between magnetism and superconductivity as the magnetically ordered state is destroyed in the fluorine doped, superconducting samples [48, 49].

In general, doping causes a suppression of both the structural and magnetic phase transitions and as these are suppressed, superconductivity emerges. The fundamental difference between materials with different rare earths comes in the behavior near the emergence of superconductivity. For $R = La$ and Pr, the structural and magnetic transitions vanish in an abrupt step-like manner as a function of doping at the onset of superconductivity [50, 51], for the case of $R = La$. For the case of $R = Ce$, the magnetic transition appears to vanish continuously to very low temperatures and superconductivity emerges at a concentration where this transition has been completely suppressed [52] .However, the structural transition has some range of concentrations where superconductivity coexists with this phase transition [52]. Finally, the case or $R = Sm$, looks similar to $R = Ce$ in that the transitions are suppressed gradually and there appears to be overlap between the structural transition and superconductivity [53]. However, unlike the case of Ce, the Sm phase diagram shows a region where magnetic ordering coexists with superconductivity [54]. This suggests that the destruction of long range magnetic order is not a necessary condition for the emergence of superconductivity.

II. 122- type family

The "122"materials have numerous doping possibilities. The family 122 has a formula AFe_2As_2 ($A = Ba, Ca, Sr$ and Eu) and compounds crystallized in the body centered tetragonal $ThCr_2Si_2$- type structure with I4/mmm space group symmetry. During cooling, $I_{4/mmm} \rightarrow F_{mmm}$ structural transformation takes place, coupled with a magnetic transition .Superconductivity is achieved through doping at A site and Fe site. An alkali metal substitute A and 3d, 4d and 5d transition metals substitute Fe [55]. As mentioned previously, the AFe_2As_2 family of materials has numerous doping possibilities. The basic behavior of the superconducting materials can be described by considering the phase diagrams for $Ba_{1-x}KxFe_2As_2$(hole doping between the $FeAs$ planes) and $BaFe_{2-x}CoxAs_2$ (electron doping within the FeAs plane). Both materials share the same $BaFe_2As_2$ parent compound. As in the case of the 1111 parent compounds, Ba-122 exhibits both a structural phase transition (in this case from the room temperature tetragonal $I_{4/mmm}$ space group to the low temperature orthorhombic

F_{mmm} space group [56, 57]) and the magnetic transition to a long range ordered, SDW state. However, unlike the 1111 materials, both the structural and magnetic phase transitions occur at the same temperature in the Ba-122 parent compound [56–58]. Doping with either K or Co causes a suppression of the structural and SDW transitions as in the 1111 materials. For Co doping, as x increases, the two transitions no longer appear at the same temperature with the structural transition occurring first in both cases, superconductivity emerges as the SDW order is suppressed. For K doping, the superconducting region starts for $x \sim 0.1$ and the maximum Tc of 38 K is reached for $x \sim 0.4$ [59, 60]. For $(Fe_{1-x}Cox)_2As_2$, superconductivity is first observed for $x \sim 0.03$ and the maximum T_C of 23 K is seen.

III. 111-type family

The simplest structures in FeAs based superconductor compared to 1111-type family. The formula $AFeAs$ (A=Li and Na, called 111 phase) and has a transition temperature of 23 K in $NaFeAs$, have the CeFeSi structural space group $P_{4/nmm}$ [61].

IV. 11 -Type family

The simplest structures among all known iron-based superconductors are 11 families. This 11-type consists of compounds with the $\alpha - PbO$-type of structure and highest T_c of 27K obtained in $FeSe$. It adopts a space group of P_4/nmm. As mentioned previously, these materials form with excess Fe with the largest amount of extra Fe observed near the Te rich side of the phase diagram. Initial measurements of the $Fe_{1+y}Te_{1-x}Sex$ [62] family of compounds showed superconductivity with T_C as high as 15 K for $x \sim 0.5$ existing for all values of x except very near $x = 0$ where superconductivity is destroyed. This suggests a different phase diagram from other Fe-based superconductors. However, single crystal specific heat measurements on the Te rich side of the phase diagram indicate bulk superconductivity only for concentrations near $x = 0.5$ [63]. With this in mind, the phase moment diagram was re–investigated and indicated magnetic order for small x which coexists with superconductivity over a range of concentrations [64] in a manner very similar to the doped 122 materials and $SmFeAsO_{1-x}Fx$. As mentioned previously, materials with low Se concentrations have a tendency to form with excess Fe.

Measurements of the phase diagram with samples intentionally grown with Fe_{11} [65] show an additional spin glass phase which coexists with superconductivity over much of the

measured concentration range. This shows the sensitivity of these materials to stoichiometry and, in particular, the amount of excess Fe present. Although, as discussed above, there are some differences in the concentration dependent phase diagrams of various Fe- based superconductors, inspection of phase diagrams for pnictides family shows that there are some common features. All materials exhibit a SDW state at low concentrations and this state is suppressed with doping allowing for the emergence of superconductivity. This shows strong similarity to the generic cuprates phase diagram and is evidence for the interplay of magnetism and superconductivity.

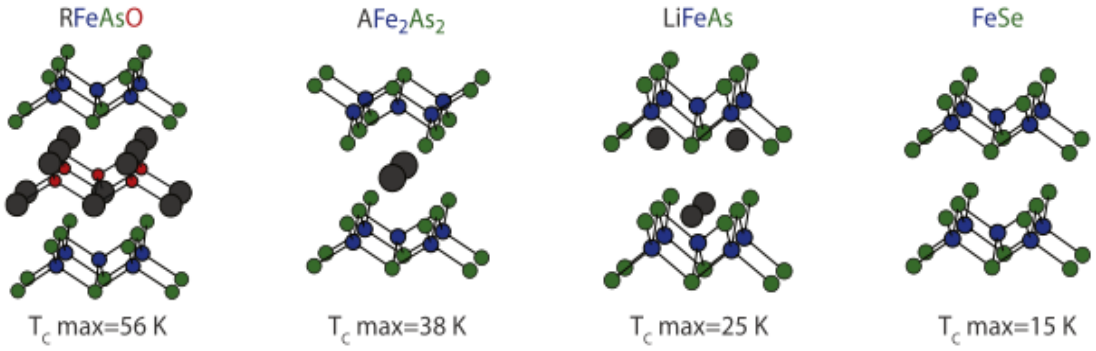

(a)1111 (b) 122 (c) 111 (d) 11

Figure 2.1: Several representative classes of the iron-based materials [34]

The structures of the 1111, 122, 111 and 11 families of materials are shown in Figure 2.1 above, the common feature is the presence of an identical $FeAs$ (or $FeSe$) plane. An interesting trend can be the larger the separation between layers, the higher the observed optimal transition temperature [66].

2.5 Barium iron arsenide ($BaFe_2As_2$)

$BaFe_2As_2$ is the parent compound of the iron -based superconductors belonging to "122" family i. e a member of the ternary iron arsenide family. It crystallizes in a tetragonal structure (space group I_4/mmm) and is built up by layers of edge-sharing $FeAs_{4/4}$ tetrahedral simply alternating with barium atoms. The synthesis of $BaFe_2\ As_2$ was already reported in 1980 but except for the crystal structure and some indeterminate magnetic data no physical properties were known. The magnetic nature of the structural phase transition in $BaFe_2As_2$ has been demonstrated by the Mossbauer spectra at low temperatures discussed above. With respect to the susceptibility data,

antiferromagnetic order was expected. Neutron diffraction experiments with polycrystalline $BaFe_2As_2$ by Huang *et al.* [67] clarified the complete spin structure, which is illustrated in Figure (2.2) $BaFe_2As_2$.

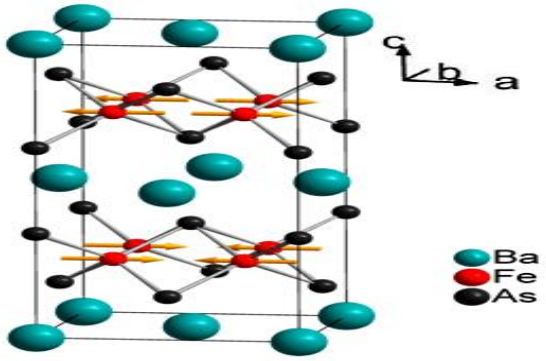

Figure 2.2: Crystal structure of $BaFe_2As_2$

The magnetic moment is 0.83 μB / Fe. [67] .The fundamental magnetic wave vector is q = 0, thus the magnetic moments are anti-parallel aligned to the longer orthorhombic *a*-axis and also antiferromagnetic ally along the *c*-axis. Along *b* (longer Fe–Fe distance in rectangular Fe nets) the moments form ferromagnetic chains. Thus, $BaFe_2As_2$ shows a stripe-type antiferromagnetic order at low temperatures. About the same time neutron diffraction experiments were carried out using single crystals of $BaFe_2\ As_2$ which were grown from a tin flux.[68] Due to approximately five percent tin incorporation, these specimens showed substantially different phase transition and magnetic ordering temperatures of about 90 K. The determined magnetic structure, however, agrees with the powder results of Huang *et al.*, [67] which show the magnetic transition at $T_N \approx 143$ K. Later, the experiments were conducted with tin-free crystals. [69] The results confirmed the spin structure again and proved that the tin incorporation affected the transition temperatures, but not the magnetic structure. The properties of the ternary iron arsenide $BaFe_2As_2$ with the $ThCr2Si2$-type structure have been proved to be remarkably similar to those of $LaFeAsO$, which is the first parent compound of the new class of high-*T*C superconductors. Both materials are poor metals at room temperature and undergo second-order structural and magnetic phase transitions. The Fe Mossbauer data of $BaFe_2As_2$ show hyperfine field splitting below 140 K, which hints at antiferromagnetic ordering.

Neutron diffraction experiments revealed the magnetic structure, which is largely the same as in $LaFeAsO.BaFe_2As_2$ differs most significantly from $LaFeAsO$ in the structural and magnetic phase transition temperatures. While the antiferromagnetic transition seemingly occurs at the same temperature as the structural transition in $BaFe_2As_2$, in all previously measured 1111-type compounds the structural and magnetic phase transitions are separated. Nevertheless, a broadening of the experimental line width in the 57Fe Mossbauer spectra of $BBaFe_2$ at 155 K hints already at short range or nematic order well above 140 K.Most likely, long-range antiferromagnetic ordering occurs right before the structural distortion emerges.

Magnetic fluctuations that lead to magnetic ordering are presumably the driving force for the structural phase transition. As a consequence, also the resistivity drops sharply at 140 K, because scattering of the conduction electrons due to magnetic fluctuations is strongly reduced and the electrical resistance is therefore decreasing. Thus, $BaFe_2As_2$ exhibits the same SDW anomaly at 140 K as $LaFeAsO$ at 150 K. Since the SDW instability is an important prerequisite for high-TC superconductivity in iron arsenide's, the results discussed above strongly suggest that $BaFe_2As_2$ can serve as a parent compound for another, oxygen-free class of iron arsenide superconductors with $ThCr_2Si_2$type structure. There is everything to suggest that superconductivity can be induced either by electron or hole doping. If the latter is the case it would conclusively prove that superconductivity originates from the $FeAs$ layers, regardless of the separating sheets.

2.6 Sodium doped $BaFe_2As_2$ ($Ba_{1-x}Na_xFe_2As_2$)

Hole doping of the 122 system is possible by substitution of an alkaline-earth ion site with an appropriate alkali ion (e.g. Na substitution of the Ba site).Due to Na doping in the Ba site of $BaFe_2As_2$ compound the high temperature anomaly is suppressed and then superconductivity occurs in $Ba_{0.6}Na_{0.4}Fe_2As_2$ compound .The magnetic and superconducting properties exhibited by the $Ba_{1-x}Na_xFe_2As_2$ system are quite similar to those of the homologous $Ba_{1-x}K_xFe_2As_2$ system; even though the large mismatch between the Ba^{2+} and Na^{+} ionic radii, no evidence for ordering was observed.

The structural and magnetic phase transitions are coincident and both 1st order. A first systematic study concluded that the tetragonal-to-orthorhombic transformation occurs during cooling up to $x = 0.35$, while for larger Na-content, the tetragonal I4/mmm is retained down to the lowest temperature [72]. Subsequently, a peculiar magnetic phase was detected in the compositional range

$0.22 \leq x \leq 0.28$ [73], where superconductivity coexists with spin density wave at low temperatures. More interestingly, these compositions were found to first undergo a tetragonal-to-orthorhombic structural transformation during cooling; in a second stage, as the temperature is further decreased, a spin re-orientation occurs and the orthorhombic phase becomes unstable. As a result, a 1st order transition takes place and the orthorhombic phase is partly transformed into the pristine tetragonal one; both phases display antiferromagnetic ordering and appear to be superconductive [71, 73]. The structure of the low-temperature tetragonal phase is stretched in the ab plane and compressed along the c-axis, whereas the magnetic structure of the orthorhombic phase does not qualitatively change across the transition [74]. The magnetic structure associated with the tetragonal phase is described by an antiferromagnetic stripe model with moments that are polarized along the c-axis [74].

The re-entrant magneto structural transitions characterizing this system were analyzed for both magnetically and orbit ally driven mechanisms, but at present, the underlying physical mechanism has not yet been unveiled [74].These results clearly indicate that magnetism competes with superconductivity; for this reason, it was first suggested that the sematic order is possibly of magnetic origin [73], but a subsequent analysis concluded that the structural transition has a purely electronic origin [74]. In any case, the occurrence of a magnetic phase associated with the tetragonal structure, localized only within a two-phase field, raises some concerns: it is in fact not clear why it is completely suppressed as the orthorhombic phase disappears. The strongly strained nature of the tetragonal 28 phase in the bi-phasic field likely plays a dominant role. We note that in the phase diagrams drawn in ref. [71, 73], the phase field pertaining to the so-called C4 phase is actually a biphasic field, in which the orthorhombic and tetragonal structures coexist [71, 73]. In this system, the two-phase field is likely very narrow above 50 K, but broadens as the temperature is further cooled. This gives rise to the rather unusually extended separation between the tetragonal and the orthorhombic phase fields at low temperatures, which is not observed in the other 122-type systems.

Another question concerns the homogenous variation of T_c with composition throughout the orthorhombic-to-tetragonal phase field. In fact, no net discontinuity is observed at the structural transition in all of the reported phase diagrams for 122- and 1111-type systems. This phenomenon becomes extraordinarily apparent in the $Ba_{1-x}Na_xFe_2As_2$ phase diagrams of ref. [71, 73], in which this homogenous variation crosses a relatively wide and peculiar two-phase field. the

reentrant structural transformation, remixing and the tetragonal magnetic phase were not confirmed by a new study based on neutron diffraction analyses of single-crystal samples [75]; in this case, the analytical results pointed to a spin reorientation along the c-axis in the orthorhombic magnetic phase, inducing structural changes in the orthorhombic crystalline structure itself. As a result, spin re-orientation appears as the characterizing feature of the low-temperature transition, whereas no evidence for a coexisting tetragonal phase was found [75].

Recently a wholly new magnetic phase with C_4-symmetry in the lattice was found to exist at the boundary between superconductivity and stripe magnetism in $Ba_{1-x}Na_xFe_2As_2$ by high resolution neutron diffraction experiments [76]. For several doping levels: $x = 0.22$, 0.26, 0.27 and 0.28 in the coexistence regime of anti-ferromagnetism (or spin density wave (SDW)) and superconductivity, an emergent C_4 symmetric SDW phase was found above the superconducting transition. This discovery has important implications for the origin of magnetic and structural transitions in iron-based superconductors. The results agree with the prediction of the spin-nematic models that a C_4 phase can become degenerate with the C_2 phase only at higher doping when hole and electron Fermi surfaces are not well nested, and that the stability of the C_4 phase would be limited to a very narrow region close to the suppression of anti-ferromagnetism.

For $x = 0.22$ this sample lies outside of the emergent C_4 phase in the phase diagram of $Ba_{1-x}Na_xFe_2As_2$ and we don't see any new phase transition in our data. However, our results confirm a T_c at 18K and a T_N at 98K, which agrees with results from neutron diffraction measurements and provides more accurate transition temperatures. It also gives us a general idea of the quality of the sample and how the AFM transition looks like in specific heat.

For $x = 0.26$ doping level, neutron diffraction results tell us that there would be 3 phase transitions: one AFM/SDW transition at ~80K, one re-entrant C_2 to C_4 symmetry structural transition at ~ 45K and one superconducting transition at ~25K. We performed specific heat measurement of this sample at a frequency of 34Hz (determined by a frequency scan at 40K) with a heating current of 120 μA from 20K to 105K.A weak anomaly can be seen at around 25K in the specific heat data which marks the superconducting transition at this doping level in the sample. In addition to this feature, another weak feature can be seen in specific heat at around T* = 45K which possibly signifies the reentrant C_2 to C_4 transition in the sample. Considering that the T_c for $x = 0.26$ sample is also higher (25K comparing to 18K), the results are consistent. However, we

have to emphasize again that the value is considerably smaller (~ a factor of 10) than that from measurements of a similar single crystal Sample $Ba_{0.77}\ K_{0.23}\ Fe_2\ As_2$with about the same T_c which can be attributed to the poor quality of the polycrystalline sample we have used. From the comparison of the results, we estimate that only ~10% of the sample is actually superconducting. Unfortunately, we are not able to distinguish another feature in the temperature region above T* that could possibly mark the AFM transition in the sample, which brings doubt to the nature of the feature at T*.

There are two possibilities: 1) T* marks the regular AFM (SDW) transition and there is not a reentrant C_4 symmetric SDW phase transition at this doping level; 2) T* indeed marks the new phase transition. However, due to certain reasons (e.g. sample quality), we cannot locate the regular AFM (SDW) transition. To further investigate and verify the phase transitions we found in specific heat, we also performed SQUID magnetization measurements on powder samples of $Ba_{0.74}Na_{0.26}Fe_2As_2$ from the same batch. In addition to the superconducting transition, which is manifested as a drop in the magnetization with a onset of 25K , we found that there is a kink in the M/T vs T curve at 45K for all three different applied magnetic fields (H=2kG, 1T and 2T) with either ZFC (Zero-field cooled) or FC (Field cooled) conditions. The transition temperatures agree with that from specific heat measurements. No evidence for another phase transition above 45K can be found, which also agrees with the specific heat measurement results. Thus the existence of the re-entrant C4 AFM (SDW) transition is not clear based on our experimental data.

For $x = 0.28$, two samples, sample 1 and sample 2, of $Ba_{1-x}Na_xFe_2As_2$ at doping level of $x = 0.28$ have also been measured. According to neutron diffraction data [5 8], this sample should have T_c in the range of 25 to 30K, T_r (reentrant C_4 symmetry SDW transition) in the range of 40 to 50K and T_N in the range of 65 to 75K. Our specific heat results show that the samples are actually multi-phased and doping level has variations from sample to sample, which again brought doubt to the interpretation of data from neutron diffraction measurements. The specific heat of sample 1 (size: 88μm x 78μm x 15μm) is measured from 20K to 80k. A step like anomaly is found strangely at around 34K. This contradicts the T_c value of ~26K as given for $x = 0.28$ doping level and in fact agrees more with the literature T_c Value for a $Ba_{1-x}Na_xFe_2As_2$ $x = 0.4$ single crystal sample at Debye temperature of θ_D= 297 K. For applied field along the crystalline c-axis considering that the sample we measured is polycrystalline and the alignment of the field could be off from c axis by quite a bit. The slightly higher value we got for the upper critical field slope is

quite reasonable. Because of the good agreement of our data with the literature data for $Ba_{0.6}Na_{0.4}Fe_2As_2$ we conclude that sample 1 actually has a doping level of 0.4, rather than 0.28. What this indicates is that the powdered $Ba_{1-x}Na_xFe_2As_2$ sample $(x = 0.28)$ we used in our measurements is not homogenous and some of them is actually optimum doped$(x = 0.4)$.

In an attempt to verify our conclusion, we measured the heat capacity of another sample (sample 2 from the same batch of powered polycrystals.Temperature dependence of the heat capacity of sample 2 of $Ba_{1-x}Na_xFe_2As_2$ $(x = 0.28)$ .Two small anomalies at 34K and 29.5K. The feature at 34K, as we have seen in sample 1, is the superconducting transition temperature for $Ba_{0.6}Na_{0.4}Fe_2As_2$ i.e., $x = 0.4$. The nature of the 29K feature was confirmed as another superconducting transition. This results, combined with the results from sample 1, confirmed that the sample we obtained were not homogeneous and thus not useful for identifying the reentrant C_4 symmetric SDW transition claimed by neutron diffraction measurements. The conclusion from our investigation of the emergent reentrant C_4 SDW phase transition in $Ba_{1-x}Na_xFe_2As_2$ is that there might be a reentrant C_4 phase in $Ba_{1-x}Na_xFe_2As_2$ at doping level of x=0.26. However, to make a firmer conclusion we would need to obtain a high quality single crystal for specific heat measurements. High quality samples for the whole range from x=0.24 to x=0.3 would be helpful for us to determine the exact phase boundaries of this emergent phase in the temperature-doping phase diagram.

Specific heat measurements indicates that substitution of Ba by Na leads to the suppression of SDW ordering and induces superconductivity up to 34 K for x = 0.4. The positive Hall coefficient of $Ba_{0.6}Na_{0.4}Fe_2As_2$ confirms that Na substitution results in hole doping similar to K doping in Ba1-xKxFe$_2$As$_2$. Angle-resolved photoemission spectroscopy measurements were carried out on freshly cleaved surfaces of $Ba_{1-x}Na_xFe_2As_2$samples with x=0.4. Exemplarily shows a typical photoemission intensity distribution at the Fermi level, a so-called Fermi surface map, of the $Ba_{1-x}Na_xFe_2As_2$ sample with x = 0.4. In general, the FS of all $Ba_{1-x}Na_xFe_2As_2$ samples consists of hole like sheets at the center of the Brillion zone and of a propeller like structure at the BZ corner (x point) with hole like propeller blades and small electron like FS sheets in the center. Thus, the FS of Na-substituted $BaFe_2As_2$is to a large extent the same as the FS found for K-substituted $BaFe_2As_2$ suggesting that the substitution of Ba by either Na or K affects the electronic band dispersion at the Fermi level in a verisimilar way. An energy-momentum cut, passing through

the point, reveals not only well-defined band dispersions for the inner and outer barrels, but also a superconducting gap with a larger magnitude for the inner barrels and with a smaller magnitude for the outer one. The analysis of the temperature dependence of the electronic spectrum of the sample with x=0.4 ($Tc = 34k$) for different locations in the momentum space allows us to conclude that the superconducting gap distribution is very close to the one observed for the optimally doped $Ba_{1-x}\ K_x\ \ Fe_2\ As_2$.

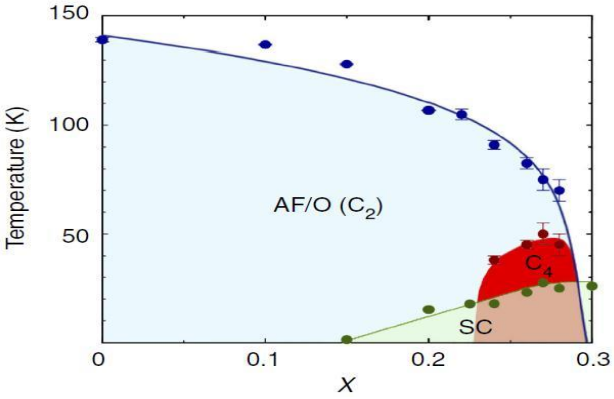

Figure 2.3: phase diagram of $Ba_{1-x}Na_xFe_2As_2$

From the above Figure blue points indicate coincident antiferromagnetic and Tetragonal to Orthorhombic structural transition temperatures, T_m. Red points indicate observed transition temperatures, T_r, into the C_4 phase, all measured by neutron diffraction. Green points indicate superconducting transition temperatures, T_C, determined from magnetization data [77].In an attempt to map out with more precision the transition temperatures of this new emergent C_4 symmetric magnetic phase, we performed heat capacity measurements of a samples of $Ba_{1-x}Na_xFe_2As_2$ at doping levels of x=0.4 antiferromagnetic order parameter (M),antiferromagnetic transition temperature (T_m), superconducting transition temperature (T_c), and superconducting order parameter (Δ) and we will plot the phase diagrams (T_c vs Δ) , (T_m vs M) and Tc vs M to study the competition between superconductivity and spin density wave in hole- doped barium iron arsenic superconductor.

2.5 Spin Density Wave (SDW)

The spin density wave state is a kind of AFM state with electronic spin density forming a static wave. It occurs at low temperature in anisotropic low dimensional material, low dimension materials or in metals that have high densities of states at the Fermi level N (Ef). Other low temperature ground states that occur in such materials are superconductivity. Also SDW couples to the spin, it indicates to the periodic modulation of spin density with a periodic (T) determined by the Fermi wave number. The density varies at right angle as the function of position with no net magnetization in the entire volume. In the normal state, the density $\rho\uparrow(r)$ of electron spins polarized vertically upward with respect to any quantization axis is completely deleted by $\rho\downarrow(r)$ of downward polarized spins. So the difference is finite and modulates in space as the function of the position vector in the SDW state .The SDW state such tendency of forming SDW ground state takes place when possesses nested pieces of Fermi surface together with intermediate coulomb correlation structure of alternating layers of Fe-As where Fe-As layers are thought to be responsible for superconductivity [79, 80]. The spin density wave transition arise when the spatial spin density modulation is due to delocalize or itinerant electrons rather than localize ones.

Coexistence of spin density wave (SDW) and superconductivity in multiple iron based materials have been reported [78].A development of spin density wave is accompanied by the slight distortion from the tetragonal to the orthorhombic unit cell. Therefore, one can present a model to study the coexistence of superconductivity and anti-ferromagnetic, that in corporate two competing physical processes involving electron hole AFM like of opposite spins with a net moment difference vector (Q) between the conjugates and electron electron(superconducting) pairing of opposite spins with total momentum zero. Iron arsenic layers are responsible for the generation of spin density wave [81].

Figure 2.4: Spin Density Waves (SDW)

CHAPTER THREE

3. Methodology

3.1 The green function formalism

The green's function techniques have been used in order to study the competition between superconductivity and magnetism in $Ba_{1-x}Na_xFe_2As_2$ superconductor. The term is used in physics especially in quantum field theory, electrodynamics and statistical field theory, to refer to various types of correlation functions, even those that do not fit the mathematical definition. The Green's function technique is one of the most powerful techniques suitable for solving strongly-correlated many body particle problems. These functions have been applied in quantum field theory (mean-field theory) to statistical problems. In quantum field theory, Green functions are known as propagator [82]. This name is based on the idea that, in order to find the important physical properties of a system. Green functions are essentially useful for summing over the restricted classes of perturbation theory diagrams and are very powerful when combined with spectral representations. The Green's function method is a very useful method in the theory of ordinary and partial differential equations, and all the physical quantities can be derived from the Green's functions.

There are different types of green's such as: one particle, two particle, zero-temperature, time-dependent or finite temperature, n-particle, advanced, retarded double-time temperature dependent, and non-equilibrium. The Double time temperature dependent Green's function equal to the change of the average value of some dynamic quantity by the time t and useful because they can be used to describe the effect of retarded interactions and all quantities of physical interest can be derived from them. To get the equation of motion in our thesis we use the retarded double time temperature dependent Green function. The definition of a retarded double-time Green's function propagators for any time dependent Heisenberg operators $\hat{A}(t)$ and $\hat{B}(t')$ expressed as;-

$$G^r_{A,B}(t, t') = \langle\langle\ \hat{A}_{(t),}\ \hat{B}_{(t')}\ \rangle\rangle = -i\theta(t-t')\langle\ \left[\hat{A}(t)\ \hat{B}(t')\right]\ \rangle \tag{3.1}$$

Hence $[\hat{A}(t),\ \hat{B}(t')] = \hat{A}(t)\hat{B}(t') - \hat{B}(t')\hat{A}(t)$,

where $\hat{A}$ and $\hat{B}$ are Heisenberg operators and θ(t-t‘) is the Heaviside step function, $\langle\langle$ -- $\rangle\rangle$ is denoted for Green function, $\langle$ --- $\rangle$ denotes thermal average and ‘r’ means retarded. $\hat{A}$ and $\hat{B}$ are follow commutation or anti commutation. That is;-

[A, B] = AB - BA = 0 commutation operator and

[A, B] = AB - BA $\neq$ 0 ant commutation operators (no commutation operators).

3.2 Equation of motion

To solve the many body particle problems the kinds of Green’s function formalism we applied have been the retarded double time temperature dependent Green’s function formalism of the kind that possess the Heaviside step function form. In order to obtain the equation of motion for the Green’s function, we differentiate equation (3.1) with respect to time;-

$$\frac{d}{dt}G_r(t\text{-}t') = \frac{d}{dt}\langle\langle\ \hat{A}(t),\ \hat{B}(t')\ \rangle\rangle$$

$$\frac{d}{dt}G_r(t\text{-}t') = -\frac{d}{dt}i\ \theta(t\text{-}t')\langle\ [\hat{A}(t)\hat{B}(t')]\ \rangle$$

$$\frac{d}{dt}G_r(t\text{-}t') = -i\frac{d}{dt}\theta(t\text{-}t)\ \langle\ [\hat{A}(t),\hat{B}(t')]\ \rangle\ - i\theta(t\text{-}t')<[\frac{d}{dt}\ \hat{A}(t)\ ,\hat{B}\ (t')]>$$

Multiplying both sides of the above equation by ‘i’ we can obtain;

$$-i\frac{d}{dt}G_r(t-t') = \frac{d}{dt}\theta(t-t')\ \langle\ [\hat{A}(t),\hat{B}(t')]\ \rangle + \theta(t-t('\langle\ [\frac{d}{dt}\ \hat{A}(t),\hat{B}(t')] \qquad (3.2)$$

From $\hbar\frac{d}{dt}\hat{A}(t) = [\hat{A}(t),\hat{H}],$ if $\hbar = 1$

By applying Dirac delta function, we can write equation (3.2)

$$i\frac{d}{dt}G_r(t\text{-}t') = \delta(t\text{-}t')\langle\ [\hat{A}(t)\hat{B}(t')]\ \rangle + \langle\langle\ [\hat{A}(t),\hat{H}]\hat{B}(t')\ \rangle\rangle$$

A careful analysis shows that the function depends on time t and t’ through (t-t’). Thus we can write

G (t, t′) =G (t, 0)

Let G (t, 0) be the Fourier transformation of G (t, 0)

$$\text{Then,} \quad G(t\text{-}0) = \int_{-\infty}^{\infty} G(\omega) exp^{(-i\omega(t-0)} d\omega G_{(t-0)}$$

$$= \int_{-\infty}^{\infty} G_{(t-0)}\, exp^{(-i\omega(t-0)} d \tag{3.3}$$

And δ the Dirac delta function can be defined as

$$\delta_{(t-0)} = \int_{-\infty}^{\infty} exp^{(-i\omega(t-0)}\, d\omega \tag{3.4}$$

Therefore equation (3.3) becomes

$$\omega G_{(\omega)} = <[\, \hat{A}_{(t)}; \hat{B}_{(0)}\,]> + \ll \left[\hat{A}_{(t)},\, \hat{H}\right] \tag{3.5}$$

The ωG (ω) can be written as

$$\omega \ll A, B \gg = <[\, A, B\,]> \; + \ll [\, A, H\,]; B \gg \tag{3.6}$$

$$\omega \ll A, B \gg = <[\, A, B\,]> + \ll [AH - HA\,]; B \gg \tag{3.7}$$

Since, $\ll A, B \gg$ denotes the Fourier transform of the Green functions involving the operator $\hat{A}$ and $\hat{B}$, now to get the equation of motion we apply Green's function techniques; Let us define: $\ll G^{\uparrow\uparrow}{}_{KK} \gg = \ll \hat{C}^{\dagger}{}_{K\uparrow} \hat{C}_{k\uparrow} \gg$

Hence, the equation of motion becomes

$$\omega G_{(\omega)} = <[\, \hat{A}_{(t)}; \hat{B}_{(0)}\,]> + \ll \left[\hat{A}_{(t)},\, \hat{H}\right]; \hat{B}_{(0)} \gg \tag{3.8}$$

$$\omega \ll \hat{C}^{\dagger}{}_{K\uparrow} \hat{C}_{k\uparrow} \gg = <\hat{C}^{\dagger}{}_{K\uparrow} \hat{C}_{k\uparrow} \gg + \ll [\hat{C}_{k\uparrow}, \mathrm{H}] \quad \hat{C}^{\dagger}{}_{K\uparrow} \gg$$

$$[\hat{A}, \hat{B}\hat{C}] = [\hat{A}, \hat{B}]\hat{C} + \hat{B}[\hat{A}, \hat{C}]$$

$$[\hat{A}\hat{B}, \hat{C}] = \hat{A}[\hat{B}\,, \hat{C}] + [\hat{A}, \hat{C}]\hat{B}$$

$$[\hat{A}\hat{B}, \hat{C}] = \hat{A}\{\hat{B}, \hat{C}\} - \{\hat{A}, \hat{C}\}\hat{B} \text{ And}$$

$[C_{k\sigma}, C^{\dagger}{}_{k'\sigma}] = \delta_{kk'}$=1 if $k = k'$, other wise 0

$$[C_{k\sigma}, C_{k\sigma}] = \quad [C^{\dagger}{}_{k\sigma}, C^{\dagger}{}_{k\sigma}$$

CHAPTER FOUR

4. Formulation of the problem

4.1 The model Hamiltonian

To study the competition between superconductivity and spin density wave in hole doped barium iron arsenide ($Ba_{1-x}Na_xFe_2As_2$) based on the multi band nature of iron based superconductor, two band model Hamiltonian was considered. The model Hamiltonian fore coexistence of SDW and superconducting in these compounds can be expressed as:-

$$\hat{H} = \hat{H}_0 + \hat{H}_1 + \hat{H}_2 + \hat{H}_3 \qquad (4.1)$$

Where $\hat{H}_0 = \sum_{k\sigma} \in_C \hat{C}^{\dagger}_{k\sigma} \hat{C}_{k\sigma}$ (4.2)

$$\hat{H}_1 = \sum_{k\sigma} \in_p p^{\dagger}_{k\sigma} p_{k\sigma} \qquad (4.3)$$

$$\hat{H}_2 = \sum_{k,k'} V^s_{(k,k')} \hat{C}^{\dagger}_{k\uparrow} \hat{C}^{\dagger}_{-k\downarrow} \hat{p}_{-k\downarrow} P_{k\uparrow +} \hat{p}^{\dagger}_{k\uparrow} \hat{p}^{\dagger}_{-k\downarrow} \hat{C}_{-k\downarrow} \hat{C}_{k\uparrow} \qquad (4.4)$$

$$\hat{H} = \sum_{k,k'} V^M_{(k,k')} \hat{C}^{\dagger}_{k\sigma} \hat{p}_{k\sigma} C \hat{p}^{\dagger}_{k\sigma} \qquad (4.5)$$

Substituting Equation (4.2), (4.3), (4.4) and (4.5) in to Equation (4.1) then we can get;-

$$\hat{H} = \sum_{k\sigma} \in_C \hat{C}^{\dagger}_{k\sigma} C + \sum_{k\sigma} \in_P p^{\dagger}_{k\sigma} p_{k\sigma} + \sum_{kk'} V^s_{kk'} (C^{\dagger}_{k\uparrow} \hat{C}^{\dagger}_{-k\downarrow} \hat{p}_{-k\downarrow} \hat{p}_{k\uparrow} + \hat{p}^{\dagger}_{k\uparrow} \hat{p}^{\dagger}_{-k\downarrow} C_{-k\downarrow} C_{k\uparrow})$$

$$+ \sum_{kk'\sigma} V^m_{kk\sigma} C^{\dagger}_{k\sigma} \hat{p}_{k\sigma} C_{k\sigma} \hat{p}^{\dagger}_{k\sigma} \qquad (4.6)$$

Where in this model Hamiltonian, the first term ($\hat{H}_0$)describes the itinerant electrons forming the hole Fermi pocket near the Fermi energy, the second term ($\hat{H}_1$) describes the itinerant electron forming the electron Fermi pocket near the Fermi energy. These electrons are responsible for the third term ($\hat{H}_2$) is superconducting interaction and the fourth term ($\hat{H}_3$) describes Magnetic interactions. $\in_C$And $\in_P$ is the dispersion near the two pockets independent of spin σ. And $V^s_{kk'}$ and $V^m_{kk'}$ the interaction potential for superconducting and magnetism respectively. Are the creation (annihilation n $\hat{C}^{\dagger}_{k\sigma}(\hat{C}_{k\sigma})$,$\hat{p}^{\dagger}_{k\sigma}(\hat{p}_{k\sigma})$n or destruction) operator of hole and electrons specified by the wave vector k and the spin σ.

4.2 Pure superconducting state for hole doping barium iron arsenide superconductors

Pure superconducting state means there is no magnetic order or on the other hand magnetic effect is zero.To proceed with this Hamiltonian we can make use of the equation of motion Fourier transformation which is:

$$\omega G^{r}_{A,B}(\omega) = < [\hat{A}, \hat{B}] > + \ll [\hat{A}, \hat{H}]; \hat{B} \gg \quad (4.2.1)$$

It is possible to take the advantage of the following relation as *definition*

$$G^{r}_{A,B}(t) = \ll \hat{A}, \hat{B} \gg = \ll \hat{C}_{k\uparrow}, \hat{c}^{\dagger}_{k\downarrow} \gg$$

Then, the equation of motion in Fourier transform from Equation (4.2.1) becomes

$$\omega G^{r}_{A,B}(\omega) = < [\hat{c}_{k\uparrow}, \hat{c}^{\dagger}_{k\downarrow}] > + \ll [\hat{c}_{k\uparrow}, \hat{H}]; \hat{c}_{k\uparrow} \quad (4.2.2)$$

The Equation (4.2.2) reproduces s a series of equations. The preferable method to solve it is using the part of Hamiltonian one by one in turn in the components of $[\hat{c}_{k\uparrow}, \hat{H}]$.First let as solve the kinetic energy of the hole component. In order to solve it we use the computation relation of three operators, and as given below for hole case.

[A, BC] = [A, B] C-B [A, C] for fermions

[A, BC] = [A, B] C+B [A, C] for bosons

$[\hat{c}_{k\uparrow}, \hat{c}_{k\uparrow}] = 0$

$[\hat{c}_{k\uparrow}, \hat{c}^{\dagger}_{k\uparrow}] = \delta_{kk}\delta\uparrow\uparrow = 1$

$[\hat{C}^{\dagger}_{k\uparrow}, \hat{C}^{\dagger}_{k\downarrow}] = 0$

Now let as evaluate $[\hat{c}_{k\uparrow}, \hat{H}]$

$$\hat{H} = \hat{H}_{O} + \hat{H}_{1} + \hat{H}_{2} + \hat{H}_{3} \quad (4.2.3)$$

$$[C_{k\uparrow}\hat{H}] = [C_{k\uparrow}, \hat{H}_{O} + \hat{H}_{1} + \hat{H}_{2} + \hat{H}_{3} \quad (4.2.4)$$

$$= [C_{k\uparrow}, \hat{H}_{O}] + [C\hat{H}_{1}] + [C_{k\uparrow}, \hat{H}_{2}] + [C\hat{H}_{3}]$$

Then now let us commute the first term

$$[C_{k\uparrow}, \hat{H}_O] = [C_{k\uparrow,} CC^{\dagger}{}_{k\sigma} C_{k\sigma}]$$

$$= \sum_{k\sigma} \in_{\sigma} \{[C, C^{\dagger}{}_{k\sigma} C]\}$$

$$= C\{[C,\ C^{\dagger}{}_{k\sigma} C_{k\sigma} - C_{k\sigma} C^{\dagger}{}_{k\sigma}]\}$$

$$= \sum_{k\sigma} \in_{C} (\ C_{k\uparrow})$$

$$= \in_{C} C_{k\uparrow} \tag{4.2.5}$$

$$[Cs_{k\uparrow,} \hat{H}_1] = 0 \tag{4.2.6}$$

The superconducting part

$$[C_{k\uparrow}, \hat{H}_2] = [C_{k\uparrow}, \sum_k V^s{}_k \hat{C}^{\dagger}{}_{k\uparrow} \hat{C}^{\dagger}{}_{-k\downarrow} \hat{p}_{-k\downarrow} \hat{p}_{k\uparrow} + \hat{p}^{\dagger}{}_{k\uparrow} \hat{p}^{\dagger}{}_{-k\downarrow} \hat{C}_{-k\downarrow} \hat{C}_{k\uparrow}]$$

$$= \sum_k V^s{}_{(k)} [C, C_{k\uparrow} \hat{C}^{\dagger}{}_{-k\downarrow} \hat{p}_{-k\downarrow} \hat{p}_{k\uparrow}]$$

$$= \sum_{k,} V^s{}_{(k)} \hat{p}_{-k\downarrow} \hat{p}_{k\uparrow} \{[C, C_{k\uparrow} \hat{C}^{\dagger}{}_{-k\downarrow}]\}$$

$$= \sum_{k,} V^s{}_{(k)} \hat{p}_{-k\downarrow} \hat{p}_{k\uparrow} \{\delta_{kk} \delta_{\uparrow\uparrow} \hat{C}^{\dagger}{}_{-k\downarrow}\}$$

where, $\sum_{k,} V^s{}_{(k)} < \hat{p}_{-k\downarrow} \hat{p}_{k\uparrow} > = \Delta_p$s

$$= \Delta_p C^{\dagger}{}_{-k\downarrow} \tag{4.2.7}$$

Substituting Equation (4.2.5), (4.2.6), (4.2.7) into Equation (4.2.3), we get

$$[C_{k\uparrow}, \hat{H}] = \in_C C + \Delta_p \hat{C}^{\dagger}{}_{-k\downarrow} \tag{4.2.8}$$

With Equation (4.2.8) and (4.2.4), the Equation of motion for Fourier transform G (ώ) of G(t, t′) becomes

$$\omega G_{(\omega)} = < CkC^{\dagger}{}_{k\downarrow} > + \ll \in_{k\uparrow} C_{k\downarrow} + \Delta_p \hat{C}^{\dagger}{}_{-k\downarrow} \gg \tag{4.2.9}$$

Δ_p – Represent the superconductor parameter.

$[C_{k\uparrow}, C^{\dagger}{}_{k\downarrow}] = 1$, $[C^{\dagger}{}_{k\uparrow}, C^{\dagger}{}_{k\downarrow}] = 0$ so, Equation (4.2.9) becomes:

$$\omega \ll C_{\ k\uparrow,} C^{\dagger}{}_{k\downarrow} \gg = < C_{k\uparrow,} C^{\dagger}{}_{k\downarrow} > + \in_C \ll C_{k\downarrow} C^{\dagger}{}_{k\downarrow} \gg$$

$$\omega \ll C_{k\uparrow,} C^{\dagger}{}_{k\downarrow} >> = \quad 1+\epsilon_C \ll C_{k\downarrow} C^{\dagger}{}_{k\downarrow} \gg \; + \; \Delta_p \ll \hat{C}^{\dagger}{}_{-k\downarrow} C^{\dagger}{}_{k\downarrow} \gg \tag{4.9}$$

$$[C^{\dagger}{}_{-k\uparrow,} \hat{H}] \quad = \quad [C^{\dagger}{}_{-k\uparrow,} \hat{H}o \; + \hat{H}_1 \; + \hat{H}_2 + \hat{H}_3 \,] \tag{4.11}$$

$$(\omega - \epsilon_C) \ll C_{k\downarrow}, C^{\dagger}{}_{k\downarrow} \gg = 1 + \; \Delta_p \ll \hat{C}^{\dagger}{}_{-k\downarrow} C^{\dagger}{}_{k\downarrow} \gg \tag{4.12}$$

Similarly, we can evaluate $\omega \ll C^{\dagger}{}_{-k\uparrow}, C^{\dagger}{}_{k\downarrow} \gg$

$$\omega \ll C^{\dagger}{}_{-k\uparrow}, C^{\dagger}{}_{k\downarrow} \gg = < [C^{\dagger}{}_{-k\uparrow}, C^{\dagger}{}_{k\downarrow}] > + \ll \left[C^{\dagger}{}_{-k\uparrow}, \hat{H}\right], C^{\dagger}{}_{k\downarrow} \; \gg \tag{4.13}$$

First evaluate $\left[C^{\dagger}{}_{-k\uparrow}, \hat{H}\right]$ $= [C^{\dagger}{}_{-k\uparrow,} \hat{H}o\,] + [C^{\dagger}{}_{-k\uparrow,} \hat{H}1\,] \quad + \left[C^{\dagger}{}_{-k\uparrow,} \hat{H}2\right] + [C^{\dagger}{}_{-k\uparrow,}, \hat{H}_3\,]$ (4.12)

Now let us do the first term we get

$$[C^{\dagger}{}_{-k\uparrow,} \hat{H}o\,] \; = [C^{\dagger}{}_{-k\uparrow,} \textstyle\sum_{k\sigma} \epsilon_k \, C^{\dagger}{}_{k\sigma} C_{k\sigma}]$$

$$= \textstyle\sum_{k\sigma} \epsilon_j [C^{\dagger}{}_{-k\uparrow,} C^{\dagger}{}_{k\sigma} C_{k\sigma}]$$

$$= - \textstyle\sum_{-k\uparrow} \epsilon_C \, C_{-k\uparrow} = -\epsilon_C \tag{4.14}$$

$$[C^{\dagger}{}_{-k\uparrow,} \hat{H}_1] = 0 \tag{4.15}$$

$$[C^{\dagger}{}_{-k\uparrow,} \hat{H}2\,] = [C^{\dagger}{}_{-k\uparrow,} \textstyle\sum_k V^s{}_k \, \hat{C}^{\dagger}{}_{k\uparrow} \hat{C}^{\dagger}{}_{-k\downarrow} \hat{p}_{-k\downarrow} \hat{p}_{k\uparrow} + \hat{p}^{\dagger}{}_{k\uparrow} \hat{p}^{\dagger}{}_{-k\downarrow} \hat{C}_{-k\downarrow} \hat{C}_{k\uparrow}]$$

$$= \textstyle\sum_k V^s{}_k \{\hat{p}^{\dagger}{}_{k\uparrow} \hat{p}^{\dagger}{}_{-k\downarrow} [C^{\dagger}{}_{-k\uparrow,} \hat{C}_{-k\downarrow} \hat{C}_{k\uparrow}]\}$$

Where, $\textstyle\sum_k V^s{}_k < \hat{p}^{\dagger}{}_{k\uparrow} \hat{p}^{\dagger}{}_{-k\downarrow} > \;\; = \Delta_p$ then,

$$= \Delta_p \hat{C}_{k\uparrow} \tag{4.116}$$

Now substituting Equation (4.14), (4.15), (4.16) in to (4.11we get

$$[C^{\dagger}{}_{-k\uparrow,} \hat{H}] = -\epsilon_C \; C + \; \Delta_p \hat{C}_{k\uparrow} \tag{4.17}$$

Substituting with Equation (4.17) in to Equation (4.13) the equation of motion for Fourier transform becomes

$$\omega \ll C^{\dagger}_{-k\uparrow}, C^{\dagger}_{k\downarrow} \gg = < [C^{\dagger}_{-k\uparrow} C^{\dagger}_{k\downarrow}] > + \ll \left[C^{\dagger}_{-k\uparrow,} \hat{H}\right], C^{\dagger}_{k\downarrow} \gg$$

$$\omega \ll C^{\dagger}_{-k\uparrow}, C^{\dagger}_{k\downarrow} \gg = -\epsilon_C \ll C_{-k\uparrow}, C^{\dagger}_{k\downarrow} \gg + \Delta_p \ll \hat{C}_{k\uparrow}, C^{\dagger}_{k\downarrow} \gg$$

$$(\omega + \epsilon_C) \ll C^{\dagger}_{-k\uparrow}, C^{\dagger}_{k\downarrow} \gg = \Delta_p \ll \hat{C}_{k\uparrow}, C^{\dagger}_{k\downarrow} \gg \quad (4.18)$$

The two equation of motion are from Equation (4.12) and (4.18)

$$(\omega - \epsilon_C) \ll C_{k\uparrow,} C^{\dagger}_{k\downarrow} \gg = 1 + \Delta_p \ll \hat{C}^{\dagger}_{-k\downarrow} C^{\dagger}_{k\downarrow} \gg \text{ and}$$

$$(\omega + \epsilon_C) \ll C^{\dagger}_{-k\uparrow}, C^{\dagger}_{k\downarrow} \gg = \Delta_p \ll \hat{C}_{k\uparrow}, C^{\dagger}_{k\downarrow}$$

Combine these Equation (4.12) and Equation (4.18) we will get this expression

$$\ll C_{k\uparrow,} C^{\dagger}_{k\downarrow} \gg = \frac{1}{\omega - \epsilon_C} (1 + \Delta_p \ll \hat{C}^{\dagger}_{-k\downarrow} C^{\dagger}_{k\downarrow} \gg)$$

$$\ll C^{\dagger}_{-k\uparrow}, C^{\dagger}_{k\downarrow} >> = \frac{1}{\omega + \epsilon_C} (\Delta_p \ll \hat{C}_{k\uparrow}, C^{\dagger}_{k\downarrow} \gg)$$

$$\ll \hat{C}^{\dagger}_{-k\downarrow}, C^{\dagger}_{k\uparrow} \gg = \frac{\Delta_p}{\omega^2 - \epsilon^2_{C-} \Delta_p{}^2} \quad (4.19)$$

We can follow similar way to find Δ_a from Equation (3.8) the equation of motion expressed as:

$$\omega G_{(\omega)} = < [p_{k\uparrow}, p^{\dagger}_{k\downarrow}] > + \ll [p_{k\uparrow}, H] ; p^{\dagger}_{k\uparrow} \gg \quad (4.19a)$$

$$[p_{k\uparrow,} \hat{H}] = [C_{k\uparrow}, \hat{H}o + \hat{H}_1 + \hat{H}_2] \quad (4.19b)$$

Now evaluate $[\, p_{k\uparrow}, H \,]$

$$[\, P_{k\uparrow,} \hat{H}_o \,] = [P_{k\uparrow,} \textstyle\sum_{k\sigma} \epsilon_a \hat{a}^{\dagger}_{k\sigma} \hat{a}_{k\sigma}] = 0 \quad (4.19c)$$

$$[p_{k\uparrow}, \hat{H}_1] = [\, p_{k\uparrow}, \textstyle\sum_{k\sigma} \epsilon_p \hat{p}^{\dagger}_{k\sigma} \hat{p}_{k\sigma}]$$

$$= \textstyle\sum_{k\sigma} \epsilon_p \; [p_{k\uparrow}, \hat{p}^{\dagger}_{k\sigma} \hat{p}_{k\sigma} - \hat{P}_{k\sigma} \hat{p}^{\dagger}_{k\sigma}]$$

$$= \textstyle\sum_{k\sigma} \epsilon_p \; \{p_{k\uparrow}\}$$

$$= \epsilon_p \, p_{k\uparrow} \quad (4.19d)$$

The superconducting term is similarly calculated

$$[\,p_{k\uparrow}\hat{H}_2\,] = [p_{k\uparrow}, \sum_{k,k'} V^s{}_{(k,k')}\,\hat{p}^\dagger{}_{k\uparrow}\,\hat{p}^\dagger{}_{-k\downarrow}\hat{p}_{-k\downarrow}\hat{p}_{k\uparrow} + \hat{p}^\dagger{}_{k\uparrow}\,\hat{p}^\dagger{}_{-k\downarrow}\hat{C}_{-k\downarrow}\hat{C}_{k\uparrow}]$$

$$= \sum_{k,k'} V^s{}_{(k,k')}\,([p_{k\uparrow}, \hat{p}^\dagger{}_{k\uparrow}]\hat{p}^\dagger{}_{-k\downarrow}\}\hat{C}_{-k\downarrow}\hat{C}_{k\uparrow})$$

Hence $\sum_{k,k'} V^s{}_{(k,k')} < \hat{C}_{-k\downarrow}\hat{C}_{k\uparrow} > \; = \; \Delta_C$

$$= \; \Delta_C \hat{p}^\dagger{}_{-k\downarrow} \qquad (4.19e)$$

Substituting, Equation (4.19c),(4.19d), (4.19e) then Equation (4.19b) become

$$[p_{k\uparrow,}\hat{H}] = \; \in_p \; p_{k\uparrow} + \quad \Delta_C \hat{p}^\dagger{}_{-k\downarrow} \qquad (4.19f)$$

Also substituting Equation (4.19f) in to Equation (4.19a) we get

$$\omega G_{(\omega)} \; = \; < \left[p_{k\uparrow}, p^\dagger{}_{k\downarrow}\right] > + \ll \in_p \; p_{k\uparrow} + \quad \Delta_C \hat{p}^\dagger{}_{-k\downarrow,} \quad p^\dagger{}_{k\uparrow} \gg$$

$$\omega \ll p_{k\uparrow}, p^\dagger{}_{k\downarrow} = 1 + \in_p \ll \; p_{k\uparrow} \quad p^\dagger{}_{k\uparrow} \gg + \; \Delta_C \ll \hat{p}^\dagger{}_{-k\downarrow,} \quad p^\dagger{}_{k\uparrow} \gg$$

$$(\,\omega - \in_p) \ll p_{k\uparrow}, p^\dagger{}_{k\downarrow} = 1 + \; \Delta_C \ll \hat{p}^\dagger{}_{-k\downarrow,} \quad p^\dagger{}_{k\uparrow} \gg \qquad (4.19g)$$

Now following similar way to find $\ll \hat{d}^\dagger{}_{-k\downarrow,} \quad d^\dagger{}_{k\uparrow} \gg$ from Equation (4.19g)

$$\ll \hat{p}^\dagger{}_{-k\downarrow,} \quad p^\dagger{}_{k\uparrow} \gg = < [\hat{p}^\dagger{}_{-k\downarrow,} \quad p^\dagger{}_{k\uparrow}\,] > + \left[\hat{p}^\dagger{}_{-k\downarrow,}, H\right], p^\dagger{}_{k\uparrow} \gg \qquad (4.20)$$

First we can evaluate

$$[\hat{p}^\dagger{}_{-k\downarrow}, \hat{H}] = [\hat{p}^\dagger{}_{-k\downarrow,} \hat{H}\,\mathrm{o} + \hat{H}1 + \hat{H}\,2] \qquad (4.20a)$$

$$[\hat{p}^\dagger{}_{-k\downarrow,} \hat{H}_o\,] \; = 0 \qquad (4.20b)$$

$$[\;\hat{p}^\dagger - k_\downarrow \; \hat{H}_1 = [\hat{p}^\dagger{}_{-k\downarrow,}, \sum_{k\sigma} \in_p \hat{p}^\dagger_{k\sigma}\hat{p}_{k\sigma}]$$

$$= \sum_{-k\uparrow} \in_p \hat{p}^\dagger_{-k\downarrow} \qquad (4.20c)$$

$$[\hat{p}^\dagger{}_{-k\downarrow,} \hat{H}_2\,] \; = [\hat{P}_{-k\downarrow,} \sum_{k,k'} V^s{}_{(k,k')}\,\hat{C}^\dagger{}_{k\uparrow}\,\hat{C}^\dagger{}_{-k\downarrow}\hat{p}_{-k\downarrow}\hat{p}_{k\uparrow} + \hat{p}^\dagger{}_{k\uparrow}\,\hat{p}^\dagger{}_{-k\downarrow}\hat{C}_{-k\downarrow}\hat{C}_{k\uparrow}]$$

$$= \; \sum_{k,k'} V^s{}_{(k,k')} \left\{[\hat{p}^\dagger{}_{-k\downarrow,}\hat{C}^\dagger{}_{k\uparrow}\,\hat{C}^\dagger{}_{-k\downarrow}\hat{p}_{-k\downarrow}\hat{p}_{k\uparrow}\right] + [\hat{p}^\dagger{}_{-k\downarrow,}\hat{p}^\dagger{}_{k\uparrow}\,\hat{p}^\dagger{}_{-k\downarrow}\hat{C}_{-k\downarrow}\hat{C}_{k\uparrow}]$$

$$= \; \sum_{k,k'} V^s{}_{(k,k')}\,C^\dagger{}_{k\uparrow}\hat{C}^\dagger{}_{-k\downarrow}[\hat{p}^\dagger{}_{-k\downarrow,}\hat{p}_{-k\downarrow}\hat{p}_{k\uparrow}\,]$$

where $\sum_{k,k'} V^{s}_{(k,k')} < \hat{C}^{\dagger}_{k\uparrow} \hat{C}^{\dagger}_{-k\downarrow} > = \Delta_C$

$$= \Delta_C [\hat{p}^{\dagger}_{-k\downarrow,} \hat{p}_{-k\downarrow} \hat{p}_{k\uparrow}]$$

$$= \Delta_C \hat{p}_{k\uparrow} \qquad (4.20d)$$

Then substituting Equation (4.20b), (4.20c), (4.20d) in to (4.20a)

$$[\hat{p}^{\dagger}_{-k\downarrow,} H] = \sum_{-k\uparrow} \in_p \hat{p}^{\dagger}_{-k\downarrow} + \Delta_C \hat{p}_{k\uparrow} \qquad (4.20e)$$

Inserting Equation (4.20.e) in to (4.20) then equation of motion becomes

$$\omega G_{(\omega)} = < \left[\hat{p}^{\dagger}_{-k\downarrow,} \; p^{\dagger}_{k\uparrow} \right] > = - \ll \in_p \hat{p}^{\dagger}_{-k\downarrow} + \Delta_C \hat{p}_{k\uparrow}, \; p^{\dagger}_{k\uparrow} \gg \qquad (4.20f)$$

$$\omega \ll \hat{p}^{\dagger}_{-k\downarrow,} p^{\dagger}_{k\uparrow} \gg = - \in_p \ll \hat{p}^{\dagger}_{-k\downarrow}, \; p^{\dagger}_{k\uparrow} \gg + \Delta_C \ll \hat{p}_{k\uparrow}, \; p^{\dagger}_{k\uparrow} \gg$$

$$\omega + \in_p \ll \hat{p}^{\dagger}_{-k\downarrow,} p^{\dagger}_{k\uparrow} \gg = \Delta_C \ll \hat{p}_{k\downarrow}, \; p^{\dagger}_{k\uparrow} \gg \qquad (4.20g)$$

Combining the equation of motion Equation (4.19g) and (4.20g) these are

$$\ll p_{k\uparrow}, p^{\dagger}_{k\downarrow} \gg = \frac{1}{\omega - \in_p} (1 + \Delta_C \ll \hat{p}^{\dagger}_{-k\downarrow,} \; p^{\dagger}_{k\uparrow} \gg$$

$$\ll \hat{p}^{\dagger}_{-k\downarrow}, p^{\dagger}_{k\uparrow} \gg = \frac{1}{\omega + \in_p} (\Delta_C \ll \hat{p}_{k\downarrow}, \; p^{\dagger}_{k\uparrow} \gg) \quad \text{then we get}$$

$$\ll \hat{p}^{\dagger}_{-k\downarrow}, p^{\dagger}_{k\uparrow} \gg = \frac{\Delta_C}{\omega^2 - \in^2_p - \Delta_C{}^2} \qquad (4.21)$$

From Equation (4.19) and (4.21) the two order parameter calculated as

$$\ll \hat{C}^{\dagger}_{-k\downarrow}, C^{\dagger}_{k\uparrow} \gg = \frac{\Delta_C}{\omega^2 - \in^2_C - \Delta_p{}^2}.$$

$$\ll \hat{p}^{\dagger}_{-k\downarrow,} \; p^{\dagger}_{k\uparrow} \gg = \frac{\Delta_C}{\omega^2 - \in^2_p - \Delta_C{}^2}$$

The superconducting order parameter is given by

$$\Delta_C = \frac{V}{\beta} \sum \ll C^{\dagger}_{-k\uparrow}, C^{\dagger}_{k\downarrow} \gg \qquad (4.22)$$

and

$$\Delta_p = \frac{V}{\beta}\sum \ll {p^\dagger}_{-k\downarrow}, {p^\dagger}_{k\uparrow} \tag{4.23}$$

First we can evaluate Equation (4.22)

$$\Delta_C = \frac{V}{\beta}\sum \ll {C^\dagger}_{-k\uparrow}, {C^\dagger}_{k\downarrow} \gg \tag{4.24}$$

$$\Delta_C = \frac{V}{\beta}\Sigma \frac{\Delta_p}{\omega^2 - {\epsilon^2}_{C-}\ {\Delta_p}^2} \tag{4.25}$$

And the summation may be changed into the integral by introducing density of state that defined as

$$\mathrm{N}(\in) = \frac{1}{V}\sum_n \to \frac{1}{(2\pi)^3}\int dk^3 = \int_{-\infty f}^{\infty} d \in N(\in).$$

The summation with respect to k and n extends over all allowed pair states. Therefore;

$$\Delta_C = \frac{V}{\beta}\sum_{k,n} \int_{-\in f}^{\infty} d \in N(\in)\frac{\Delta_p}{\omega^2 - {\epsilon^2}_{C-}\ \ {\Delta_p}^2} \tag{4.26}$$

The attractive interaction is effective in the region between $-\hbar\omega_b < \in < \hbar\omega_b$ and assuming the density of states does not vary over this integral then the expression becomes.

$$\Delta_C = \frac{2VN(\in)}{\beta}\sum \int_0^{\hbar\omega_b} d \in \frac{\Delta_p}{\omega^2 - {\epsilon^2}_{C-}\ \ {\Delta_p}^2} \tag{4.27}$$

ω in to $i\omega_n$ using Matsubara frequency $\omega_n = [(2n+1)\pi]/\beta$

By Squaring both sides $\omega^2 = \frac{(2n+1)^2\pi^2}{\beta^2}$

And replacing $\in^2 = {\epsilon_C}^2 - {\Delta_p}^2$

Then after substituting Equations (4.27) becomes

$$\Delta_C = \frac{2VN(\in)}{\beta}\sum \int_0^{\hbar\omega b} d \in \frac{\Delta_p}{\dfrac{(2n+1)^2\pi^2 +}{\beta^2}\in^2}$$

$$= \frac{2VN(\in)}{\beta}\sum \int_0^{\hbar\omega b} d \in \frac{\Delta_p}{(2n+1)^2\pi^2 + \beta^2\in^2} \tag{4.28}$$

Let define $x = \beta \in$ and

Using the relation $\sum_n \frac{1}{(2n+1)^2\pi^2+x^2} = \frac{\tanh(\frac{x}{2})}{2x} = \frac{1}{2x}tanh\frac{x}{2}$ where x = $\beta \in$

Then we can write the above equation as follows

$$\Delta_c = 2VN(0)\beta \int_0^{\hbar\omega b} d \in (\Delta_p)\frac{1}{2\beta}\tanh\frac{\beta\in}{2} \tag{4.29}$$

$$\text{Let } VN(0) = N_1V_1$$

$$\Delta_C = N_1V_1 \int_0^{\hbar\omega b} d \in (\Delta_p)\frac{1}{2\beta\in}\tanh\frac{\beta\in}{2} \tag{4.30}$$

Now using the same step from the above to find Δ_p

$$\Delta_p = \frac{V}{\beta}\sum \ll p^\dagger{}_{-k\downarrow}, p^\dagger{}_{k\uparrow} \gg$$

$$\text{Since } \ll p^\dagger{}_{-k\downarrow}, p^\dagger{}_{k\uparrow} \gg = \frac{\Delta_C}{\omega^2 - \in^2{}_p - \Delta_C{}^2}$$

$$\frac{V}{\beta}\sum \frac{\Delta_C}{\omega^2 - \in^2{}_p - \Delta_C{}^2} \tag{4.31}$$

And the sum may be changed into the integral by introducing density of state that defined as:

$$\text{N}(\in) = \frac{1}{V}\sum_n \to \frac{1}{(2\pi)^3}\int dk^3 = \int_{-\infty f}^{\infty} d \in N(\in).$$

The summation with respect to k and n extends over all allowed pair states.

Therefore;

$$\Delta_p = \frac{V}{\beta}\sum_{k,n} \int_{-\in f}^{\infty} d \in N(\in)\frac{\Delta_C}{\omega^2 - \in^2{}_p - \Delta_C{}^2}$$

$$= \frac{2VN(\in)}{\beta}\sum \int_0^{\hbar\omega b} d \in \frac{\Delta_C}{\omega^2 - \in^2{}_p - \Delta_C{}^2} \tag{4.26}$$

ω Changed in to $i\omega_n$, using Matsubara frequency

$$\omega_n = \frac{(2n+1)\pi}{\beta}$$

And

$$\omega^2 = \frac{(2n+1)^2\pi^2}{\beta^2}$$

Replacing $\in^2 = \in_p{}^2 - \Delta_C{}^2$

Then after substituting Equation (4.26) become

$$\Delta_p = \frac{2VN(\in)}{\beta}\sum\int_0^{\hbar\omega b} d\in \frac{\Delta_C}{\frac{(2n+1)^2\pi^2 +}{\beta^2}\in^2}$$

$$= \frac{2VN(\in)}{\beta}\sum\int_0^{\hbar\omega b} d\in \frac{\Delta_C}{(2n+1)^2\pi^2+\beta^2\in^2} \quad (4.27)$$

Let define $x = \beta\in$ and

Using the relation $\sum_n \frac{1}{(2n+1)^2\pi^2+x^2} = \frac{\tanh(\frac{x}{2})}{2x} = \frac{1}{2x}\tanh\frac{x}{2}$

Then we can write the above equation as follows

$$\Delta_p = 2VN(0)\beta\int_0^{\hbar\omega b} d\in(\Delta_C)\frac{1}{2\beta\in}\tanh\frac{\beta\in}{2} \quad (4.28)$$

Let $VN(0) = N_2V_2$ and $let \quad V_1 = V_2$

$$\Delta_p = N_2V_2\,\beta\int_0^{\hbar\omega b} d\in(\Delta_C)\frac{1}{\beta\in}\tanh\frac{\beta\in}{2} \quad (4.29)$$

Then from Equation (4.24) and (4.29) we get the two equations are

$$\Delta_C = N_1V_1\int_0^{\hbar\omega b} d\in(\Delta_p)\frac{1}{\beta\in}\tanh\frac{\beta\in}{2}$$

$$\Delta_p = N_2V_2\int_0^{\hbar\omega b} d\in(\Delta_C)\frac{1}{\beta\in}\tanh\frac{\beta\in}{2}$$

Then substitute the second Equation Δ_P in t the first one Δ_C

$$\Delta_C = N_1V_1\int_0^{\hbar\omega b} d\in(\Delta_p)\frac{1}{\beta\in}\tanh\frac{\beta\in}{2}$$

$$\Delta_C = N_1V_1\int_0^{\hbar\omega b} d\in N_2V_2\int_0^{\hbar\omega b} d\in(\Delta_C)\frac{1}{\beta\in}\tanh\frac{\beta\in}{2}\frac{1}{\beta E}\tanh\frac{\beta\in}{2} \quad (4.30)$$

$$N_1V_2\int_0^{\hbar\omega b} d\in\int_0^{\hbar\omega b} N_2V_2\, d\in\frac{1}{\beta\in}\tanh\frac{\beta\in}{2}\frac{1}{\beta\in}\tanh\frac{\beta\in}{2}=1 \tag{4.31}$$

Rearranging this Equation we get

$$N_2V^2\int_0^{\hbar\omega b} d\in\frac{1}{\beta\in}\tanh\frac{\beta\in}{2}\frac{1}{2\,\beta\in}\tanh\frac{\beta\in}{2}\ =1 \tag{4.32}$$

When the temperature approaches to the transition temperature the superconducting order parameter approach to zero and using integration by parts, we have

$$N_1N_2V^2\left[ln\left(\frac{\beta\hbar\omega b}{2}\right)^2-\int_0^{\infty} dx\frac{\ln(x)}{cosh^2(x)}\right]=1 \tag{4.33}$$

For low temperature

$$\tanh(\frac{\hbar\omega_b}{2k_BT})\rightarrow 1$$

$$=N_1N_2V^2\left[ln\left(\frac{\beta\hbar\omega b}{2}\right)^2-ln\left(\frac{\pi}{4e^{\gamma}}\right)\right]$$

$$2N_1N_2V^2\ ln\left(\frac{\beta\hbar\omega b}{2}\right)-ln\left(\frac{\pi}{4e^{\gamma}}\right)=1$$

$$\frac{1}{e^{2N_1N_2V^2}}=\left(\frac{\hbar\omega b}{2K_BT_C}\right)-ln\left(\frac{\pi}{4e^{\gamma}}\right) \tag{4.34}$$

$$=ln\left(\frac{2e^{\gamma}\beta\hbar\omega b}{\pi}\right)$$

$$\text{Let }\left(\frac{-1}{2N_1N_2V^2}\right)=\left(\frac{-1}{\lambda_1}\right)k_BT_c=1.13\hbar\omega_b exp\left(\frac{-1}{2N_1N_2V^2}\right)$$

After rearranging Equation (4.34) we get Where γ = 0.772156649 is the Euler Mascheronic constant. This Equation be solved to give:

$$K_BT_C=\frac{2e^{\gamma}}{\pi}\hbar\omega b\ exp\ (\frac{-1}{\lambda_1})\approx 1.13\ \hbar\omega b\ e^{\ \frac{-1}{\lambda_1}}$$

$$T_c=\frac{1.13\ \hbar\omega b}{K_B}e^{-\frac{1}{\lambda}} \tag{4.35}$$

4.3 Calculating Superconducting transition temperature with magnetic order parameter

To decuple the Hamiltonian we use mean filed approximation and thus the mean filed Hamiltonian of superconducting state is expressed as;

$$H_{Mf} = \hat{H}_1 + \hat{H}_2 + \hat{H}_3 + \hat{H}_4 + \hat{H}_5 \tag{4.3.1}$$

$$H_{Mf} = \sum_{K\sigma} \in_C (\mathrm{k})\, C^{\dagger}_{k\sigma} C_{\kappa\sigma} + \sum_{k\sigma} \in_p (\mathrm{k}) p^{\dagger}_{k\sigma} p_{k\sigma} + \sum_k \Delta_h (C^{\dagger}_{k\uparrow} C^{\dagger}_{-k\downarrow} + \mathrm{h.c}) + \sum_{k,} \Delta_e (\mathrm{k})\, (\hat{p}^{\dagger}_{k\uparrow} \hat{p}^{\dagger}_{-k\downarrow} + \mathrm{h.c})$$
$$+ \sum_{K\sigma} M(\, C^{\dagger}_{k\sigma} p_{k+q\sigma} + h.c) \tag{4.3.2}$$

The mean filed are

$$\Delta_h = \sum_k V^1{}_{(k)} < p^{\dagger}{}_{k\uparrow}, p^{\dagger}{}_{-k\downarrow} >$$

$$\Delta_e = \sum_k V^2{}_{(k)} < C^{\dagger}{}_{k\uparrow}, C^{\dagger}{}_{-k\downarrow} >$$

$$\Delta_m = \sum_k M_{(k)} < C^{\dagger}{}_{k\sigma}, p_{K+q\sigma} >$$

Where h.c is Herniation conjugate, q is magnetic wave vector and σ is the spin. In our present analysis to obtain $T_c and\ T_m$ we apply green formalism. Let as define the following:

$$G^{\uparrow\uparrow}_{K,K}{}' = \ll C_{k\uparrow}, C^{\dagger}{}_{k\uparrow} \gg \tag{4.2.3}$$

And writing Equation of motion as

$$\omega \ll C_{k\uparrow}, C^{\dagger}{}_{k\uparrow} \gg = < [C_{k\uparrow}, C^{\dagger}{}_{k\uparrow}] > \tag{4.2.4}$$

First let us calculate the commutation $[a_{k\uparrow}, H]$ using the Hamiltonian Equation (4.2.2) then, the equation of motion for $\ll C_{k\uparrow}, C^{\dagger}{}_{k\uparrow} \gg$ is given by

$$\omega \ll C_{k\uparrow}, C^{\dagger}{}_{k\uparrow} \gg = \delta_{kk'} + \ll [C_{k\uparrow}, H]\, ; C^{\dagger}{}_{k\uparrow} \gg \tag{4.2.5}$$

Using commutation relation, now let us eliminate $[C_{k\uparrow}, H]$ Therefore,

$$[C_{k\uparrow}, H] = \left[C_{k\uparrow}, \hat{H}_1 + \hat{H}_2 + \hat{H}_3 + \hat{H}_4 + \hat{H}_5\right] \tag{4.2.6}$$

$$[C_{k\uparrow}, \hat{H}_1] = [C_{k\uparrow}, \sum_{K\sigma} \in_C C^{\dagger}_{k\sigma} C_{\kappa\sigma}]$$

$$= \in_C C_{k\uparrow} \tag{4.2.7}$$

$$[C_{k\uparrow}, \hat{H}_2] = 0 \tag{4.2.8}$$

$$[C_{k\uparrow}, \hat{H}_3] = [C_{k\uparrow,} \sum_k \Delta_h (C^{\dagger}_{k\uparrow} C^{\dagger}_{-k\downarrow} + \text{h.c})]$$

$$= \sum_k \Delta_h [C_{k\uparrow,} C^{\dagger}_{k\uparrow} C]$$

$$= \sum_k \Delta_h \delta_{kK'} \delta_{\uparrow\uparrow} C^{\dagger}_{-k\downarrow}$$

$$= \Delta_h \tag{4.2.9}$$

$$[C_{k\uparrow}, \hat{H}_4] = 0 \tag{4.2.10}$$

$$[C_{k\uparrow}, \hat{H}_5] = [C_{k\uparrow,} \sum_{K\sigma} M(C^{\dagger}_{k\sigma} p_{k+q\sigma} + h.c)]$$

$$= \sum_{K\sigma} M [C_{k\uparrow,} C^{\dagger}_{k\sigma} p_{k+q\sigma}]$$

$$= \sum_{K\sigma} M \left[C_{k\uparrow,} C^{\dagger}_{k\sigma}\right] p_{k+q\sigma} - C^{\dagger}_{k\sigma} [C_{k\uparrow,} p_{k+q\sigma}]$$

$$= \sum_{K\sigma} M \left[C_{k\uparrow,} C^{\dagger}_{k\sigma}\right] p_{k+q\sigma}$$

$$= \sum_{K\sigma} M \delta_{kK'} \delta_{\sigma\sigma} p_{k+q\uparrow}$$

$$= M p_{k+} \tag{4.2.11}$$

After substation in general our equation of motion becomes;

$$\omega \ll C_{k\uparrow}, C^{\dagger}{}_{k\uparrow} \gg = 1 + \ll \in_C C_{k\uparrow} C^{\dagger}{}_{k\uparrow}, \gg + \ll \Delta_h C^{\dagger}_{-k\downarrow,} C^{\dagger}{}_{k\uparrow} \gg + \ll M p_{k+q\uparrow,} C^{\dagger}{}_{k\uparrow} \gg \tag{4.2.12}$$

$$\omega - \in_C \ll C_{k\uparrow}, C^{\dagger}{}_{k\uparrow} \gg = 1 + \Delta_h \ll C^{\dagger}_{-k\downarrow,} C^{\dagger}{}_{k\uparrow} \gg + M \ll p_{k+q\uparrow,} C^{\dagger}{}_{k\uparrow} \gg \tag{4.2.13}$$

Similarly the equation of motion of Greens function $\ll C^{\dagger}_{-k\downarrow,} C^{\dagger}{}_{k\uparrow} \gg$ can be obtained as before by evaluating the relevant commentators. Then the Equation of motion for $\ll C^{\dagger}_{-k\downarrow,} C^{\dagger}{}_{k\uparrow} \gg$ becomes;

$$\omega \ll C^{\dagger}_{-k\downarrow,} C^{\dagger}{}_{k\uparrow} \gg = \ll \left[C^{\dagger}_{-k\downarrow,} H\right] \tag{4.2.14}$$

Then solving for the commutation $\left[C^{\dagger}_{-k\downarrow,} H\right]$

$$\left[C^{\dagger}_{-k\downarrow,} H\right] = \left[C^{\dagger}_{-k\downarrow,} \hat{H}_1 + \hat{H}_2 + \hat{H}_3 + \hat{H}_4 + \hat{H}_5\right]$$

$$\left[C^{\dagger}_{-k\downarrow,} \hat{H}_1\right] = \left[C^{\dagger}_{-k\downarrow,} \sum_{K\sigma} \in_C C^{\dagger}_{k\sigma} C_{\kappa\sigma}\right]$$

$$= -\in_C C^{\dagger}_{-k\downarrow,} \tag{4.2.15}$$

$$\left[C^{\dagger}_{-k\downarrow,} \hat{H}_2 = 0\right.$$

$$\left[C^{\dagger}_{-k\downarrow,} \hat{H}_3\right] = \left[C^{\dagger}_{-k\downarrow,} \sum_k \Delta_h (C^{\dagger}_{k\uparrow} C^{\dagger}_{-k\downarrow} + \text{h.c})\right] \quad , \text{h.c} = C_{k\uparrow} C_{-k\downarrow}$$

$$= \sum_k \Delta_h - C_{k\uparrow} \left[C^{\dagger}_{-k\downarrow,} C_{-k\downarrow}\right]$$

$$= -\Delta_h C_{k\uparrow}$$

$$\left[C^{\dagger}_{-k\downarrow,} \hat{H}_4\right] = 0 \tag{4.2.16}$$

$$\left[C^{\dagger}_{-k\downarrow,} \hat{H}_5\right] = C \sum_{K\sigma} M(C^{\dagger}_{k\sigma} p_{k+q\sigma} + h.c)]$$

$$= \sum_{K\sigma} M \left[C^{\dagger}_{-k\downarrow,} C^{\dagger}_{k\sigma} p_{k+q\sigma} + h.c)\right] \ , h.c = p_{-(k+q\sigma)} C_{-k\sigma}$$

$$= \sum_{K\sigma} M \left[C^{\dagger}_{-k\downarrow,} C^{\dagger}_{k\sigma} p_{k+q\sigma} + p_{-(k+q\sigma)} C_{-k\sigma}\right]$$

$$= \sum_{K\sigma} M([C^{\dagger}_{-k\downarrow,} C^{\dagger}_{k\sigma} p_{k+q\sigma}] +, [C^{\dagger}_{-k\downarrow,} p_{-(k+q\sigma)} C_{-k\sigma}])$$

$$= \sum_{K\sigma} M \left[C^{\dagger}_{-k\downarrow,} p_{-k+q\sigma} C_{-k\sigma}\right])$$

$$= \sum_{K\sigma} M C p_{-k+q\sigma}] C_{-k\sigma} - p_{-(k+q\sigma)} \left[C^{\dagger}_{-k\downarrow,} C_{-k\sigma}\right]$$

$$= -\sum_{K\sigma} M p_{-k+q\sigma} \left[C^{\dagger}_{-k\downarrow,} C_{-k\sigma}\right]$$

$$= -Mp_{-k-q\downarrow} \tag{4.2.17}$$

After substation in general our equation of motion becomes;

$$\omega \ll C C^{\dagger}_{k\uparrow} \gg = \ll \left(-\in_C C - \Delta_h C_{k\uparrow} - M p_{-k-q\downarrow}\right), C^{\dagger}_{k\uparrow} \tag{2.18}$$

$$\omega + \in_C \ll C^{\dagger}_{-k\downarrow,} C^{\dagger}_{k\uparrow} \gg = -\Delta_h \ll C_{k\uparrow}; C^{\dagger}_{k\uparrow} \gg -M \ll p_{-k-q\downarrow} , C^{\dagger}_{k\uparrow} \tag{4.2.19}$$

Similarly the equation of motion of Green's function $\ll p_{k+q\uparrow,}\ C^{\dagger}{}_{k\uparrow} \gg$ can be obtained as before by evaluating the relevant commentators'. Writing the Equation of motion,

$$\omega \ll p_{k+q\uparrow,}\ C^{\dagger}{}_{k\uparrow} \gg = < \left[p_{k+q\uparrow,}\ C^{\dagger}{}_{k\uparrow}\right] > = \ll \left[p_{k+q\uparrow,H}\ \right], C^{\dagger}{}_{k\uparrow} \gg \tag{4.2.20}$$

$$\omega \ll p_{k+q\uparrow,}\ C^{\dagger}{}_{k\uparrow} \gg = \delta_{k+q,k'} + \ll \left[p_{k+q\uparrow,H}\ \right], C^{\dagger}{}_{k\uparrow} \gg \tag{4.2.21}$$

valuating the commutation $[p_{k+q\uparrow,H}\ ]$ using the Hamiltonian in Equation (4.2.2)

$$[p_{k+q\uparrow,}\hat{H}\ = [p_{k+q\uparrow,}\ \hat{H}_1\ + \hat{H}_2\ + \hat{H}_3 + \hat{H}_4\ + \hat{H}_5]$$

$$\left[p_{k+q\uparrow,}\ \hat{H}_1\right] = 0 \tag{4.2.22}$$

$$\left[p_{k+q\uparrow,}\ \hat{H}_2\right] = [p_{k+q\uparrow,}\ \sum_{k\sigma} \in_p p^{\dagger}_{k\sigma} p_{k\sigma}]$$

$$= \sum_{k\sigma} \in_p [p_{k+q\uparrow,}\ p^{\dagger}_{k\sigma} p_{k\sigma}]$$

$$= \sum_{k\sigma} \in_p p_{k+q\uparrow}$$

$$= \in_p p_{k+q\uparrow} \tag{4.2.23}$$

$$\left[p_{k+q\uparrow,}\ \hat{H}_3\right] = 0 \tag{4.2.24}$$

$$\left[p_{k+q\uparrow,}\ \hat{H}_4\right] = [p_{k+q\uparrow,}\ \sum_{k'} \Delta_e\ (\hat{p}^{\dagger}_{k\uparrow} \hat{p}^{\dagger}_{-k\downarrow} + \text{h.c})]$$

$$= \sum_{k'} \Delta_e\ [p_{k+q\uparrow,}\ \hat{p}^{\dagger}_{k\uparrow} \hat{p}^{\dagger}_{-k\downarrow}]$$

$$= \sum_{k'} \Delta_e\ [p_{k+q\uparrow,}\ \hat{p}^{\dagger}_{k\uparrow}] \hat{p}^{\dagger}_{-k\downarrow} - \hat{p}^{\dagger}_{k\uparrow} [p_{k+q\uparrow,}\ \hat{p}^{\dagger}_{-k\downarrow}]$$

$$= \sum_{k'} \Delta_e\ [p_{k+q\uparrow,}\ \hat{p}^{\dagger}_{k\uparrow}] \hat{p}^{\dagger}_{-k\downarrow}$$

$$= \Delta_e \hat{p}^{\dagger}_{-(k+q)\downarrow} \tag{4.2.25}$$

$$\left[p_{k+q\uparrow,}\ \hat{H}_5\right] = [p_{k+q\uparrow,}\ \sum_{K\sigma} M(\ C^{\dagger}_{k\sigma} p_{k+q\sigma}\ + h.c)] \quad , h.c = \hat{p}^{\dagger}_{-(k+q)\sigma} + C_{-k\sigma}$$

$$= \sum_{K\sigma} M\ [p_{k+q\uparrow,}\ \ C^{\dagger}_{k\sigma} p_{k+q\sigma}\ ] + [p_{k+q\uparrow,}\ , \hat{p}^{\dagger}_{-(k+q)\sigma} + p_{-k\sigma}\ ]$$

$$= \sum_{K\sigma} M\ [p_{k+q\uparrow,}\ , \hat{p}^{\dagger}_{-(k+q)\sigma} + C_{-k\sigma}\ ]$$

$$= \sum_{K\sigma} M\,[p_{k+q\uparrow},\ \hat{p}^{\dagger}_{-(k+q)\sigma}]C_{-k\sigma}\ - \hat{p}^{\dagger}_{-(k+q)\sigma}[p_{k+q\uparrow},\ C_{-k\sigma}\ ]$$

$$= \sum_{K\sigma} M\,[p_{k+q\uparrow},\ \hat{p}^{\dagger}_{-(k+q)\sigma}]p_{-k\sigma}$$

$$= MC_{k\uparrow} \qquad 2.26)$$

After substation

$$[p_{k+q\uparrow,}\,\hat{H}\,] = \ll \in_p p_{k+q\uparrow}\ + \Delta_e \hat{p}^{\dagger}_{-(k+q)\downarrow} + \ MC_{k\uparrow} \qquad (4.2.2)$$

Then our equation of motion become

$$\omega \ll p_{k+q\uparrow,}\ C^{\dagger}{}_{k\uparrow} \gg = \delta_{k+q,k'} + \in_p \ll p_{k+q\uparrow,}\ C^{\dagger}{}_{k\uparrow} \gg + \Delta_e \ll \hat{p}^{\dagger}_{-(k+q)\downarrow}, C^{\dagger}{}_{k\uparrow} \gg + MC_{k\uparrow\,,C^{\dagger}{}_{k\uparrow}} \gg$$

$$\omega - \in_p \ll p_{k+q\uparrow,}\ C^{\dagger}{}_{k\uparrow} \gg = \delta_{k+q,k'} + \Delta_e \ll \hat{p}^{\dagger}_{-(k+q)\downarrow}, C^{\dagger}{}_{k\uparrow} \gg + MC_{k\uparrow\,,C^{\dagger}{}_{k\uparrow}} \gg \qquad (4.2.28)$$

Similarly the Equation of motion of Green's function$\ll p_{-(k+q)\downarrow,}\ C^{\dagger}{}_{k\uparrow} \gg$ can be obtained as above Equation (4.2.28) by evaluating the relevant commentators. Writing the equation of motion,

$$\omega \ll \hat{p}^{\dagger}_{-(k+q)\downarrow}, C^{\dagger}{}_{k\uparrow} \gg\ = < \left[\hat{p}^{\dagger}_{-(k+q)\downarrow}, C^{\dagger}{}_{k\uparrow}\right] > + \ll \left[\hat{p}^{\dagger}_{-(k+q)\downarrow}, C^{\dagger}{}_{k\uparrow}\right], C^{\dagger}{}_{k\uparrow} \gg$$

$$\omega \ll \hat{p}^{\dagger}_{-(k+q)\downarrow}, C^{\dagger}{}_{k\uparrow} \gg\ = \ll \left[\hat{p}^{\dagger}_{-(k+q)\downarrow}, \hat{H}\,\right], p^{\dagger}{}_{k\uparrow} \qquad (4.2.29)$$

Evaluating the commutation $[p_{-(k+q)\downarrow,}\,\hat{H}\,]$ using the Hamiltonian Equation (4.2.2)

$$\widehat{[p}^{\dagger}_{-(k+q)\downarrow},\,\hat{H}\,] = [p_{-(k+q)\downarrow,}\hat{H}_1\ + \hat{H}_2\ + \hat{H}_3 + \hat{H}_4\ + \hat{H}_5]$$

$$\widehat{[p}^{\dagger}_{-(k+q)\downarrow}, \hat{H}_1] = 0 \qquad (4.2.30)$$

$$\widehat{[p}^{\dagger}_{-(k+q)\downarrow}, \hat{H}_2\ = \ [\hat{p}^{\dagger}_{-(k+q)\downarrow}, \sum_{k\sigma} \in_p p^{\dagger}_{k\sigma} p_{k\sigma}]$$

$$= \sum_{k\sigma} \in_p [\hat{p}^{\dagger}_{-(k+q)\downarrow}, p^{\dagger}_{k\sigma} p_{k\sigma}]$$

$$= -\sum_{k\sigma} \in_p p^{\dagger}_{-(k+q)\downarrow}$$

$$= -\in_p p^{\dagger}_{-(k+q)\downarrow} \qquad (4.2.31)$$

$$\left[\hat{p}^{\dagger}_{-(k+q)\downarrow}, \hat{H}_3\right] = 0 \tag{4.2.32}$$

$$\left[\hat{p}^{\dagger}_{-(k+q)\downarrow}, \hat{H}_4\right] = \widehat{[p}^{\dagger}_{-(k+q)\downarrow},\ \sum_{k'} \Delta_e \left(\hat{p}^{\dagger}_{k\uparrow}\hat{p}^{\dagger}_{-k\downarrow} + \text{h.c}\right)] \quad , \text{h.c} = p_{k\uparrow}p_{-k\downarrow}$$

$$= \sum_{k'} \Delta_e \left[\hat{p}^{\dagger}_{-(k+q)\downarrow}, \hat{p}^{\dagger}_{k\uparrow}\hat{p}^{\dagger}_{-k\downarrow}\right] + \left[\hat{p}^{\dagger}_{-(k+q)\downarrow}, p_{k\uparrow}p_{-k\downarrow}\right]$$

$$= \sum_{k'} \Delta_e \left[\hat{p}^{\dagger}_{-(k+q)\downarrow}, p_{k\uparrow}p_{-k\downarrow}\right]$$

$$= \sum_{k'} \Delta_e \left[\hat{p}^{\dagger}_{-(k+q)\downarrow}, p_{k\uparrow}\right]p_{-k\downarrow} - p_{k\uparrow}\left[\hat{p}^{\dagger}_{-(k+q)\downarrow}p_{-k\downarrow}\right]$$

$$= -\sum_{k'} \Delta_e\, p_{k\uparrow}\left[\hat{p}^{\dagger}_{-(k+q)\downarrow}, p_{-k\downarrow}\right]$$

$$= -\Delta_e p_{k+q\uparrow} \tag{4.2.33}$$

$$\left[\hat{p}^{\dagger}_{-(k+q)\downarrow}, \hat{H}_5\right] = \left[\hat{p}^{\dagger}_{-(k+q)\downarrow}, \sum_{K\sigma} M\left(C^{\dagger}_{k\sigma}p_{k+q\sigma} + h.c\right)\right]$$

$$= \sum_{K\sigma} M\left[\hat{p}^{\dagger}_{-(k+q)\downarrow},\ C^{\dagger}_{k\sigma}p_{k+q\sigma}\right]$$

$$= \sum_{K\sigma} M\left[\hat{p}^{\dagger}_{-(k+q)\downarrow},\ C^{\dagger}_{k\sigma}\right]p_{k+q\sigma} - C^{\dagger}_{k\sigma}\left[\hat{p}^{\dagger}_{-(k+q)\downarrow}, p_{k+q\sigma}\right]$$

$$= -\sum_{K\sigma} M\, C^{\dagger}_{k\sigma}\left[\hat{p}^{\dagger}_{-(k+q)\downarrow}, C_{k+q\sigma}\right]$$

$$= -MC^{\dagger}_{-k\downarrow} \tag{4.2.34}$$

After substation of Equation (4.2.31), (4.2.33), (4.2.34)

$$\left[\hat{p}^{\dagger}_{-(k+q)\downarrow}, \hat{\mathrm{H}}\right] = \ll -\epsilon_p\, p^{\dagger}_{-(k+q)\downarrow} - \Delta_e p_{k+q\uparrow} - MC^{\dagger}_{-k\downarrow} \tag{4.2.35}$$

Then our Equation of motion become

$$\omega \ll \hat{p}^{\dagger}_{-(k+q)\downarrow}, C^{\dagger}{}_{k\uparrow} \gg = \ll \left(-\epsilon_p\, p^{\dagger}_{-(k+q)\downarrow} - \Delta_e p_{k+q\uparrow} - MC^{\dagger}_{-k\downarrow}\right), C^{\dagger}{}_{k\uparrow} \gg$$

$$\omega + \epsilon_p \ll \hat{p}^{\dagger}_{-(k+q)\downarrow}, C^{\dagger}{}_{k\uparrow} \gg = -\Delta_e \ll p_{k+q\uparrow}, C^{\dagger}{}_{k\uparrow} \gg - M \ll C^{\dagger}_{-k\downarrow}, C^{\dagger}{}_{k\uparrow} \gg \tag{4.2.36}$$

We have assumed that

$\omega - \epsilon_C = \omega - \epsilon_k$, $\omega + \epsilon_C = \omega + \epsilon_{-k}$ and $\Delta_{e=}\Delta$, $\Delta_h = \Delta$, $\frac{\omega - \epsilon_k}{\omega + \epsilon_k} \cong 1$, $\delta_{k,k'=1}$

$$\delta_{k+q,k'=0} \text{ If } k = k'$$

After rearranging the equation becomes: Generally we have four coupled equations of motion, they are;

$$\ll C_{k\uparrow}, C^{\dagger}{}_{k\uparrow} \gg = \frac{1}{\omega - \epsilon_k}(1 - \Delta \ll C^{\dagger}_{-k\downarrow}, C^{\dagger}{}_{k\uparrow} \gg + M \ll p_{k+q\downarrow}, C^{\dagger}{}_{k\uparrow} \gg \quad (4.3.1)$$

$$\ll CC^{\dagger}{}_{k\uparrow} = \frac{1}{\omega + \epsilon_{-k}}\left(\Delta \ll C_{k\uparrow}; C^{\dagger}{}_{k\uparrow} \gg - M \ll p_{-k-q\downarrow}, C^{\dagger}{}_{k\uparrow} \gg\right) \quad (4.3.2)$$

$$\ll p_{k+q\downarrow}, C^{\dagger}{}_{k\uparrow} \gg = \frac{1}{\omega - \epsilon_{k+q}} \Delta \ll \hat{p}^{\dagger}_{-(k+q)\downarrow}, C^{\dagger}{}_{k\uparrow} \gg + M \ll C_{k\uparrow, C^{\dagger}{}_{k\uparrow}} \gg) \quad (4.3.3)$$

$$\ll \hat{p}^{\dagger}_{-(k+q)\downarrow}, C^{\dagger}{}_{k\uparrow} \gg = \frac{1}{\omega + \epsilon_{-k-q}} (\Delta \ll p_{k+q\downarrow}, C^{\dagger}{}_{k\uparrow} \gg - M \ll C^{\dagger}_{-k\downarrow}, C^{\dagger}{}_{k\uparrow} \gg \quad (4.3.4)$$

Substituting Equation (4.3.4) and (4.3.1) in to (4.3.2), yields

$$(\omega + \epsilon_{-k}) \ll C^{\dagger}_{-k\downarrow}, C^{\dagger}{}_{k\uparrow} \gg = \frac{-\Delta}{\omega + \epsilon_k}(1 - \Delta \ll C^{\dagger}_{-k\downarrow}, C^{\dagger}{}_{k\uparrow} \gg + M \ll p_{k+q\downarrow}, C^{\dagger}{}_{k\uparrow} \gg)$$

$$= -\frac{M}{\omega + \epsilon_{-k-q}}(\Delta \ll p_{k+q\downarrow}, C^{\dagger}{}_{k\uparrow} \gg - M \ll C^{\dagger}_{-k\downarrow}, C^{\dagger}{}_{k\uparrow} \gg)$$

$$\frac{\Delta}{\omega - \epsilon_k} = \left[\frac{\Delta 2}{\omega - \epsilon_k} + \frac{M^2}{\omega + \epsilon_{-k-q}} - (\omega + \epsilon_{-k})\right] \ll C^{\dagger}_{-k\downarrow}, C^{\dagger}{}_{k\uparrow} \gg$$

$$= \Delta M \left[\frac{1}{\omega - \epsilon_k} + \frac{1}{\omega + \epsilon_{-k-q}}\right] \ll C^{\dagger}_{-k\downarrow}, C^{\dagger}{}_{k\uparrow} \quad (4.3.5)$$

Similarly substituting Equation (4.3.1) and (4.3.4) in to (4.3.3), yields;

$$(\omega - \epsilon_{k+q}) \ll p_{k+q\downarrow}, C^{\dagger}{}_{k\uparrow} \gg = \frac{\Delta}{\omega + \epsilon_{-k-q}}\left(\Delta \ll p_{k+q\downarrow}, C^{\dagger}{}_{k\uparrow} \gg - M \ll C^{\dagger}_{-k\downarrow}, C^{\dagger}{}_{k\uparrow}\right)$$

$$+ \frac{M}{\omega - \epsilon_k}\left(1 - \Delta \ll C^{\dagger}_{-k\downarrow}, C^{\dagger}{}_{k\uparrow} \gg + M \ll p^{\dagger}{}_{k+q\downarrow}, C^{\dagger}{}_{k\uparrow}\right)$$

$$-\frac{M}{\omega - \epsilon_k} = \left[\frac{\Delta^2}{\omega + \epsilon_{-k-q}} + \frac{M^2}{\omega - \epsilon_k} - (\omega - \epsilon_{k+q})\right] \ll p^{\dagger}{}_{k+q\downarrow}, C^{\dagger}{}_{k\uparrow} \gg$$

$$\Delta M \left[\frac{1}{\omega + \epsilon_{-k-q}} + \frac{1}{\omega - \epsilon_k}\right] \ll C^{\dagger}_{-k\downarrow}, C^{\dagger}{}_{k\uparrow} \gg \quad (4.3.6)$$

Rearranging the above Equation (4.3.5) and (4.3.6) yields

$$-\Delta = [\omega^2 - \epsilon_k^2 - (\Delta^2 + M^2)] \ll C_{-k\downarrow}^{\dagger}, C^{\dagger}{}_{k\uparrow} \gg + 2\Delta M \ll p_{k+q\downarrow,} C^{\dagger}{}_{k\uparrow} \gg \quad (4.3.7)$$

$$\Delta M = [\omega^2 - \epsilon_k^2 - ((\Delta^2 + M^2)] \ll p_{k+q\downarrow,} C^{\dagger}{}_{k\uparrow} \gg + 2\Delta M \ll C_{-k\downarrow}^{\dagger}, C^{\dagger}{}_{k\uparrow} \gg \quad (4.3.8)$$

Now solving for $\ll C_{-k\downarrow}^{\dagger}, C^{\dagger}{}_{k\uparrow} \gg$ and $\ll p_{k+q\downarrow,} C^{\dagger}{}_{k\uparrow} \gg$ respectively

$$\ll C_{-k\downarrow}^{\dagger}, C^{\dagger}{}_{k\uparrow} = \frac{-\Delta^2[\omega^2 - \epsilon_k^2 - (\Delta^2 + M^2) + 2M^2]}{[\omega^2 - \epsilon_k^2 - (\Delta_S^2 + M^2)]^2 - (2\Delta M)^2} \quad (4.3.9)$$

$$\ll p_{k+q\downarrow,} C^{\dagger}{}_{k\uparrow} = \frac{M[\omega^2 - \epsilon_k^2 - (\Delta^2 + M^2) + 2\Delta^2]}{[\omega^2 - \epsilon_k^2 - (\Delta^2 + M^2)]^2 - (2\Delta M)^2} \quad (4.3.10)$$

Applying factorization theorem for Equation (4.3.9) above we have;

$$\ll C_{-k\downarrow}^{\dagger}, C^{\dagger}{}_{k\uparrow} \gg = \frac{-\Delta[\omega^2 - \epsilon_k^2 - (\Delta^2 + M^2)]}{[\omega^2 - \epsilon_k^2 - (\Delta^2 + M^2) - (2M\Delta)][\omega^2 - \epsilon_k^2 - (\Delta^2 + M^2) + (2M\Delta)]}$$

$$= \frac{A}{[\omega^2 - \epsilon_k^2 - (\Delta^2 + M^2) + (2M\Delta)]} + \frac{B}{[\omega^2 - \epsilon_k^2 - (\Delta^2 + M^2) - (2M\Delta)]} \quad (4.3.10a)$$

Hence, $A + B = -\Delta$, and $2M(B - A) = 0$

$A = \frac{-M}{2}$, $B = \frac{-M}{2}$ And the second term become

$$\frac{-2\Delta M}{[\omega^2 - \epsilon_k^2 - ((\Delta^2 + M^2) - (2M\Delta)][\omega^2 - \epsilon_k^2 - (\Delta^2 + M^2) + (2M\Delta)]} \quad (4.3.10b)$$

$$= \frac{A}{[\omega^2 - \epsilon_k^2 - (\Delta^2 + M^2) + (2M\Delta)]} + \frac{B}{[\omega^2 - \epsilon_k^2 - (\Delta + M^2) - (2M\Delta)]}$$

$A + B = 0$, $2M\Delta(B - A) = -(2M\Delta A = \frac{-M}{2}$, $B = \frac{M}{2}$

$$\ll C_{-k\downarrow}^{\dagger}, C^{\dagger}{}_{k\uparrow} \gg = \frac{-\Delta}{[\omega^2 - \epsilon_k^2 - (+M^2) + 2M\Delta)]} - \frac{\Delta}{[\omega^2 - \epsilon_k^2 - (\Delta^2 + M^2) - 2M\Delta)]} \quad (4.3.11)$$

$$+ \frac{M}{[\omega^2 - \epsilon_k^2 - (\Delta^2 + M^2) + 2M\Delta)]} - \frac{M}{[\omega^2 - \epsilon_k^2 - (\Delta^2 + M^2) - 2M\Delta)]}$$

Finally collecting the terms which have similar denominator we obtain;

$$\ll C_{-k\downarrow}^{\dagger}, C^{\dagger}{}_{k\uparrow} \gg = \frac{-(\Delta + M)}{2[\omega^2 - \epsilon_k^2 - (\Delta^2 + M^2)]} \quad (4.3.12)$$

In similar fashion, applying factorization theorem for $\ll p_{k+q\downarrow,} C^{\dagger}{}_{k\uparrow} \gg$

$$\ll p_{k+q\downarrow}, C^{\dagger}{}_{k\uparrow} \gg = \frac{M[\omega^2 - \epsilon_k^2 - (\Delta^2 + M^2) + 2\Delta]}{[\omega^2 - \epsilon_k^2 - (\Delta + M^2)]^2 - (2\Delta M)^2}$$

$$= \frac{M[\omega^2 - \epsilon_k^2 - (\Delta^2 + M^2)]}{[\omega^2 - \epsilon_k^2 - (\Delta^2 + M^2) - 2M\Delta)][\omega^2 - \epsilon_k^2 - (\Delta^2 + M^2) + 2M\Delta)]} \quad (4.3.13)$$

$$= \frac{A}{[\omega^2 - \epsilon_k^2 - (\Delta + M^2) + (2M\Delta)]} + \frac{B}{[\omega^2 - \epsilon_k^2 - (\Delta + M^2) - (2M\Delta)]} \quad (4.3.14)$$

$$A + B = M, \quad B = A, \quad A = \frac{M}{2}, \quad B = \frac{M}{2},$$

And the second term become

$$\frac{-2\Delta M}{[\omega^2 - \epsilon_k^2 - (\Delta + M^2) - (2\,M\Delta)][\omega^2 - \epsilon_k^2 - (\Delta + M^2) + (2M\Delta)]} \quad (4.3.15)$$

$$= \frac{A}{[\omega^2 - \epsilon_k^2 - (\Delta - M^2) + (2\,M\Delta)]} + \frac{B}{[\omega^2 - \epsilon_k^2 - (\Delta - M^2) - (2M\Delta)]} \quad (4.3.16)$$

$$A + B = 0\,,\, B - A = \Delta$$

$$A = \frac{\Delta}{2}, B = \frac{\Delta}{2},$$

$$\ll p_{k+q\downarrow}, C^{\dagger}{}_{k\uparrow} \gg = \frac{M}{[\omega^2 - \epsilon_k^2 - (\Delta + M^2) + (2M\Delta)]} + \frac{M}{[\omega^2 - \epsilon_k^2 - (\Delta + M^2) - (2M\Delta)]} - \frac{\Delta}{[\omega^2 - \epsilon_k^2 - (\Delta - M^2) + (2\,M\Delta)]} + \frac{\Delta}{[\omega^2 - \epsilon_k^2 - (\Delta + M^2) - (2M\Delta)]} \quad (4.3.17)$$

Collecting the terms which have similar denominator we obtain;

$$\ll p_{k+q\downarrow}, C^{\dagger}{}_{k\uparrow} \gg = \frac{M}{[(\omega^2 - \epsilon_k^2 - (\Delta + M^2)) + (2M\Delta)]} + \frac{\Delta}{[(\omega^2 - \epsilon_k^2 - (\Delta - M^2)) + (2M\Delta)]}$$

$$+ \frac{M}{[(\omega^2 - \epsilon_k^2 - (\Delta + M^2)) - (2M\Delta)]} + \frac{\Delta_s}{[(\omega^2 - \epsilon_k^2 - (\Delta + M^2)) - (2M\Delta)]}$$

$$\ll p_{k+q\downarrow}, C^{\dagger}{}_{k\uparrow} \gg = \frac{\Delta + M}{2[\omega^2 - \epsilon_k^2 - (\Delta + M)^2]} + \frac{M - \Delta}{2[\omega^2 - \epsilon_k^2 - (\Delta - M)^2]} \quad (4.3.18)$$

We can use equation (4.3.12)

$$\ll C_{-k\downarrow}^{\dagger}, C^{\dagger}{}_{k\uparrow} \gg = \frac{-(\Delta + M)}{2[\omega^2 - \epsilon_k^2](\Delta + M)^2} - \frac{(\Delta - M)}{2[\omega^2 - \epsilon_k^2(\Delta - M)^2]}$$

where, Δ are the superconducting order parameter (analogues to the BCS order parameter) and $M\ is$ the magnetic order parameter?

using the relation for Δ.

$$\Delta = \frac{V}{\beta}\sum_{k,n} \ll C^{\dagger}_{-k\downarrow}, C^{\dagger}{}_{k\uparrow} \gg \qquad (4.3.19)$$

And the sum may be changed in to an integral by introducing the density of states,

$$\mathrm{N}(\in = \frac{1}{V}\sum_{k} \rightarrow \frac{1}{(2\pi)^3}\int dk^3 = \int_{-\infty f}^{\infty} d \in N(\in)$$

The summation with respect to k and n extends over all allowed pair states. Therefore;

$$\Delta = \frac{V}{\beta}\sum_{k,n} \left\{\frac{-(\Delta+M)}{2\left[\omega^2-\epsilon_k^2-(\Delta+M)^2\right]} - \frac{(\Delta-M)}{2\left[\omega^2-\epsilon_k^2--(\Delta-M)^2\right]}\right\} N(\in) d \in$$

$$= \frac{V}{\beta}\sum_{k,n} \int_{-\infty f}^{\infty} d \in N(\in)\left\{\frac{-(\Delta+M)}{2\left[\omega^2-\epsilon_k^2-(\Delta+M)^2\right]} - \frac{(\Delta-M)}{2\left[\omega^2-\epsilon_k^2-(\Delta-M)^2\right]}\right\} \qquad (4.3.20)$$

Attractive interaction is effective for the region $-\hbar\omega_b < \in < \hbar\omega_b$, assuming the density of states doesn't vary over this integral. Then the expression becomes;

$$\Delta = 2N(\in)\frac{V}{\beta}\sum_{k,n} \int_0^{\hbar\omega_b} d \in \left[\frac{-(\Delta+M)}{2\left[\omega^2-\epsilon_k^2-(\Delta+M)^2\right]} - \frac{(\Delta-M)}{2\left[\omega^2-\epsilon_k^2-(\Delta-M)^2\right]}\right] \qquad (4.3.21)$$

$\omega \rightarrow \omega_n$ And using the Matsubara frequency;

$$\omega_n = \frac{(2n+1)\pi}{\beta} \quad \text{and} \quad \omega_n^2 = \frac{(2n+1)^2\pi^2}{\beta^2}$$

$$2\Delta = 2N(0)\frac{V}{\beta}\sum_{k,n} \int_0^{\hbar\omega b} d \in \left[\frac{-(\Delta+M)}{\left[\frac{(2n+1)^2\pi^2}{\beta^2} - \epsilon_k^2 - (+M)^2\right]}\right]$$

$$= -2N(0)\frac{V}{\beta}\sum_{k,n} \int_0^{\hbar\omega b} d \in \left[\frac{(\Delta-M)}{\left[\frac{(2n+1)^2\pi^2}{\beta^2} - \epsilon_k^2 - (\Delta-M)^2\right]}\right] \qquad (4.3.22)$$

Let $\quad \in_1{}^2 = \epsilon_k^2 + (\Delta + M)^2$ and $\in_2{}^2 = \epsilon_k^2 + (\Delta - M)^2$

$$2\Delta_s = 2N(0)V\beta\sum_n \int_0^{\hbar\omega_b} d \in \left[\frac{(\Delta+M)}{\left[(2n+1)^2\pi^2+\beta^2\in_1^2\right]} + \frac{(\Delta-M)}{\left[(2n+1)^2\pi^2+\beta^2\in_2^2\right]}\right] \qquad (4.3.23)$$

Using the relation $\frac{\tanh(\frac{x}{2})}{2x} = \sum_n \frac{1}{(2n+1)^2\pi^2+x^2}$ where $x = \beta \in_1, x = \beta \in_2, x^2 = \beta^2 \in_1^2$

So we can rewrite Equation (4.3.23) as

$$2\Delta = 2N(0)V\beta \sum_n \int_0^{\hbar\omega_b} d \in \left\{ (\Delta + M)\frac{\tanh(\frac{x}{2})}{2\beta \in_1} + (\Delta - M)\frac{\tanh(\frac{x}{2})}{2\beta \in_2} \right\}$$

$$2\Delta = \lambda \int_0^{\hbar\omega b} d \in \left\{ \left[\frac{\Delta+M}{\sqrt{\in_k^2+(\Delta+M)^2}} \right] \tanh \frac{\beta(\sqrt{\in_k^2+(\Delta+M)^2}}{2} \right\}$$

$$+ \left\{ \left[\frac{\Delta-M}{\sqrt{\in_k^2-(\Delta+M)^2}} \right] \tanh \frac{\beta(\sqrt{\in_k^2+(\Delta+M)^2}}{2} \right\} \qquad (4.3.24)$$

Let us study the above equation for the case temperature approach to critical temperature as order parameter approach to zero using Equation (4.3.24)

$$\frac{\lambda}{2} = \int_0^{\hbar\omega b} d \in \left[\frac{1+\frac{M}{\Delta}}{\sqrt{\in_k^2+(\Delta+M)^2}} \right] \tanh \frac{\beta(\sqrt{\in_k^2+(\Delta+M)^2}}{2}$$

$$+ \int_0^{\hbar\omega b} d \in \left[\frac{1-\frac{M}{\Delta}}{\sqrt{\in_k^2+(\Delta+M)^2}} \right] \tanh \frac{\beta(\sqrt{\in_k^2+(\Delta+M)^2}}{2} \qquad (4.3.25)$$

Let: $\frac{\lambda}{2} = I + L \qquad (4.3.26)$

Now the first integral is I and the second is L

$$I = \int_0^{\hbar\omega b} \in \left[\frac{1+\frac{M}{\Delta}}{\sqrt{\in_k^2+(\Delta+M)^2}} \right] \tanh \frac{\beta(\sqrt{\in_k^2+(\Delta+M)^2}}{2} \qquad 4.3.26a)$$

$$L = \int_0^{\hbar\omega b} d \in \left[\frac{1-\frac{M}{\Delta}}{\sqrt{\in_k^2+(\Delta+M)^2}} \right] \tanh \frac{\beta(\sqrt{\in_k^2+(\Delta+M)^2}}{2} \qquad (4.3.26b)$$

Now solve the first integral

$$I = \int_0^{\hbar\omega b} d \in \left[\frac{1+\frac{M}{\Delta}}{\sqrt{\in_k^2+(\Delta+M)^2}}\right] \tanh\frac{\beta(\sqrt{\in_k^2+(\Delta+M)^2}}{2}$$

$$= \int_0^{\hbar\omega b} d \in \left[\frac{1}{\sqrt{\in_k^2+(\Delta+M)^2}}\right] \tanh\frac{\beta(\sqrt{\in_k^2+(\Delta+M)^2}}{2} + \int_0^{\hbar\omega b} d \in \qquad (4.3.27)$$

At $T = T_C, \Delta = 0$

The first integral of Equation (4.3.27) say I_1 can be calculated as follows using the relation,

$$\frac{\tanh(\frac{x}{2})}{2x} = \sum_n \frac{1}{(2n+1)^2\pi^2 + x^2}$$

$$I_1 = \int_0^{\hbar\omega b} d \in \left[\frac{1}{\sqrt{\in_k^2+(\Delta+M)^2}}\right] \tanh\frac{\beta(\sqrt{\in_k^2+(\Delta_s+M)^2}}{2} = \int_0^{\hbar\omega b} d \in \frac{2}{\beta}\sum_{n=-\infty}^{n=\infty} \frac{1}{\omega_n^2+\epsilon_k^2+M^2} \qquad (4.3.28)$$

Using Laplace's transform and Matsubara frequency $\omega_n = \frac{(2n+1)\pi}{\beta}$ the above integral becomes

$$I_1 = \int_0^{\hbar\omega b} d \in \frac{2}{\beta}\sum_{n=-\infty}^{n=\infty} \frac{1}{\omega_n^2+\epsilon_k^2} - \int_0^{\hbar\omega b} M^2 d \in \frac{2}{\beta}\sum_{n=-\infty}^{n=\infty} \frac{1}{(\omega_n^2+\epsilon^2)^2} \qquad (4.3.29)$$

$$= \int_0^{\hbar\omega b} \frac{\tanh(\frac{\beta\epsilon}{2})}{\epsilon} - \int_0^{\hbar\omega b} M^2 d \in \frac{2}{\beta}\sum_{n=-\infty}^{n=\infty} \frac{1}{\left\{\frac{(2n+1)^2\pi^2 n}{\beta^2 \quad n} + \epsilon^2\right\}^2} + \ldots.$$

The summation become $\frac{2}{\beta}\sum_{n=-\infty}^{n=\infty} \frac{1}{\left\{\frac{(2n+1)^2\pi^2}{\beta^2}\frac{(2n+1)^2\pi^2}{\beta^2}\right.}$ $= 2\sum_{n=-\infty}^{n=\infty} \frac{1}{\left\{\frac{(2n+1)^2\pi^2}{\beta^2} + \epsilon^2\right\}^2}$

After some manipulation

$$\sum_{n=-\infty}^{n=\infty} \frac{1}{\left\{\frac{(2n+1)^2\pi^2}{\beta^2} + \epsilon^2\right\}^2} = 2\sum_{n=-\infty}^{n=\infty} \frac{1}{a^4(1+x^2)^2} \quad \text{so,}$$

$$I_1 = \int_0^{\hbar\omega b} \frac{\tanh(\frac{\beta\epsilon}{2})}{\epsilon} - \int_0^{\hbar\omega b} M^2 d \in \frac{4}{\beta}\sum_{n=0}^{n=\infty} \frac{1}{a^4(1+x^2)^2}$$

Let $I_1 = I_{1a} + I_{1b}$ (4.3.30)

$$I_{1a} = \int_0^{\hbar\omega b} \frac{\tanh(\frac{\beta\in}{2})}{\in} \quad \text{And} \quad I_{1b} = -\int_0^{\hbar\omega b} M^2 d\in \frac{4}{\beta}\sum_{n=0}^{n=\infty} \frac{1}{a^4(1+x^2)^2}$$

Then evaluate

$$I_{1a} = \int_0^{\hbar\omega b} \frac{\tanh(\frac{\beta\in}{2})}{\in} \quad \text{Let,} \quad y = \frac{\beta E}{2} d\in = \frac{2}{\beta} \text{dy}$$

$$= lny \tanh y\,(y-0) - \int_0^y \frac{lny}{cosh^2 y} \quad \text{at low temperature } \frac{\tanh y}{2K_B T_c} \to 1$$

$$= lny - ln\left(\frac{\pi}{4e^{\gamma}}\right), \text{ Where } \gamma \text{ is the Euler's constant. } \gamma = 1.78$$

$$= ln1.13\left(\frac{\hbar\omega b}{K_B T_c}4\right) \tag{4.3.31}$$

$$I_{1b} = -\int_0^{\hbar\omega b} M^2 d\in \frac{2}{\beta} 2\sum_{n=0}^{n=\infty} \frac{1}{a^4(1+x^2)^2} x^2 = \frac{\in^2}{a^2}, adx = d\in$$

$$= -\int_0^{\hbar\omega b} M^2 \frac{4}{\beta}\sum_0^{\infty} \frac{1}{a^4(1+x^2)^2} a^2 = \frac{(2n+1)^2\pi^2}{\beta^2}$$

$$= -\frac{4}{\beta} M^2 \sum_0^{\infty} \frac{1}{a^4} \int_0^{\hbar\omega b} adx \frac{1}{a^4(1+x^2)^2} + \cdots = -\frac{4}{\beta} M^2 \sum_0^{\infty} \frac{1}{a^3} \int_0^{\hbar\omega b} dx \frac{1}{a^3(1+x^2)^2} + ..$$

After some manipulation and sing from the laws series and Zeta function we get

$$= \int_0^{\hbar\omega b} \frac{1}{(1+x^2)^2} dx = \frac{\pi}{4}\sum_0^{\infty} \frac{1}{[(1+x)]^p} = (1 - 2^{-p})\, \zeta(p) \text{ so; } \sum_0^{\infty} \frac{1}{[2n+1]^3} = \frac{7}{8}\zeta(3), \zeta(3) = 1.202$$

Therefore, $$I_{1b} = -\left(\frac{M}{\pi K_B T_C}\right)^2 \frac{8.414}{8} \tag{4.3.32}$$

Then Equation (4.3.30) or I_1 is the sum of equation (4.3.31) and equation (4.3.32)

$$I_1 = ln1.13\left(\frac{\hbar\omega b}{K_B T_c}\right) - \frac{M^2}{(\pi K_B T_C)}\frac{8.414}{8} \tag{4.3.33}$$

The second integral in Equation (4.3.27) is let we can say I_2

$$I_2 = \int_0^{\hbar\omega b} d\in \left[\frac{M}{\Delta\sqrt{\in_k^2 + (\Delta+M)^2}}\right] \tanh \frac{\beta(\sqrt{\in_k^2 + (\Delta+M)^2}}{2}$$

$$I_2 = \int_0^{\hbar\omega b} d \in \left[\frac{M}{\Delta\sqrt{\epsilon_k^2+(\Delta+M)^2}}\right]\tanh\left\{(\beta\frac{\sqrt{\epsilon_k^2+(\Delta+M)^2}}{2}\right\}$$

Applying L'Hopital's rule

$$I_2 = \int_0^{\hbar\omega b}\lim_{\Delta\to 0}\left\{\frac{d}{d\Delta}\left(d \in \left[\frac{M}{\Delta\sqrt{\epsilon_k^2+(\Delta+M)^2}}\tanh\beta\frac{\sqrt{\epsilon_k^2+(\Delta+M)^2}}{2}\right]\right)\right\} \quad (4.3.34)$$

$$\frac{d}{d\Delta}\left((d \in \tanh(\beta\frac{\sqrt{\epsilon_k^2+(\Delta+M)^2}}{2}\right) = sech^2\left\{(\beta\frac{\sqrt{\epsilon_k^2+(\Delta+M)^2}}{2}\right\}\left\{\frac{\beta(+M)}{2\sqrt{\epsilon_k^2+(\Delta+M)^2}}\right\} \quad (4.3.35a)$$

$$\text{And}\frac{d}{d\Delta}\left(\Delta\sqrt{\epsilon_k^2+(\Delta+M)^2}\right) = \sqrt{\epsilon_k^2+(\Delta+M)^2} + \Delta\left\{\frac{2\beta\ (\Delta+M)}{2\sqrt{\epsilon_k^2+(\Delta+M)^2}}\right\} \quad (4.3.35b)$$

Then substitute Equation (4.3.35a) & (4.3.35b) in to (4.3.34) we get

$$I_2 = \int_0^{\hbar\omega b} d \in \frac{M^2\beta\ sech^2\frac{\beta}{2}\sqrt{\epsilon_k^2+M^2}}{2(\epsilon_k^2+M^2)} \quad (4.3.36)$$

Combing Equation (4.3.33) & (4.3.36)

$$I = I_1 + I_2 = ln1.13\left(\frac{\hbar\omega b}{K_B T_c}\right) - \frac{M^2}{(\pi K_B T_C)}\frac{8.414}{8} + \int_0^{\hbar\omega b} d \in \frac{M^2\beta\ sech^2\frac{\beta}{2}\sqrt{\epsilon_k{}^2+M^2}}{2(\epsilon_k^2+M^2)} \quad (4.3.37)$$

Using the relation $\Rightarrow sech^2 x = 1 - tanh^2$

$$I = ln1.13\left(\frac{\hbar\omega b}{K_B T_c}\right) - M^2\left(\frac{1}{\pi K_B T_c}\right)^2\frac{8.414}{8} + \int_0^{\hbar\omega b} d \in \frac{M^2}{2K_B T_c(\epsilon_k^2+M^2)}$$

$$- \int_0^{\hbar\omega b} d \in \frac{M^2 tanh^2\frac{\beta}{2}\sqrt{\epsilon_k^2+M^2}}{2K_B T_c(\epsilon_k^2+M^2)} \quad (4.3.38)$$

From the integral of special functions and the help of FORTRAN language;

$$\int_0^{\hbar\omega b} d \in \frac{M^2}{2K_B T_c(\epsilon_k^2+M^2)} = \frac{M^2}{2K_B T_c} arctan\left(\frac{\hbar\omega b}{M}\right)$$

$$I = ln1.13\left(\frac{\hbar\omega b}{K_B T_c}\right) - M^2\left(\frac{1}{\pi K_B T_c}\right)^2 \frac{8.414}{8} + - \int_0^{\hbar\omega b} d \in \frac{M^2 tanh^2 \sqrt{\epsilon_k^2 + M^2}}{2K_B T_c(\epsilon_k^2 + M^2)}$$

$$- \int_0^{\hbar\omega b} d \in \frac{M^2 tanh^2 \frac{\beta}{2}\sqrt{\epsilon_k^2 + M^2}}{2K_B T_c(\epsilon_k^2 + M^2)}$$

$$= \frac{M}{4K_B T_c)} ln\left| \frac{\hbar\omega b + M}{\hbar\omega b - M} \right| \qquad (4.3.39)$$

Similarly, let us solve for L from Equation (4.3.26b)

$$L = \int_0^{\hbar\omega b} d \in \left[\frac{1 - \frac{M}{\Delta}}{\sqrt{\epsilon_k^2 + (\Delta - M)^2}}\right] \tanh \frac{\beta(\sqrt{\epsilon_k^2 + (\Delta - M)^2}}{2}$$

$$L = \int_0^{\hbar\omega b} d \in \left[\frac{1}{\sqrt{\epsilon_k^2 - (\Delta - M)^2}}\right] \tanh\left\{\frac{\beta(\sqrt{\epsilon_k^2 + (\Delta - M)^2}}{2}\right\}$$

$$- \int_0^{\hbar\omega b} d \in \left[\frac{M}{\sqrt{\epsilon_k^2 + (\Delta - M)^2}}\right] \tanh\left\{\frac{\beta(\sqrt{\epsilon_k^2 + (\Delta - M)^2}}{2}\right\} \qquad (4.3.40)$$

At $T = T_{C,}$ $\Delta = 0$ Now, the first integral in Equation (4.3.40) can be calculated by applying the previous method; $\Delta = 0$ Let

$$L_1 = \int_0^{\hbar\omega b} d \in \left[\frac{1}{\sqrt{\epsilon_k^2 + M^2}}\right] \tanh\left\{\frac{\beta(\sqrt{\epsilon_k^2 + M^2}}{2}\right\} \qquad (4.3.41)$$

$$L_2 = - \int_0^{\hbar\omega b} d \in \left[\frac{M}{\Delta\sqrt{\epsilon_k^2 + (\Delta - M)^2}}\right] \tanh\left\{\frac{\beta(\sqrt{\epsilon_k^2 + (\Delta - M)^2}}{2}\right\} \qquad (3.4.42)$$

Now evaluate L_1

$$L_1 = \int_0^{\hbar\omega b} d \in \left[\frac{1}{\sqrt{\epsilon_k^2 + M^2}}\right] \tanh\left\{\frac{\beta(\sqrt{\epsilon_k^2 + M^2}}{2}\right\} \qquad (4.3.43)$$

$= \int_0^{\hbar\omega b} d \in \frac{2}{\beta} \sum_{-\infty}^{\infty} \frac{1}{\omega_n^2 + \epsilon_k^2 + M^2}$, Since $\frac{\tanh(\frac{x}{2})}{2x} = \sum_n \frac{1}{(2n+1)^2\pi^2 + x^2}$ where,$(\omega_n = \frac{(2n+1)\pi}{\beta}$

$$L_1 = \int_0^{\hbar\omega b} d\in \frac{2}{\beta}\sum_{-\infty}^{\infty} \frac{1}{\omega_n^2+\in_k^2} - \int_0^{\hbar\omega b} M^2 d\in \frac{2}{\beta}\sum_{-\infty}^{\infty} \frac{1}{(\omega_n^2+\in_k^2)^2} + ..$$

$$= \int_0^{\hbar\omega b} d\in \frac{2}{\beta} tanh\beta \frac{(\frac{\beta\in}{2})}{\in} - \int_0^{\hbar\omega b} M^2 d\in \frac{2}{\beta}\sum_{-\infty}^{\infty} \frac{1}{\left\{\frac{(2n+1)^2\pi^2}{\beta^2} + \in^2\right\}^2} + .. \qquad (4.3.44)$$

But the summation becomes

$$\sum_{n=-\infty}^{n=\infty} \frac{1}{\left\{\frac{(2n+1I_1)^2\pi^2\in}{\beta^2\ n}\right\}^2} = 2\sum_{n=-\infty}^{n=\infty} \frac{1}{\left\{\frac{(2n+1)^2\pi^2}{\beta^2} + \in^2\right\}^2} \quad \text{after some manipulation}$$

$$2\sum_{n=-\infty}^{n=\infty} \frac{1}{\left\{\frac{(2n+1)^2\pi^2}{\beta^2} + \in^2\right\}^2} = 2\sum_{n=0}^{n=\infty} \frac{1}{a^4(1+x^2)^2} \qquad (4.3.45)$$

$$L_1 = \int_0^{\hbar\omega b} \frac{\tanh(\frac{\beta\in}{2})}{E} - \int_0^{\hbar\omega b} M^2 d\in 2\sum_{n=0}^{n=\infty} \frac{1}{a^4(1+x^2)^2} \quad \text{let the first integral } L_{1a} \text{ and } L_{1b}$$

$$L_{1a} = \int_0^{\hbar\omega b} \frac{\tanh(\frac{\beta\in}{2})}{E} \quad \text{And} \quad L_{1b} = -\int_0^{\hbar\omega b} M^2 d\in \frac{4}{\beta}\sum_{n=0}^{n=\infty} \frac{1}{a^4(1+x^2)^2}$$

Then the value of L_{1a} and L_{1b} can be obtained using the method that used previously to solve *I*

$$L_{1a} = ln1.13\left(\frac{\hbar\omega b}{K_B T_c}\right) \qquad (4.3.46)$$

$$L_{1b} = -\left(\frac{M}{\pi K_B T_C}\right)^2 \frac{8.414}{8} \qquad (4.3.47)$$

Then Equation (4.3.41) or become the sum of Equation (4.3.46) & Equation (4.3.47)

$$L_1 = ln1.13\left(\frac{\hbar\omega b}{K_B T_c}\right) - \left(\frac{M}{\pi K_B T_C}\right)^2 \frac{8.414}{8} \qquad (4.3.48)$$

The second integral Equation (4.3.42)

$$L_2 = -\int_0^{\hbar\omega b} d\in \left[\frac{M}{\Delta\sqrt{\in_k^2+(\Delta-M)^2}}\right] \tanh\left\{\frac{\beta(\sqrt{\in_k^2+(\Delta-M)^2}}{2}\right\}$$

Applying L 'Hospital's rule

$$L_2 = \int_0^{\hbar\omega b} \lim_{\Delta\to 0} \left\{ \frac{d}{d\Delta} \left(d \in \left[\frac{M}{\Delta\sqrt{\epsilon_k^2+(\Delta-M)^2}} \tanh\beta \frac{\sqrt{\epsilon_k^2+(\Delta+M)^2}}{2} \right] \right) \right.$$

$$\frac{d}{d\Delta}\left(tanh(\beta \frac{\sqrt{\epsilon_k^2+(\Delta-M)^2}}{2} \right) = sech^2 \left\{ (\beta \frac{\sqrt{\epsilon_k^2+(\Delta-M)^2}}{2} \right\} \left\{ \frac{\beta(\Delta+M)}{\sqrt{\epsilon_k^2+(\Delta+M)^2}} \right\} \quad (4.3.49a)$$

$$\text{and } \frac{d}{d\Delta}\left(\Delta\sqrt{\epsilon_k^2+(\Delta-M)^2}\right) = \sqrt{\epsilon_k^2+(\Delta-M)^2} - \quad (4.3.49b)$$

Then substitute Equations (4.3.49a) & (4.3.49b) in to (4.3.42) we get:

$$L_2 = \int_0^{\hbar\omega b} d \in \frac{M^2\beta\, sech^2 \frac{\beta}{2}\sqrt{\epsilon_k^2+M^2}}{2(\epsilon_k^2+M^2)} \quad (4.3.50)$$

Therefore combining Equations (4.3.48) and (4.3.50) we get

$$L = L_1 + L_2 = ln1.13\left(\frac{\hbar\omega b}{K_B T_c}\right) - \frac{M^2}{(\pi K_B T_C)}\frac{8.414}{8} + \int_0^{\hbar\omega b} d \in \frac{M^2\beta\, sech^2 \frac{\beta}{2}\sqrt{\epsilon_k^2+M^2}}{2(\epsilon_k^2+M^2)}$$

Using the trigonometric relation $\Rightarrow sech^2 x = 1 - tanh^2$

$$L = ln1.13\left(\frac{\hbar\omega b}{K_B T_c}\right) - M^2\left(\frac{1}{\pi K_B T_c}\right)^2 \frac{8.414}{8} + \int_0^{\hbar\omega b} d \in \frac{M^2}{2K_B T_c(\epsilon_k^2+M^2)}$$

$$- \int_0^{\hbar\omega b} d \in \frac{M^2 tanh^2 \frac{\beta}{2}\sqrt{\epsilon_k^2+M^2}}{2K_B T_c(\epsilon_k^2+M^2)} \quad (4.3.50a)$$

From the integral of special functions and the help of FORTRAN language

$$\int_0^{\hbar\omega b} d \in \frac{M^2\beta\, sech^2 \frac{\beta}{2}\sqrt{\epsilon_k^2+M^2}}{2(\epsilon_k^2+M^2)} = \frac{M^2}{2K_B T_c} arctan\left(\frac{\hbar\omega b}{M}\right) = \frac{M}{4K_B T_c)}\, ln \left| \frac{\hbar\omega b+M}{\hbar\omega b-M} \right| \quad (4.3.51)$$

$$L = ln1.13\left(\frac{\hbar\omega b}{K_B T_c}\right) - M^2\left(\frac{1}{\pi K_B T_c}\right)^2 \frac{8.414}{8} + \int_0^{\hbar\omega b} d \in \frac{M^2}{2K_B T_c(\epsilon_k^2+M^2)}$$

$$- \int_0^{\hbar\omega b} d \in \frac{M^2 tanh^2 \frac{\beta}{2}\sqrt{\epsilon_k^2+M^2}}{2K_B T_c(\epsilon_k^2+M^2)} \quad (4.3.52)$$

$$L = ln1.13\left(\frac{\hbar\omega b}{K_B T_c}\right) - M^2\left(\frac{1}{\pi K_B T_c}\right)^2 \frac{8.414}{8} + \int_0^{\hbar\omega b} d \in \frac{M^2}{2K_B T_c(\epsilon_k^2+M^2)}$$

$$- \int_0^{\hbar\omega b} d \in \frac{M^2 tanh^2 \frac{\beta}{2}\sqrt{\in_k^2 + M^2}}{2K_B T_c(\in_k^2 + M^2)}$$

Since $\frac{2}{\lambda} = I + L$, then from Equations (4.3.38) and 4.3.50a)

$$\frac{2}{\lambda} = 2ln1.13\left(\frac{\hbar\omega b}{K_B T_c}\right) - 2M^2\left(\frac{1}{\pi K_B T_c}\right)^2 \frac{8.414}{8} + 2 \int_0^{\hbar\omega b} d \in + \frac{M^2}{2K_B T_c(\in_k^2 + M^2)}$$

$$-2 \int_0^{\hbar\omega b} d \in \frac{M^2 tanh^2 \frac{\beta}{2}\sqrt{\in_k^2 + M^2}}{2K_B T_c(\in_k^2 + M^2)} \quad (4.3.53)$$

Using Equations (4.3.51) and (4.3.53) can be written as

$$\frac{1}{\lambda} = ln1.13\left(\frac{\hbar\omega b}{K_B T_c}\right) + \frac{M}{4K_B T_c)} ln \left| \frac{\hbar\omega b + M}{\hbar\omega b - M} \right| - M^2\left(\frac{1}{\pi K_B T_c}\right)^2 \frac{8.414}{8}$$

$$- \int_0^{\hbar\omega b} d \in \frac{M^2 tanh^2 \frac{\beta}{2}\sqrt{\in_k^2 + M^2}}{2K_B T_c(\in_k^2 + M^2)} \quad (4.3.54)$$

Since Δ is very small so Δ^2 also become we can ignore the second and the fourth term

Let $= \frac{1}{4K_B T_c)} ln \left| \frac{\hbar\omega b + M}{\hbar\omega b - M} \right|$, $y = \left(\frac{1}{\pi K_B T_c}\right)^2 \frac{8.414}{8}$ and $z = \int_0^{\hbar\omega b} d \in \frac{M^2 tanh^2 \frac{\beta}{2}\sqrt{\in_k^2 + M^2}}{2K_B T_c(\in_k^2 + M^2)}$

$$\frac{1}{\lambda} = ln1.13\left(\frac{\hbar\omega b}{K_B T_c}\right) + Mx - M^2 y - M^2 z \quad (4.3.55)$$

Rearranging the above equation

$$\left(\frac{1}{\lambda} + M^2 y + M^2 z - Mx\right) = ln1.13\left(\frac{\hbar\omega b}{K_B T_c}\right)$$

$$K_B T_c = 1.13\hbar\omega b \exp - \left(\frac{1}{\lambda} + M^2 y + M^2 z + Mx\right)$$

$$= 1.13\hbar\omega b e^{-\left(\frac{1}{\lambda} + M^2 y + M^2 z - Mx\right)}$$

$$T_c = \frac{1.13\hbar\omega b}{K_B} e^{-\left(\frac{1}{\lambda} + Mx\right)} \quad (4.3.56)$$

This Equation (4.3.56) indicates that superconducting transition temperature varies exponentially with magnetic ordering parameter.

4.4 Magnetic transition temperature and magnetic order parameter

$\ll p_{k+q\downarrow,} C^{\dagger}{}_{k\uparrow} \gg \; = \frac{\Delta+M}{2[\omega^2-\epsilon_k^2(\Delta+M)^2]} + \frac{M-\Delta}{2[\omega^2-\epsilon_k^2(\Delta-M)^2]}$, from Equ (4.3.18).

Where, Δ are the superconducting order parameter and M *is* the magnetic order parameter?

Using the relation for M i.e;

$$\Delta_m = \frac{u}{\beta}\sum_{k,n} \; \ll p_{k+q\downarrow,} C^{\dagger}{}_{k\uparrow} \gg \qquad (4.3.57)$$

$$\Delta_m = \frac{u}{\beta}\sum_{k,n} \; \frac{\Delta+M}{2[\omega^2-\epsilon_k^2(\Delta+M)^2]} + \frac{M-\Delta}{2[\omega^2-\epsilon_k^2(\Delta-M)^2]}$$

And the sum may be changed in to an integral by introducing the density of states, N(∈)

$$\sum_k \rightarrow \frac{1}{(2\pi)^3}\int dk^3 = \int_{-\infty f}^{\infty} d \in N(\in)$$

The summation with respect to k and n extends over all allowed pair states. Therefore

$$M = \frac{u}{\beta}\sum_{k,n} \; \int_{-\infty f}^{\infty} d \in N(\in)\left[\frac{\Delta+M}{2[\omega^2-\epsilon_k^2(\Delta+M)^2]} + \frac{\Delta-M}{2[\omega^2-\epsilon_k^2(\Delta-M)^2]}\right]$$

The tractive interaction is effective for the region -ħω_b <∈< ħω_b. Assuming the density of states doesn't vary over this integral. Then the expression becomes;

$$M = \frac{u}{\beta}\sum_{k,n} \; \int_{0}^{\hbar\omega_b} d \in N(\in)\left[\frac{\Delta+M}{2[\omega^2-\epsilon_k^2(\Delta+M)^2]} + \frac{\Delta-M}{2[\omega^2-\epsilon_k^2(\Delta-M)^2]}\right]$$

$\omega \rightarrow \omega_n$ And using the Matsubara frequency;$\omega_n = \frac{(2n+1)\pi}{\beta}$ and $\omega_n^2 = \frac{(2n+1)^2\pi^2}{\beta^2}$

And the relation, $\frac{\tanh(\frac{x}{2})}{2x} = \sum_n \frac{1}{(2n+1)^2\pi^2+x^2}\frac{\tanh(\frac{x}{2})}{2x}$

$$2M = 2N(0)u\beta\,\Sigma_n \int_0^{\hbar\omega_b} d \in \left\{-\Delta + M\frac{\tanh\left(\frac{\beta\epsilon_1}{2}\right)}{2\beta\,\in_1} + \;\; \Delta - M\frac{\tanh\left(\frac{\beta\,\in_2}{2}\right)}{2\beta\,\in_2}\right\} \qquad (4.3.58)$$

Let N (0) u = λ and $\epsilon_1^2 = \epsilon_k^2(\Delta + M)^2$, $\epsilon_2^2 = \epsilon_k^2(\Delta - M)^2$

$$\frac{2M}{\lambda} = \Sigma_n \int_0^{\hbar\omega_b} d \in \left\{\left[\frac{-\Delta + M}{(\sqrt{\epsilon^2{}_k + ((\Delta+M)^2}}\right] + \tanh\frac{(\beta\sqrt{\epsilon^2{}_k + ((\Delta+M)^2}}{2}\right\}$$

$$-\int_0^{\hbar\omega_b} d \in \left\{\left[\frac{\Delta - M}{(\sqrt{\epsilon^2{}_k + ((\Delta - M)^2}}\right] + \tanh\frac{(\beta\sqrt{\epsilon^2{}_k + ((\Delta + M)^2}}{2}\right\} \qquad (4.3.59)$$

Let us study the above equation for the case as temperature approach to magnetic order transition temperature magnetic order parameter approach to zero.

Using Equation (4.3.59)

$$\frac{2}{\lambda} = \int_0^{\hbar\omega b} d \in \left[\frac{-\left(1 + \frac{\Delta}{M}\right)}{\sqrt{\epsilon_k^2 + (\Delta + M)^2}}\right] \tanh\frac{\beta(\sqrt{\epsilon_k^2 + (\Delta + M)^2}}{2}$$

$$-\int_0^{\hbar\omega b} \in \left[\frac{\left(1 - \frac{\Delta}{M}\right)}{\sqrt{\epsilon_k^2 + (\Delta - M)^2}}\right] \tanh \qquad (4.3.60)$$

where $\frac{2}{\lambda} = I + R$ (4.3.61)

$$= \int_0^{\hbar\omega b} \in \left[\frac{-\left(1 + \frac{\Delta}{M}\right)}{\sqrt{\epsilon_k^2 + (\Delta + M)^2}}\right] \tanh\frac{\beta(\sqrt{\epsilon_k^2 + (\Delta + M)^2}}{2} \qquad (4.3.61a)$$

$$R = -\int_0^{\hbar\omega b} d \in \left[\frac{\left(1 - \frac{\Delta}{M}\right)}{\sqrt{\epsilon_k^2 + (\Delta - M)^2}}\right] \tanh\frac{\beta(\sqrt{\epsilon_k^2 + (\Delta - M)^2}}{2} \qquad (4.3.61b)$$

Let as solve for I

$$I = -\int_0^{\hbar\omega b} d \in \left[\frac{1}{\sqrt{\epsilon_k^2 + (\Delta + M)^2}}\right] \tanh\left\{\frac{\beta(\sqrt{\epsilon_k^2 + (\Delta + M)^2}}{2}\right\}$$

$$-\int_0^{\hbar\omega b} d \in \left[\frac{\Delta}{\sqrt{\epsilon_k^2 + (\Delta - M)^2}}\right] \tanh\left\{\frac{\beta(\sqrt{\epsilon_k^2 + (\Delta + M)^2}}{2}\right\} \qquad (4.3.62)$$

Let the first integral in Equation (4.3.62) =I_1 and second integral is I_2

$$I_1 = -\int_0^{\hbar\omega b} d \in \left[\frac{1}{\sqrt{\in_k^2+(\Delta+M)^2}}\right] \tanh\left\{\frac{\beta(\sqrt{\in_k^2+(\Delta+M)^2}}{2}\right\}.$$

For $M = 0$

$$I_1 = -\int_0^{\hbar\omega b} d \in \left[\frac{1}{\sqrt{\in_k^2+\Delta^2}}\right] \tanh\left\{\frac{\beta(\sqrt{\in_k^2+\Delta^2}}{2}\right\} = \int_0^{\hbar\omega b} d \in \frac{2}{\beta}\sum_{-\infty}^{\infty} \frac{1}{\omega_n^2+\in_k^2+\Delta^2} \qquad (4.3.63)$$

$$\text{Since,} \frac{\tanh(\frac{x}{2})}{2x} = \sum_n \frac{1}{(2n+1)^2\pi^2+x^2}$$

$$\text{Where, } (\omega_n = \frac{(2n+1)\pi}{\beta}, \quad \in_1^2 = \in_k^2 + (\Delta+M)^2$$

Using Laplace's transform and Matsubara frequency the above integral can be

$$I_1 = -\left(\int_0^{\hbar\omega b} d \in \frac{2}{\beta}\sum_{-\infty}^{\infty} \frac{1}{\omega_n^2+\in_k^2} - \int_0^{\hbar\omega b} \Delta^2 d \in \frac{2}{\beta}\sum_{-\infty}^{\infty} \frac{1}{(\omega_n^2+\in_k^2)^2} + ..\right)$$

$$= -\left(\int_0^{\hbar\omega b} d \in \frac{2}{\beta} tanh\beta\frac{(\frac{\beta\in}{2})}{\in} - \int_0^{\hbar\omega b} \Delta^2 d \in \frac{2}{\beta}\sum_{-\infty}^{\infty} \frac{1}{\{\frac{(2n+1)^2\pi^2}{\beta^2}+\in^2\}^2} + .\right)$$

But the summation becomes

$$\sum_{n=-\infty}^{n=\infty} \frac{1}{\{\frac{(2n+1I_1)^2\pi^2}{\beta^2}\}} 2 = 2\sum_{n=-\infty}^{n=\infty} \frac{1}{\{\frac{(2n+1)^2\pi^2}{\beta^2}+E^2\}^2} = 2\sum_{n=0}^{n=\infty} \frac{1}{a^4(1+x^2)^2}$$

$$-\int_0^{\hbar\omega b} d \in \left[\frac{1}{\sqrt{\in_k^2+(\Delta+M)^2}}\right] \tanh\left\{\frac{\beta(\sqrt{\in_k^2+(\Delta+M)^2}}{2}\right\}$$

$$= -\left(\int_0^{\hbar\omega b} \frac{\tanh(\frac{\beta\in}{2})}{\in} - \int_0^{\hbar\omega b} \Delta^2 d \in 2\sum_{n=0}^{n=\infty} \frac{1}{a^4(1+x^2)^2}\right)$$

Let the first integral I_{1a} and I_{1b}

$$I_{1a} = -\int_0^{\hbar\omega b} \frac{\tanh(\frac{\beta\in}{2})}{\in} \quad \text{And} \quad I_{1b} = -\int_0^{\hbar\omega b} \Delta^2 d \in \frac{4}{\beta}\sum_{n=0}^{n=\infty} \frac{1}{a^4(1+x^2)^2}$$

Then the value of I_{1a} and I_{1b} can be obtained using the method that used previously to solve *I*

$$= -\int_0^{\hbar\omega b} \frac{\tanh(\frac{\beta \in}{2})}{\in}$$

$$-ln1.13\left(\frac{\hbar\omega b}{K_B T_m}\right) \qquad (4.3.64)$$

$$\mathrm{I}_{1b} = \left(\frac{\Delta}{\pi K_B T_m}\right)^2 \frac{8.414}{8} \qquad (4.3.65)$$

Therefore combining Equation (4.3.64) and (4.3.65) i.e;

$$\mathrm{I}_1 = \mathrm{I}_{1a} + \mathrm{I}_{1b} = -\int_0^{\hbar\omega b} d \in \left[\frac{1}{\sqrt{\in_k^2 + \Delta^2}}\right] \tanh\left\{\frac{\beta(\sqrt{\in_k^2 + \Delta^2}}{2}\right\}$$

$$\mathrm{I}_1 = -ln1.13\left(\frac{\hbar\omega b}{K_B T_c}\right) + \left(\frac{\Delta}{\pi K_B T_C}\right)^2 \frac{8.414}{8} \qquad (4.3.67)$$

The second integral in equation (4.3.62) is let say I_2

$$= -\int_0^{\hbar\omega b} d \in \left[\frac{\Delta}{\Delta\sqrt{\in_k^2 + (\Delta - M)^2}}\right] \tanh\left\{\frac{\beta(\sqrt{\in_k^2 + (\Delta + M)^2}}{2}\right\}$$

I_2 = Applying 'LHopital's rule

$$\mathrm{L}_2 = \int_0^{\hbar\omega b} \lim_{M\to 0}\left\{\frac{d}{d\Delta}\left(d \in \left[\frac{\Delta}{\Delta\sqrt{\in_k^2 + (\Delta+M)^2}} \tanh\beta \frac{\sqrt{\in_k^2 + (\Delta+M)^2}}{2}\right]\right)\right\}$$

$$\frac{d}{dM}\left(\tanh(\beta \frac{\sqrt{\in_k^2 + (\Delta_s + M)^2}}{2}\right) = sech^2\left\{(\beta \frac{\sqrt{\in_k^2 + (\Delta+M)^2}}{2}\right\}\left\{\frac{\beta(\Delta+M)}{\sqrt{\in_k^2 + (\Delta+M)^2}}\right\}$$

$$\text{And } \frac{d}{dM}\left(\Delta\sqrt{\in_k^2 + (\Delta + M)^2}\right) = \sqrt{\in_k^2 + (\Delta + M)^2} + \Delta\left\{\frac{2\beta\ (\Delta+M)}{2\sqrt{\in_k^2 + (\Delta+M)^2}}\right\}$$

by Substituting the above derivatives in Equation L_2

$$\mathrm{L}_2 = -\int_0^{\hbar\omega b} \lim_{M\to 0}\left\{\frac{d \in \Delta sech^2\left\{(\beta \frac{\sqrt{\in_k^2 + (\Delta + M)^2}}{2}\right\}\left\{\frac{\beta\ (\Delta+M)}{2\sqrt{\in_k^2 + (\Delta+M)^2}}\right\}}{\sqrt{\in_k^2 + (\Delta + M)^2} + \Delta\left\{\frac{2\beta\ (\Delta+M)}{2\sqrt{\in_k^2 + (\Delta+M)^2}}\right\}}\right\}$$

$$L_2 = -\int_0^{\hbar\omega b} d \in \frac{\Delta^2 \beta\, sech^2 \frac{\beta}{2}\sqrt{\epsilon_k^2+\Delta^2}}{2\left(\epsilon_k^2+\Delta^2\right)} \tag{4.3.68}$$

Therefore combining Equation (4.3.67) and (4.3.68) gives,

$$I = -ln1.13\left(\frac{\hbar\omega b}{K_B T_m}\right) + \left(\frac{\Delta}{\pi K_B T_m}\right)^2 \frac{8.414}{8} - \int_0^{\hbar\omega b} d \in \frac{\Delta^2 \beta\, sech^2 \frac{\beta}{2}\sqrt{\epsilon_k^2+\Delta^2}}{2\left(\epsilon_k^2+\Delta^2\right)} \tag{4.3.69}$$

Using the relation of trig $sech^2\, x = 1 - tanh^2$

$$I = -ln1.13\left(\frac{\hbar\omega b}{K_B T_m}\right) + \left(\frac{\Delta}{\pi K_B T_m}\right)^2 \frac{8.414}{8} - \int_0^{\hbar\omega b} d \in \frac{{\Delta_s}^2}{2K_B T_m(\epsilon_k^2+\Delta^2)}$$

$$+ \int_0^{\hbar\omega_b} d \in \frac{\Delta^2 tanh^2 \frac{\beta}{2}\sqrt{\epsilon_k^2+\Delta^2}}{2K_B T_c\left(\epsilon_k^2+\Delta^2\right)} \tag{4.3.7}$$

From the integral of special functions and the help of FORTRAN language;

$$\int_0^{\hbar\omega_b} d \in \frac{\Delta^2}{2K_B T_m\left(\epsilon_k^2+\Delta^2\right)} = \frac{\Delta^2}{2K_B T_m} arctan\left(\frac{\hbar}{\Delta}\right) = \omega_b \frac{\Delta}{4K_B T_c)}\, l \tag{4.3.71}$$

Similarly, let us solve for R from Equation (4.3.61b)

$$R = -\int_0^{\hbar\omega b} d \in \left[\frac{\left(1-\frac{\Delta}{M}\right)}{\sqrt{\epsilon_k^2+(\Delta-M)^2}}\right] \tanh\frac{\beta(\sqrt{\epsilon_k^2+(\Delta-M)^2}}{2}$$

$$R = -\int_0^{\hbar\omega b} d \in \left[\frac{1}{\sqrt{\epsilon_k^2-(\Delta-M)^2}}\right] \tanh\left\{\frac{\beta(\sqrt{\epsilon_k^2+(\Delta-M)^2}}{2}\right\}$$

$$-\int_0^{\hbar\omega_b} d \in \left[\frac{\Delta}{\Delta\sqrt{\epsilon_k^2+(\Delta-M)^2}}\right] \tanh\left\{\frac{\beta(\sqrt{\epsilon_k^2+(\Delta-M)^2}}{2}\right\} \tag{4.3.72}$$

Let the first integral in Equation (4.3.72) R_1 and second integral is R_2

$$R_1 = -\int_0^{\hbar\omega b} d \in \left[\frac{1}{\sqrt{\epsilon_k^2+(\Delta+M)^2}}\right] \tanh\left\{\frac{\beta(\sqrt{\epsilon_k^2+(\Delta+M)^2}}{2}\right\}$$

As $T \rightarrow T_m$, M=0

$$R_1 = -\int_0^{\hbar\omega_b} d\in \left[\frac{1}{\sqrt{\in_k^2+\Delta^2}}\right] \tanh\left\{\frac{\beta(\sqrt{\in_k^2+\Delta^2}}{2}\right\} = \int_0^{\hbar\omega_b} d\in \frac{2}{\beta}\sum_{-\infty}^{\infty} \frac{1}{\omega_n^2+\in_k^2+\Delta^2} \qquad (4.3.73)$$

$$\text{Since} \quad \frac{\tanh(\frac{x}{2})}{2x} = \sum_n \frac{1}{(2n+1)^2\pi^2+x^2}$$

$$\text{where,} \quad (\omega_{n=}\frac{(2n+1)\pi}{\beta}, \in_2^2 = \in_k^2 + (\Delta - M)^2$$

Using Laplace's transform and Matsubara frequency the above integral can be

$$R_1 = -\left(\int_0^{\hbar\omega_b} d\in \frac{2}{\beta}\sum_{-\infty}^{\infty} \frac{1}{\omega_n^2+\in_k^2} - \int_0^{\hbar\omega b} \Delta^2 d\in \frac{2}{\beta}\sum_{-\infty}^{\infty} \frac{1}{(\omega_n^2+\in_k^2)^2} + ..\right)$$

$$R_1 = -\left(\int_0^{\hbar\omega_b} d\in \frac{2}{\beta} tanh\beta \frac{(\frac{\beta\in}{2})}{E} - \int_0^{\hbar\omega_b} \Delta^2 d\in \frac{2}{\beta}\sum_{-\infty}^{\infty} \frac{1}{\left\{\frac{(2n+1)^2\pi^2}{\beta^2}+\in^2\right\}^2} + ..\right)$$

But the summation becomes

$$\sum_{n=-\infty}^{n=\infty} \frac{1}{\left\{\frac{(2n+1I_1)^2\pi^2}{\beta^2}\right.} = 2\sum_{n=-\infty}^{n=\infty} \frac{1}{\left\{\frac{(2n+1)^2\pi^2}{\beta^2}+\in^2\right\}^2} = 2\sum_{n=0}^{n=\infty} \frac{1}{a^4(1+x^2)^2}$$

$$R_1 = -\int_0^{\hbar\omega b} d\in \left[\frac{1}{\sqrt{\in_k^2+(\Delta+M)^2}}\right] \tanh\left\{\frac{\beta(\sqrt{\in_k^2+(\Delta+M)^2}}{2}\right\}$$

$$= -\left(\int_0^{\hbar\omega_b} \frac{\tanh(\frac{\beta\in}{2})}{E} - \int_0^{\hbar\omega_b} \Delta^2 d\in 2\sum_{n=0}^{n=\infty} \frac{1}{a^4(1+x^2)^2}\right)$$

Let the first integral R_{1a} and R_{1b}

$$R_{1a} = -\int_0^{\hbar\omega_b} \frac{\tanh(\frac{\beta\in}{2})}{\in} \quad \text{And} \quad R_{1b} = -\int_0^{\hbar\omega_b} \Delta^2 d\in \frac{4}{\beta}\sum_{n=0}^{n=\infty} \frac{1}{a^4(1+x^2)^2}$$

Then the value of R_{1a} and R_{1b} can be obtained using the method that used previously to solve

$$, \quad R_{1a} = -ln1.13\left(\frac{\hbar\omega_b}{K_B T_m}\right) \qquad (4.3.74)$$

$$R_{1b} = \left(\frac{\Delta}{\pi K_B T_m}\right)^2 \frac{8.414}{8} \qquad (4.3.75)$$

Therefore combining Equation (4.3.74) and (4.3.75) and substitute into the first integral of $R_1 in$ Equation (4.3.73) become

$$R_1 = R_{1a} + \quad R_{1b} = -\int_0^{\hbar\omega b} d \in \left[\frac{1}{\sqrt{\in_k^2 + \Delta^2}}\right] \tanh\left\{\frac{\beta(\sqrt{\in_k^2+\Delta^2}}{2}\right\}$$

$$R_1 = -ln1.13\left(\frac{\hbar\omega_b}{K_B T_m}\right) + \left(\frac{\Delta}{\pi K_B T_m}\right)^2 \frac{8.414}{8} \tag{4.3.76}$$

The second integral of Equation (4.3.73) becomes;

$$R_2 = -\int_0^{\hbar\omega_b} d \in \left[\frac{\Delta}{\Delta\sqrt{\in_k^2+(\Delta-M)^2}}\right] \tanh\left\{\frac{\beta(\sqrt{\in_k^2+(\Delta-M)^2}}{2}\right\}$$

$$\frac{d}{dM}\left(\tanh(\beta\frac{\sqrt{\in_k^2+(\Delta+M)^2}}{2}\right) = sech^2\left\{(\beta\frac{\sqrt{\in_k^2+(\Delta-M)^2}}{2}\right\}\left\{\frac{-\beta(-M)}{\sqrt{\in_k^2+(\Delta-M)^2}}\right\}$$

$$\frac{d}{dM}\left(\Delta\sqrt{\in_k^2+(\Delta-M)^2}\right) = \sqrt{\in_k^2+(\Delta-M)^2}\Delta - \Delta\left\{\frac{-2\beta\,(\Delta-M)}{2\sqrt{\in_k^2+(\Delta-M)^2}}\right\}$$

Substituting the above derivatives in Equation R_2

$$R_2 = -\int_0^{\hbar\omega_b} \lim_{M\to 0}\left\{\frac{d\in \Delta sech^2\left\{(\beta\frac{\sqrt{\in_k^2+(\Delta-M)^2}}{2}\right\}\left\{\frac{-\beta(\Delta-M)}{2\sqrt{\in_k^2+(\Delta-M)^2}}\right\}}{\sqrt{\in_k^2+(\Delta-M)^2}-M\left\{\frac{-2\beta(\Delta-M)}{2\sqrt{\in_k^2+(\Delta-M)^2}}\right\}}\right\}$$

$$= -\int_0^{\hbar\omega b} d \in \frac{\Delta^2\beta\, sech^2\frac{\beta}{2}\sqrt{\in_k^2+\Delta^2}}{2(\in_k^2+\Delta^2)} \tag{4.3.77}$$

Then combining the first integral and the second integral i.e., Equation (4.3.76) & (4.3.77)

$$R_1 + R_2 = -ln1.13\left(\frac{\hbar\omega_b}{K_B T_m}\right) + \left(\frac{\Delta}{\pi K_B T_m}\right)^2 \frac{8.414}{8} - \int_0^{\hbar\omega b} d \in \frac{\Delta^2}{2K_B T_m(\in_k^2+\Delta^2)}$$

$$+ \int_0^{\hbar\omega_b} d \in \frac{\Delta^2\beta\, sech^2\frac{\beta}{2}\sqrt{\in_k^2+\Delta^2}}{2(\in_k^2+\Delta^2)} \tag{4.3.78}$$

Using the relation of trigonometry

$$sech^2 x = 1 - tanh^2 R = -ln1.13\left(\frac{\hbar\omega_b}{K_B T_m}\right) + \left(\frac{\Delta}{\pi K_B}\right)^2 \frac{8.414}{8} - \int_0^{\hbar\omega b} d \in \frac{\Delta^2}{2K_B T_m(\in_k^2 + \Delta^2)}$$

$$+\int_0^{\hbar\omega_b} d\epsilon \ \frac{\Delta^2 tanh^2 \frac{\beta}{2}\sqrt{\in_k^2+\Delta^2}}{2K_B T_m(\in_k^2+\Delta^2)} \qquad (4.3.79)$$

From the integral of special functions

$$\int_0^{\hbar\omega b} d \in \frac{\Delta^2}{2K_B Tm(\in_k^2+\Delta^2)} = \frac{\Delta^2}{2K_B T_m} arctan\left(\frac{\hbar\omega b}{\Delta}\right) = \frac{\Delta}{4K_B T_c)} \ ln \ \left| \ \frac{\hbar\omega_b+\Delta}{\hbar\omega_b-\Delta} \ \right| \qquad (4.3.80)$$

Since $\frac{2}{\lambda} = I + R$, using equation (4.3.70) and (4.3.79)

$$-\frac{2}{\lambda} = 2ln1.13\left(\frac{\hbar\omega_b}{K_B T_m}\right) - 2\Delta^2\left(\frac{1}{\pi K_B T_m}\right)^2 \frac{8.414}{8} - 2\int_0^{\hbar\omega_b} d \in \frac{\Delta^2}{2K_B T_m(\in_k^2+\Delta^2)}/$$

$$+2 \int_0^{\hbar\omega_b} d \in \frac{\Delta^2 tanh^2 \frac{\beta}{2}\sqrt{\in_k^2+\Delta^2}}{2K_B T_m(\in_k^2+\Delta^2)} \qquad (4.3.80)$$

Since Δ is very small we can ignore the second and the fourth term from Equation (4.3.80)

$$-\frac{1}{\lambda} = ln1.13\left(\frac{\hbar\omega_b}{K_B T_m}\right) - \frac{\Delta}{4K_B T_c)} \ ln \ \left| \ \frac{\hbar\omega_b+\Delta}{\hbar\omega_b-\Delta} \ \right| \text{ Let } \ M = \frac{1}{4K_B T_c)} \ ln \ \left| \ \frac{\hbar\omega_b+\Delta}{\hbar\omega_b-\Delta} \ \right|$$

$$-\frac{1}{\lambda} = ln1.13\left(\frac{\hbar\omega_b}{K_B T_m}\right) - \Delta M$$

$$T_m k_B = \frac{1.13\ \hbar\omega_b}{K_B} e^{-\left(\frac{1}{\lambda}-\Delta M\right)}$$

$$T_m = \frac{1.13\ \hbar\omega_b}{K_B} \qquad (4.3.81)$$

4.5 Energy gap for pure superconducting order parameter state

For pure superconducting system magnetic effect is zero, we can ignore the M term from Equation (4.3.24)

$$\frac{\Delta}{\lambda} = \frac{\Delta\left(\frac{\beta\sqrt{\in_k^2+\Delta^2}}{2}\right)}{\sqrt{\in_k^2+\Delta^2}} \ \mathrm{d} \in_k \qquad (4.3.82)$$

To obtain temperature dependent of energy gap of Equation (4.3.82).we used the same

Technique to solve the first equation on superconducting part

$$\frac{1}{\lambda} = ln1.13\left(\frac{\hbar\omega b}{K_B T_C}\right) - \left(\frac{\Delta}{\pi K_B T_c}\right)^2 \frac{8.414}{8} \tag{4.3}$$

From BCS $T = T_c$; $\frac{1}{\lambda} = ln1.13\left(\frac{\hbar\omega_b}{K_B T_m}\right)$

$$ln\frac{T}{T_{c,}} = -\Delta^2\left(\frac{1}{\pi K_B T_c}\right)^2 \frac{8.414}{8}$$

By using the relation $\ln(1-x) = -x - \frac{x^2}{2}$ ….. Then, $ln\frac{T}{T_{c,}} = 1 - \left(1 - \frac{T}{T_{c,}}\right) = -\left(1 - \frac{T}{T_{c,}}\right)$

$$-\left(1 - \frac{T}{T_{c,}}\right) = \Delta^2\left(\frac{1}{\pi K_B T_c}\right)^2 \frac{8.414}{8} = \Delta^2\left(\frac{1}{\pi K_B T_c}\right)^2 1.05175$$

$$\Delta\,(T) = \frac{(\pi K_B T_c)}{\sqrt{1.05175}}\left(1 - \frac{T}{T_{c,}}\right)$$

$$\Delta\,(T) = 3.06 K_B Tc\left(1 - \frac{T}{T_c}\right)^{\frac{1}{2}} \tag{4.3.84}$$

Equation (4.3.84) indicates that the superconducting ordering parameter (energy gap) the superconducting order parameter decreases linearly when the temperature increases.

CHAPTER FIVE

5. Results and discussion

Chapter five defines the effect of temperature (T) on superconducting order parameter. It also examined the effect of magnetic order parameter on superconducting transition temperature (T_c) and on SDW transition temperature (T_m) in $Ba_{1-x}Na_xFe_2As_2$. In chapter three and four we have used two band model Hamiltonian with retarded double time temperature dependent Green's function formalism, we have obtained mathematical expressions for superconducting transition temperature (T_c), the superconducting order parameter, magnetic order parameter and magnetic transition temperature(T_m).

In sodium doping the $Ba_{1-x}Na_xFe_2As_2$ superconductor series of phase diagram as a function of Na concentration represented by x is presents 34k for x=0.4. Using this T_c value and Equation (4.3.84) we plotted the phase diagrams of the superconducting order parameter verses temperature which is shown in Figure 5.1. In this Figure, when the temperature increases the superconducting order parameter decreases and vanishes as the temperature is equal to the critical temperatures. From Equation (4.3.81) we obtained the values of T_m and using this value, we obtained magnetic ordering parameter. The magnetic transition temperature as a function of magnetic order parameter of $Ba_{1-x}Na_xFe_2As_2$ plotted in Figure 5.2; using Equation (4.3.81) the magnetic transition temperature increases as the magnetic order parameter increases. Based on Equation (4.3.56) we plotted the phase diagram of M verses T_c Figure 5.3. This Figure indicates that, as a magnetic order parameter (M) increases the superconducting transition temperature (T_c) decreases. And finally, we merged Figure 5.2 and Figure 5.3 in order to indicate the region where both orders that superconductivity and spin density wave are coexisted Figure 5.4, where order parameters are in mille electron volt (mev) and transition temperatures are in kelvin (k).

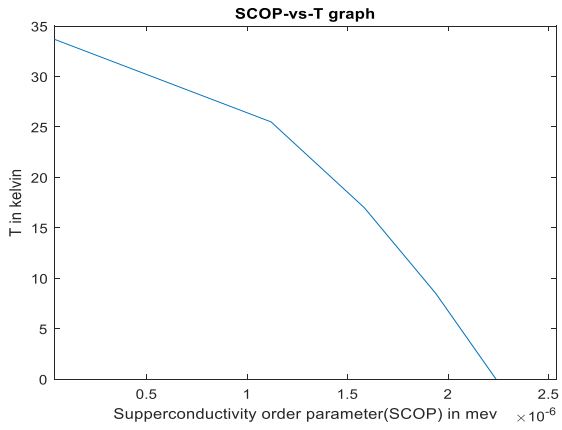

Figure 5.1 Temperature Vs Superconducting order parameter which is drawn by using Equation (4.3.84)

Figure 5.1 Shows that as the temperature increases the superconducting order parameter decreases and finally vanishes as the temperature is equal to the Critical temperature. The temperature is in kelvin and the superconducting order parameter is in mile electron volt.

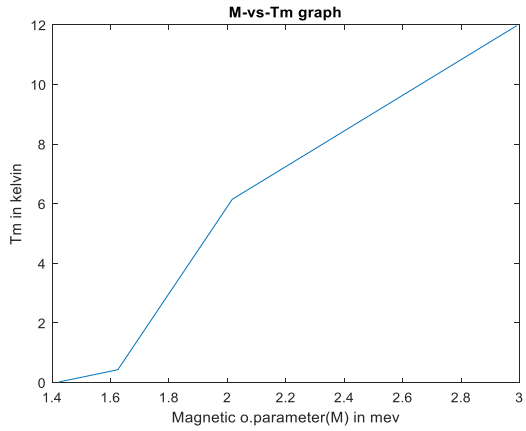

Figure 5.2: Magnetic transition temperature Vs Magnetic ordering parameter which is drawn by using Equation (4.3.81)

The above Figure describes that magnetic order parameter increases as magnetic transition temperature increases. The two parameters are directly proportional and the graph is started at the origin.

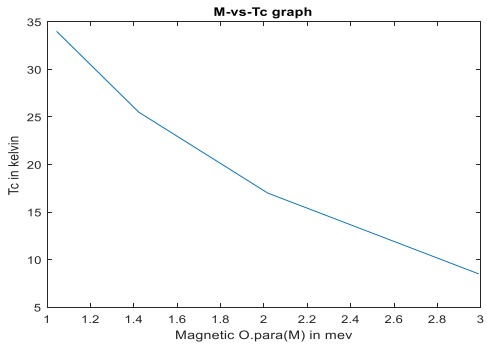

Figure 5.3: Superconducting transition temperature Vs Magnetic ordering parameter for $Ba_{1-x}Na_xFe_2As_2$ Equation (4.3.56) used to draw the graph.

The property of graph is as magnetic order parameter (M) increases the superconducting transition temperature decreases and finally it vanishes at the critical temperature. We observed that for the hole doped barium iron arsenide the magnetic order parameter is zero a temperature of 34k, this temperature is called critical temperature.

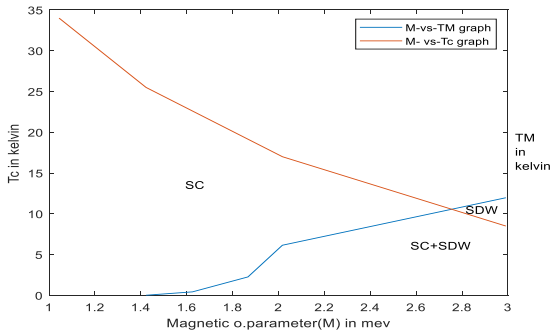

Figure 5.4: Superconducting and magnetic transition temperature as a function of magnetic order parameter of $Ba_{1-x}Na_xFe_2As_2$.

The above Figure 5.4 is drawn by using Equations (4.3.56) and (4.3.81) which describes the coexistence of superconductivity and spin density wave. The region where below the two graphs cross is the coexistence of superconductivity and spin density wave (SC+SDW).The graph shows the general property of the thesis.

CHAPTER SIX

6. Conclusions

The pairing method and symmetry of unconventional superconductivity in Fe-based superconductors is intensive investigation of these days in condensed matter physics. Since superconductivity develops in close proximity to the spin density wave phase, it is crucial to study the high-temperature superconductor mechanism by studying the competition between spin density wave and superconductivity. In this work we have studied the competition between spin density wave and superconductivity in hole doped Barium iron arsenide superconductor ($Ba_{1-x}Na_xFe_2As_2$).

The band-structure calculations have shown that the electronic states at the Fermi level are occupied predominantly by these Fe 3d electrons that changes rapidly by doping and leads to many unusual superconducting and normal state properties. To study these properties of the superconductor we have used model Hamiltonian and Green`s function formalism to obtain a mathematical expression for Superconducting order parameter, magnetic order parameter, critical temperature, and magnetic transition temperature. In so doing we explored the possible coexistence of spin density wave and superconductivity based on the experimental and theoretical hardly understanding. We have drawn different phase diagrams, such as superconducting transition temperature versus superconducting order parameter, magnetic transition temperature versus magnetic order parameter, superconducting transition temperature versus magnetic order parameter, and finally we have combined these two diagrams to obtain the coexistence of superconductivity and spin density wave in $Ba_{1-x}Na_xFe_2As_2$. All these efforts clearly specified that:

I, superconducting order parameter decreases as the temperature increases.

II, the critical temperature decreases as the magnetic order parameter increases.

III, magnetic order parameter increases with respect to magnetic transition temperature increase. Finally, the result of the two combined graphs of the Figure (5.4)

Shows that superconductivity and spin density wave coexist in the $Ba_{1-x}Na_xFe_2As_2$.

Outline of the thesis

Chapter one which defines superconductivity is a phenomenon of zero resistance. It was discovered by Heike Kamerlingh Onnes. Superconductivity is perfect diamagnetism. Chapter two took about high temperature superconductors which have a critical temperature of above 30k that includes iron based and cuprates. Unit the green‘s functions suitable modifications of functions that have been applied in quantum field theory to statistical problems. There are different types of green functions. Chapter four the model Hamiltonian to study the competition between superconductivity and spin density wave in hole doped barium iron arsenide($Ba1-xNaxFe2As2$) based on the multi band nature of iron based superconductor, two band model Hamiltonian was considered. The model Hamiltonian fore coexistence of SDW and superconducting in these compounds can be expressed us mathematically to solve the transition temperature and order parameter. Chapter five deals about how to draw the graph using different equation, it also shows the relation between order parameter and temperature. And Chapter six conclusion and summary of the hol thesis.

References

[1]. H.Kamerlingh Onnes, Akad. Weten Schappen (Amsterdam). 124c , (1911).

[2]. J. Bardeen, L. N. Cooper, and J. R. Schrie_er, Phys. Rev. 108, 1175(1957).

[3]. C. J. Gorter and Casimir, Physica. 1,306(1934)

[4]. W. H. Meissner and R. Ochsenfeld, Naturwiss. 21, 787(1933).

[5]. Shigeji Fujita and Salvador Godoy, Quantum Statistical.Theory of Superconductivity. Plenum Press, New York (1996).

[6]. G.Rickayzen, Theory of superconductivity, John Wiley and Sons, Inc., New York,1965.

[7]. E.Helfand and N.R Werthamer Phys. Rev 147,288-294(1966)

[8]. J. Flouquet and A. Buzdin, Phys. World 15,9(2002

[9]. MB.Maple, Superconductivity-a probe of the magnetic state of local moments inmetals, Appl Phys (Berl),9, 179-204(1976).

[10]. ND.Mathur , et al. Magnetically mediated superconductivity in heavy fermion compounds, Nature, 394, 39-43(1998).

[11]. S.H_ner, etal. Two gaps make a hightemperature superconductor, Rep Prog Phys, 71, 062501(2008).

[12]. H.Mizoguchi, et al. Coexistence of light and heavy carriers associated with superconductivity and antiferromagnetism in CeNi0:8Bi2 with a Bi square net, Phys Rev Lett, 106, 057002(2011).

[13]. M.Kenzelmann, et al. Coupled superconducting and magnetic order in CeCoIn5, Science, 321, 1652-1654(2008).

[14]. PC.Can_eld etal. Possible coexistence of superconductivity and weak ferromagnetism in ErNi2B2C, Physica C, 262, 249-254(1996).

[15]. J.Wen etal. Interplay between magnetism and superconductivity in ironchalco-

genide superconductors: Crystal growth and characterizations, Rep Prog Phys, 74,

124503(2011).

[16]. J. L. Sarrao and J. D. Thompson. J. Phys. Soc. Jpn., 76, 051013(2007).

[17]. Bednorz, J.G. and Müller, K.A., 1986. Possible highT c superconductivity in the Ba− La− Cu− O system. Zeitschrift für Physik B Condensed Matter, 64(2), pp.189-193 (2009).

[18]. Monthoux, P., Pines, D. and Lonzarich, G.G., Superconductivity without phonons. Nature, 450(717177 (2007).

[19]. Özdemir, Z.G., Aslan, Ö. and Onbaşlı, Ü., 2006. Determination of c-axis electrodynamics parameters of mercury cuprates. Journal of Physics and Chemistry of Solids, 67(1-3),

pp.453-456 (2008) .

[20]. Du, Q., Gunzburger, M.D. and Peterson, J.S., 1992. Analysis and approximation of the Ginzburg–Landau model of superconductivity. Siam Review, 34(1), pp.54-81 (2011). pp.453-456 (2008) .

[21]. M.D.Lumsden and A.D.Chriastonson,J.Phys.Condens.Mattter 22 (2010) 203203 (26PP)

[22]. de la Cruz C et al 2008 magnetic order close to superconductivity in the iron based layered $LaO_{1-x}F_xF$ eAs system Nature 453 ,899-902

[23]. L.B.Colman,M.J.Cohen,D.J.Sandman,F.G.Yamagishi,A,F.Garito and A.J.Heeper,Solid state Comm,12 ,1125 (1973)

[24]. Kamihara Y, Watanabe T, Hirano M and Hosono H 2008 Iron-based layered supercon- ductor $La[O_{1-x}F\ x]F$ eAs ($x = 0.050.12$) with $T_C = 26$ K J. Am. Chem. Soc. 130 3296

[25]. Wang C et al 2008 Thorium-doping-induced superconductivity up to 56 K in $Gd_{1-x}T$ hxF eAsOEurophys. Lett. 83 67006

[26]. de la Cruz C et al 2008 Magnetic order close to superconductivity in the iron-based layered $LaO_{1-x}F$ xF eAs systems Nature 453 899902

[27]. Rotter M, Tegel M and Johrendt D 2008 Superconductivity at 38 K in the iron arsenide $(Ba_{1-x}K\ x)F\ e_2As_2$ Phys. Rev. Lett.101 107006

[28]. Sefat A S, Huq A, McGuire M A, Jin R Y, Sales B C,Mandrus D, Cranswick L M D, Stephens P W andStone K H 2008 Superconductivity in LaF e1−xC oxAsO Phys. Rev. B78 104505

[29]. Sefat A S, Jin R Y, McGuiren M A, Sales B C, Singh D J and Mandrus D 2008 Superconductivity at 22 K in Co-doped BaF e2As2 crystals Phys. Rev. Lett. 101 117004

[30]. Tapp J H, Tang Z J, Lv B, Sasmal K, Lorenz B, Chu P C W and Guloy A M 2008 LiF eAs: an intrinsic FeAs-based superconductor with T_C = 18 K P hys.Rev. B 78 060505

[31]. Wang X C, Liu Q Q, Lv Y X, Gao W B, Yang L X, Yu R C,Li F Y and Jin C Q

2008 The superconductivity at 18 K in LiF eAs system SolidStateC ommun. 148 53840

[32]. Pitcher M J, Parker D R, Adamson P, Herkelrath S J C, Boothroyd A T, Ibber- son R M, Brunelli M and Clarke S J 2008 Structure and superconductivity of LiF eAs C hem.C ommun. 591820

[33]. Chu C W, Chen F, Gooch M, Guloy A M, Lorenz B, Lv B,Sasmal K, Tang Z J, Tapp J H and Xue Y Y 2009 The synthesis and characterization of LiF eAs and N aF eAs P hysica C 469 32631

[34]. M.D.Lumsden and A.D.Chriastonson,J.Phys.Condens.Mattter 22 (2010) 203203 (26PP)

[35]. Subedi A, Zhang L J, Singh D J and Du M H 2008 Density functional study of F eS, F eSe, and F eT e: electronic structure, magnetism, phonons, and superconductivity P hys.Rev. B 78 134514

[36]. Bao W etal 2009 Tunable (,)-type antiferromagnetic order in -Fe(Te, Se) super- conductors Phys. Rev. Lett. 102 247001

[37]. Bao W et al 2009 Tunable (δΠ, δΠ)-type antiferromagnetic order in α–F e(T e, Se) superconductors P hys.Rev.Lett. 102 247001

[38]. Zhu X Y, Han F, Mu G, Cheng P, Shen B, Zeng B and Wen H H 2009 Transition of stoichiometric $Sr_2V O_3F eAs$ to a superconducting state at 37.2 K P hys.Rev. B 79 220512

[39]. Chen G F, Xia T-L, Yang H X, Li J Q, Zheng P, Luo J L and Wang N L 2009 Possible high temperature superconductivity in a Ti-doped ASc F eAsO (A = Ca, Sr) system Supercond.Sci.T echnol. 22 072001

[40]. Boeri L, Dolgov O V and Golubov A A 2008 Is $LaF eAsO_{1-x}F x$ an electronphonon superconductor? P hys.Rev.Lett. 101 026403

[41]. Christianson A D etal 2008 Phonon density of states of $LaF eAsO_{1-x}F x$ P hys.Rev.Lett.101 157004

[42]. Kamihara, Y., Hiramatsu, H., Hirano, M., Kawamura, R., Yanagi, H., Kamiya, T. and Hosono, H., 2006. Iron-based layered superconductor: LaOFeP. Journal of the American Chemical Society, 128(31), pp.10012-10013 (2012).

[43]. Allen, P.B., Bedard, F.D., Belitz, D., Crow, J.E., Ferrell, R.A., Lynn, J.W., Ong, N., Santoro, A., Shelton, R.N. and Wang, C.S., High temperature superconductivity. Springer Science & Business Media (2012).

[44]. Paglione, J. and Greene, R.L., High-temperature superconductivity in iron-based materials. Nature physics, 6(9), p.645 (2010).

[45]. Wang, C., Li, L., Chi, S., Zhu, Z., Ren, Z., Li, Y., Wang, Y., Lin, X., Luo, Y., Jiang, S. and Xu, X., Thorium-doping–induced superconductivity up to 56 K in $Gd_{1-x}Th_xFeAsO$. EPL (Europhysics Letters), 83(6), p.67006 (2008).

[46]. Takahashi, H., Igawa, K., Arii, K., Kamihara, Y., Hirano, M. and Hosono, H., Superconductivity at 43 K in an iron-based layered compound LaO_{1-x} F_xFeAs. Nature, 453(7193), p.376 (2008).

[47]. Kamihara Y, Watanabe T, Hirano M and Hosono H 2008 Iron-based layered superconductor La[$O_{1-x}F_x$]F eAs ($x = 0.050.12$) with $T_C = 26$ K J. Am. Chem. Soc. 130 3296

[48]. de la Cruz C et al 2008 Magnetic order close to superconductivity in the iron-based layered $LaO_{1-x}F_x$F eAs systems Nature 453 899902

[49]. McGuire M A etal 2008 Phase transitions in LaF eAsO:structural, magnetic, elastic, and transport properties, heat capacity and Mossbauer spectra P hys.Rev. B 78 094517

[50]. McGuire M A etal 2008 Phase transitions in LaF eAsO:structural, magnetic, elastic, and transport properties, heat capacity and Mossbauer spectra P hys.Rev. B 78 094517

[51]. Rotundu C R, Keane D T, Freelon B, Wilson S D, Kim A,Valdivia P N, Bourret-Courchesne E and Birgeneau R J 2009 Phase diagram of the P rF eAs$O_{1-x}F_x$ supercon- ductor arXiv:0907.1308

[52]. Zhao J etal 2008 Structural and magnetic phase diagram of C eF eAs$O_{1-x}F_x$ and its relation to high-temperaturesuperconductivity N at.M ater. 7 9539

[53]. Zhao J etal 2008 Structural and magnetic phase diagram of C eF eAs$O_{1-x}F_x$ and its relation to high-temperaturesuperconductivity N at.M ater. 7 9539

[54]. Drew A J et al 2009 Coexistence of static magnetism and superconductivity in SmF eAs$O_{1-x}F_x$ as revealed by muon spin rotation N at.M ater. 8 3104

[55]. Kamihara, Y., Hiramatsu, H., Hirano, M., Kawamura, R., Yanagi, H., Kamiya, T. and Hosono, H., 2006. Iron-based layered superconductor: LaOFeP. Journal of the American Chemical Society, 128(31), pp.10012-10013 (2012

[56]. Rotter M, Tegel M, Johrendt D, Schellenberg I, Hermes W and Pottgen R 2008 Spin-density-wave anomaly at 140 K in the ternary iron arsenide $BaFe_2As_2$ P hys.Rev. B

78020503

[57]. Margadonna S, Takabayashi Y, Mcdonald M T, Brunelli M,Wu G, Liu R H, Chen

[58]. Kofu M, Qiu Y, Bao W, Lee S H, Chang S, Wu T, Wu G and Chen X H 2009 Neutron scattering investigation of the magnetic order in single crystalline BaF e_2As_2 N ewJ.P hys.11 055001

[59]. Rotter M, Pangerl M, Tegel M and Johrendt D 2008 Superconductivity and crystal structures of $(Ba_{1-x}K_x)F\ e_2As_2$ (x = 0–1) Angew.C hem.I nt.Edn 47 794952

[60]. Chen H et al 2009 Coexistence of the spin-density wave and superconductivity in $Ba_{1-x}K_xF\ e_2As_2$ Europhys.Lett. 85 17006

[61].Wang, X.C., Liu, Q.Q., Lv, Y.X., Gao, W.B., Yang, L.X., Yu, R.C., Li, F.Y. and Jin, C.Q., 2008. The superconductivity at 18 K in LiFeAssystem.Solid State Communications, 148(11-12), pp.538-540 (2008).

[62]. M.D.Lumsden and A.D.Chriastonson,J.Phys.Condens.Mattter 22 (2010) 03203 (26PP)

[63]. Paulose P L, Yadav C S and Subhedar K M 2009 Magnetic phase diagram of

F e_{1+y} T $e_{1-x}Se_x$ system: coexistence of spin glass behavior with superconductivity?arXiv:0907.3513

[64]. dela Cruz C et al 2008 magnetic order close to superconductivity in the iron based layered $LaO_{1-x}F_xF\ eAs$ system Nature 453 ,899-902

[65]. Klingeler R et al 2010 Local antiferromagnetic correlations in the iron pnictide superconductors $LaF\ eAsO_{1-x}F_x$ and $C\ a(F\ e_{1-x}C\ o_x)_2As_2$ as seen via normal-state suscep-tibility P hys.Rev. B 81 024506

[66]. M.k.Wu,J.R.Ashburn,C.J.Torng,P.H.hor,R.L.Meng,L.Gao,Z.J.Huang,Y.G. Wag,and C.W.Chu,Phys.Rev.Lett, 58,908 (1987)

[67]. Q. Huang, Y. Qiu, W. Bao, M. A. Green, J. W. Lynn, Y. C. Gasparovic, T. Wu, G. Wu, X. H. Chen, Phys. Rev. Lett. 2008, 101, 257003.

[68]. Y. Su, P. Link, A. Schneidewind, T. Wolf, P. Adelmann, Y. Xiao, M. Meven, R. Mittal, M. Rotter, D. Johrendt, T. Brueckel, M. Loewenhaupt, Phys. Rev. B: Condens. Matter Mater. Phys. 2009, 79, 064504.

[69]. M. Kofu, Y. Qiu, W. Bao, S. H. Lee, S. Chang, T. Wu, G. Wu, X. H. Chen, New J. Phys. 2009, 11, 055001

[70]. R. Cortes-Gil, D. R. Parker, M. J. Pitcher, J. Hadermann, S. J. Clarke, Indifference of Superconductivity and Magnetism to Size-Mismatched Cations in the Layered Iron Arsenides Ba1−xNaxFe2As2, Chem. Mater., 22 (2010) 4304

[71]. S. Avci, J. M. Allred, O. Chmaissem, D. Y. Chung, S. Rosenkranz, J. A. Schlueter, H. Claus, A. Daoud-Aladine, D. D. Khalyavin, P. Manuel, A. Llobet, M. R. Suchomel, M. G. Kanatzidis, R. Osborn, Structural, magnetic, and superconducting properties of Ba1−xNaxFe2As2, Phys. Rev. B 88 (2013) 094510

[72]. Luetkens H etal 2009 The electronic phase diagram of the $LaO_{1-x}F$ xF eAs supercon- ductor N at.M ater. 8 3059

[73]. S. Avci, O. Chmaissem, J.M. Allred, S. Rosenkranz, I. Eremin, A.V. Chubukov, D.E. Bugaris, D.Y. Chung, M.G. Kanatzidis, J.-P Castellan, J.A. Schlueter, H. Claus, D.D. Khalyavin, P. Manuel, A. Daoud-Aladine, R. Osborn. Magnetically driven suppression of nematic order in an iron-based superconductor, Nature Communications 5 (2014) 3845

[74]. D. D. Khalyavin, S. W. Lovesey, P. Manuel, F. Krüger, S. Rosenkranz, J. M. Allred, O. Chmaissem, R. Osborn, Symmetry of reentrant tetragonal phase in Ba1−xNaxFe2As2: Magnetic versus orbital ordering mechanism, Phys. Rev. B 90 (2014) 174511

[75]. F. Wasser, A. Schneidewind, Y. Sidis, S. Wurmehl, S. Aswartham, B. Büchner, M. Braden, Spin reorientation in Ba0.65Na0.35Fe2As2 studied by single-crystal neutron diffraction, Phys. Rev. B 91 (2015) 060505

[76]. I. I. Mazin and J. Schmalian, Pairing symmetry and pairing state in ferropnictides: Theoretical overview. Physica C 469, 614-623 (2009).

[77]. S. Avci, O. Chmaissem, J. M. Allred, S. Rosenkranz, I. Eremin, A. V. Chubukov, D.E. Bugaris, D. Y. Chung, M. G. Kanatzidis, J.-P. Castellan, J. A. Schlueter, H. Claus, D. D.

Khalyavin, P. Manuel, A. Daoud-Aladine, and R. Osborn, Magnetically driven suppression of nematic order in an iron-based superconductor, Nature Commun. 5,3845 (2014).

[78]. Blachowski, A., Ruebenbauer, K., Zukrowski, J., Bukowski, Z., Matusiak, M. and Karpinski, J., Interplay between spin density wave and superconductivity in'122'iron pnictides:57 (2012)

[79]. Grüner, G., The dynamics of spin density waves Reviews of modern physics, 66(1), p.1(1994).

[80]. Bonville, P., Rullier Albenque, F., Colson, D. and Forget, A., Incommensurate spin density wave in Co-doped $BaFe_2As_2$. EPL (Europhysics Letters), 89(6), p.67008 (2010).

[81]. Korshunov, M.M. and Eremin, I., Theory of magnetic excitations in iron-based layered superconductors. Physical Review B, 78(14), p.140509 (2008).Fe M\" ossbauer study.ArXiv preprint arXiv:1110.3170 (2011).

[82]. A.S.Chakravorty, Introduction to the magnetic properties of solids, John Wiley and Sons, Inc., New York, 1980.

Declaration

I hereby declare that this thesis is my original work and has not been presented for a degree in any other university. All sources of material used for the thesis have been accordingly acknowledged.

Name: Getachew Yalew Signature----------

This thesis has been submitted for the examination with my approval as university advisor.

Name: Dagne Atnafu (PhD) Signature----------

Dilla University

Department of physics

June, 2021Gc